COLORADO

Higher Education Competitive Research Authority

COLORADO HIGHER EDUCATION COMPETITIVE RESEARCH AUTHORITY

University of Colorado:Colorado State University:University of Northern Colorado:Colorado Schools of Mines:State of Colorado

March 1, 2021

Honorable Members of the House and Senate Education Committees
State Capitol
200 East Colfax
Denver, CO 80203

Re: Annual Report of the Colorado Higher Education Competitive Research Authority (CHECRA)

Dear Representatives and Senators:

Colorado Revised Statute §23-19.7-103(3) requires the Colorado Higher Education Competitive Research Authority (CHECRA), housed at the Colorado Department of Higher Education, to report annually to the Education Committees of the Colorado House of Representatives and Senate on research projects funded by the CHECRA in the previous calendar year. This letter reports on activities and projects funded in calendar year 2020.

The CHECRA was created to provide a source of matching funds for National Science Foundation (NSF) and other competitive federal grants that require or benefit from a state match. CHECRA funding has helped to bring significant research dollars to Colorado. CHECRA spent almost $1.38 million in 2020 to support five multi-year research grants that jointly are bringing over $50 million in research dollars to the state. Following is a list of the multi-year research grants that received CHECRA funding in 2020:

University of Colorado (CU)

1. In 2016, with CU Boulder as the lead awardee, the NSF awarded a $24 million, 5-year grant for the Science and Technology Center on Real-Time Functional Imaging (STROBE). STROBE brings together universities, national laboratories, industry and international partners to create a powerful new set of real-time imaging modalities. CHECRA has pledged $400,000 for five years; 2020 was the fifth year of funding.
2. The NSF Quantum Leap Challenge Institute, led by the University of Colorado Boulder, includes extensive collaborations with leaders from other academic institutions in the US and

Europe, NIST, National Laboratories, and industry to make broad, fundamental advances in quantum science and engineering. The aim is to demonstrate and leverage quantum advantages in state-of-the-art quantum sensing across the field. The Institute is designed for core integration of research with education and workforce development. CHECRA has pledged $400,000 annually for five years; 2020 was the first year of funding.

Colorado School of Mines (CSM)

3. The Colorado School of Mines is a member of the REMADE Institute—a $140 million Manufacturing USA Institute co-funded by the U.S. Department of Energy— launched in January 2017. In partnership with industry, academia, trade associations, and national laboratories, REMADE enables early-stage applied research and development of technologies that could dramatically reduce the embodied energy and carbon emissions associated with industrial-scale materials production and processing. CHECRA paid $66,435 in matching funds to the School of Mines in 2020.
4. The Re-inventing the Nation's Urban Water Infrastructure (ReNUWIt) Engineering Research Center is a $5.7 million grant for which CHECRA has provided an annual cost share of $400,000 per year for five years. With this grant from the NSF, the School of Mines joined leading universities in tackling acute water problems and needed infrastructure changes in the West. CHECRA made the final of five payments in 2020.

Colorado State University (CSU)

5. Colorado State University's Industrial Assessment Center (CSU IAC), funded by the U.S. Department of Energy, provides industrial energy audits by engineering students to small and medium sized manufacturing facilities. The CHECRA has committed to providing a total of $131,634 to the IAC over three years. CHECRA made the first and second payments (the first payment due in 2019 was inadvertently delayed) totaling $87,756 in 2020.

In addition to the payments listed above, the CHECRA provided $300,000 as a cost share for the following Major Research Instrumentation (MRI) grants received from NSF in 2020. These one-time grants provide higher education institutions with major instrumentation that supports the research and research training goals of the institution and are also used by other researchers regionally or nationally.

- **CU MRI Consortium: Development of Fiber-coupled stimulated emission depletion microscopy (STED).** With this grant, CU is developing a unique miniature optical fiber-coupled microscope that will enable flexible imaging at unprecedented spatial resolution. Developed with a diverse team that includes engineers, physicists, and neuroscientists, this cutting-edge microscope will yield far-reaching impacts through intellectual property development and future commercialization and deployment in industry. The research team will use the new instrument to expand ongoing efforts to mentor and inspire young students from groups underrepresented in Science Technology Engineering and Mathematics (STEM) fields.
- **CU MRI: Acquisition of a High-Sensitivity Low-Energy Ion Scattering (HS-LEIS) Spectrometer with Multiple Reactive Environment Transfer for Interrogating**

Surfaces and Interfaces. Materials interact with their environment through their surfaces. This spectrometer will be a vital resource for the greater Rocky Mountain Region and its many researchers studying catalysis, atomic layer deposition and coatings, photovoltaics, and solid state structure and interfaces, among other areas.

Appendices to this report include detailed information on each of the projects listed above. In addition to the millions of dollars in federal funding coming into the institutions and the state—and the impressive scientific results achieved under the projects—the research centers funded by CHECRA positively impact Colorado. These benefits include support for graduate and undergraduate students, outreach to K-12 students and teachers and economic development benefits from spin-off technologies and companies.

Following are some highlights of these benefits to Colorado.

- One of the scientists working under STROBE did research very relevant to COVID-19. As a service, he provided images of their vaccine to Moderna, to help accelerate vaccine progress.
- CSU's industrial assessment program offers an incredibly valuable service to our local manufacturing community. The assessments are offered to companies that don't have the necessary internal resources to perform the energy and waste assessments, and they provide explicit assessment reconditions. The recommendations facilitate the saving of energy while also helping our manufactures stay competitive in a dynamic manufacturing environment. The center also it provides training and applied experience for our next generation of energy engineers.
- Among other work with community partners, the Colorado School of Mines ReNUWIt Center has continued its collaboration with the City of Denver to predict changes in stormwater management and with the Southeast Metro Stormwater Authority to recover energy from wastewater using anaerobic digestion. ReNUWIt also works with Shelton Elementary School in Golden, Lakewood High School, and numerous children's camps on their Math and Science Fair and camps.

Due to the State budget impacts of the pandemic, the annual distribution of Limited Gaming Funds in the amount of $2.1 million to the Authority was suspended for two years, so CHECRA did not receive that revenue in 2020. Interest earnings on the Authority's funds totaled $77,388 in 2020. Expenses totaled $1,684,191. The CHECRA board recommends that the distribution from Limited Gaming Revenue be reinstated in FY22.

Thank you for your support of this ongoing research. We welcome any questions.

Sincerely,

Dr. Angie Paccione

Dr. Angie Paccione
Executive Director, Colorado Department of Higher Education

Cc: Dr. Alan Rudolph, Vice President for Research, Colorado State University and Vice Chair, CHECRA
Dr. Terri Fiez, Vice Chancellor for Research, University of Colorado Boulder
Colorado School of Mines
Dr. Stefanie Tompkins, Vice President for Research and Technology, Colorado School of Mines
Dr. Jeri-Ann Lyons, Associate Vice President for Research, University of Northern Colorado

Attachments:

Appendix A: University of Colorado Science and Technology Center on Real-Time Functional Imaging (STROBE)
Appendix B: MRI Consortium: Development of Fiber-coupled stimulated emission depletion microscopy (STED)
Appendix C: QLCI - CI: NSF Quantum Leap Challenge Institute for Enhanced Sensing and Distribution Using Correlated Quantum States
Appendix D: Colorado School of Mines Re-inventing the Nation's Urban Water Infrastructure (ReNUWIt) Engineering Research Center
Appendix E: Colorado School of Mines (REMADE): Sorting and Impurity Removal to Improve the Recycling of Steel Scrap from Auto Shredders
Appendix F: Colorado State University Extension Industrial Assessment Center
Appendix G: MRI: Acquisition of a High-Sensitivity Low-Energy Ion Scattering (HS-LEIS) Spectrometer with Multiple Reactive Environment Transfer for Interrogating Surfaces and Interfaces

NSF award to University of Colorado, Boulder (UCB)
NSF Award: 1548924
Title: *Science and Technology Center on Real-Time Functional Imaging (STROBE)*
Period of Performance: 10/01/2016 – 09/30/2021 ($24M over 5 yrs, renewal in progress)
Total 2020 CHECRA Funding: $400,000
Award PI's: Margaret Murnane (Director), Jianwei Miao, Markus Raschke, Naomi Ginsberg

Abstract:
Microscopy and imaging are critical for discovery and innovation in science and technology, accelerating advances in materials, bio, nano and energy sciences, as well as nanoelectronics, data storage and medicine. Although electron, X-ray and optical nano imaging methods are all undergoing revolutionary advances, no single imaging modality can address critical questions underlying much of science and technology in the 21st century. These grand challenges include: How does the local atomic and interfacial structure and interactions determine the functional properties of materials? How to image very large areas (>centimeters) at very high spatial resolution (~nanometer)? What is the 3D atomic structure of glasses and how do the atoms rearrange themselves during the glass transition? How to rapidly image viruses and vaccines, with molecular-scale information. Addressing these major scientific challenges requires the development of new multimodal multiscale imaging approaches by integrating state-of-the-art microscopes, new methods, novel sample preparation, fast detectors, big data, advanced algorithms and machine learning - which could not be accomplished without a center.

Progress made over the last year: *(focusing on key objectives or milestone reached, challenges encountered, and/or other particularly noteworthy highlights (limit answer to 1/2 page).*
STROBE brings together academia (CU Boulder, UCLA, UC Berkeley, UC Irvine, Florida International University and Fort Lewis College), national laboratories (LBNL, ORNL, NIST) and several US industries to develop and advance multimodal multiscale microscopy. One major achievement in 2020 was to go through a successful grant renewal process, so that STROBE can continue for another 5 years. A second major achievement was maintaining a safe and productive low-density research environment during covid, so that trainees could advance their careers. Please see the list and slides below for the large number of trainees, publications, collaborations and other impacts of STROBE. Most notably, STROBE technologies are now either used, or are impacting, several national laboratory facilities at NIST Boulder Labs, Lawrence Berkeley Labs, industry and elsewhere. As detailed below, UCLA STROBE scientist Hong Zhou provided images of their vaccine to Moderna, to help accelerate progress.

Outcomes/benefits of this project over the past year, including both scientific advancements as well as other benefits:
1. STROBE is attracting new collaborations from national labs, academe and industry, in particular local Colorado labs such as NREL and NIST.
2. >67 STROBE diverse graduates are now impacting the US workforce. Of these, >31 moved to industry or national labs, while >15 are in permanent academic positions. Of these trainees, ~30% were women and 10% URM.
3. UCLA STROBE scientist Hong Zhou did research very relevant to COVID-19. As a service, he provided images of their vaccine to Moderna, to help accelerate progress. For bio-materials, sub-2Å resolution is required to obtain the chemical structure to understand how

proteins function. Only the best electron imaging labs, like Zhou's, have the specialized setups to manage the immense amounts of data required to reach this resolution. He was one of the top labs tackling COVID-19 from numerous fronts, from vaccine to drug development. STROBE research into advanced algorithms that can extract structural information with less data is key for reaching molecular-level imaging and will have large future impact.

4. STROBE research advances have resulted in 200 papers that are highly cited (please see https://strobe.colorado.edu/ for Publications, News and Awards). The large majority of the papers are collaborative, cross-group, cross-node, multimodal, and/or joint university/national lab/industry work.
5. STROBE technologies are integral to ~5 joint university-industry grants with small and large businesses, and 2 Semiconductor Research center (SRC) fellowships/grants.
6. STROBE-enhanced IR sources are now available to a broad user community at the Department of Energy Synchrotron Source at UC Berkeley.
7. STROBE-enhanced advanced algorithms for X-ray imaging are now available to a broad user community at the Department of Energy Synchrotron Source at UC Berkeley.
8. STROBE-enhanced X-ray sources are now used by NIST Boulder Labs for advanced materials research.
9. CU Boulder Professor Heather Lewandowski taught a 500-person "lab" class with STROBE postdoc Dr. Alex Wurth last semester during covid (Fall 2020). They adopted STROBE mentoring training to small teams of students. The student teams analyzed real solar flare data (that had not been analyzed previously), categorizing flares etc. The feedback from the students was amazing - they really appreciated that their team felt like a community and was helpful to their learning. Students reported "feeling like a scientist for a semester" and that "this was the best class I had this semester". Heather will write up a 500-student research paper, and some education research papers also.
10. STROBE hosted and mentored >25 undergraduate students for remote research experiences in the Summer of 2020.

Fig. STROBE team at the most recent of our four Annual Retreats at UCLA.

Additional documentation:

(Additional documentation may include additional artifacts, reports, or content that should be included as an appendix or addendum to the content supplied in this form.)

Please see the slides below.

Summary 3.7 years: growth and high productivity – well done!

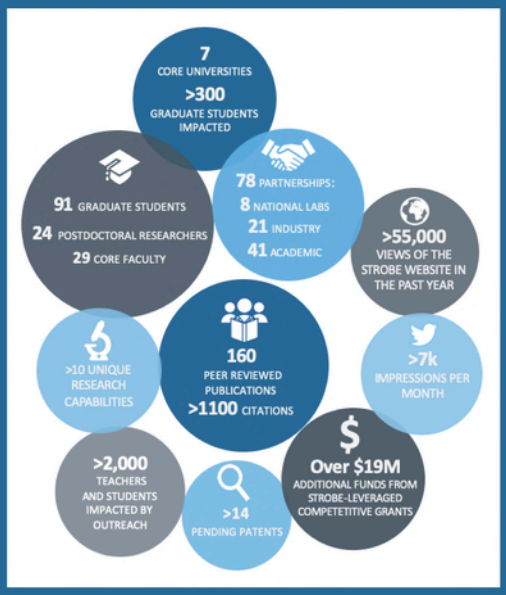

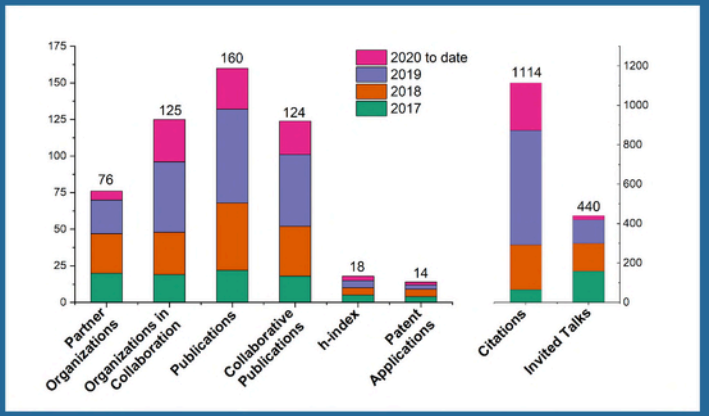

STROBE Alumni in Industry and National Laboratories
(67 grads, 31 to industry/national labs, 15 permanent academic)

- Transdisciplinary programs, professional and soft skills training; 30% women, 12% URM (US ave. <20%, <4%)

Izabella Berman
Current Affiliation: Laser Technician, KMLabs

Adam Blonsky
Current Affiliation: Lockheed Martin

Cong Chen
Current Affiliation: Product Engineer, Lam Research

Michael Chen
Current Affiliation: Research And Development Engineer, UltraSense Systems

Seth Cousin
Current Affiliation: Research Scientist, EUV/X-Ray Source Product Manager, KMLabs Inc.

Tingting Fan
Current Affiliation: Software Engineer, Tableau Software

Maithreyi Gopalakrishnan
Current Affiliation: Technical Project Manager, Quantum Thought

Wiliam Hubbard
Current Affiliation: CEO, NanoElectronic Imaging, Inc.

Simone Hyater-Adams
Current Affiliation: Education & Diversity Programs Manager, American Physical Society (APS Physics)

Robert Karl
Current Affiliation: Lockheed Martin

Omar Khatib
Current Affiliation: Bruker

Hsiou-Yuan (Herbert) Liu
Current Affiliation: Path.AI (startup)

Yuan Hung (Mike) Lo
Current Affiliation: AI Fellow, Insight Data Science

Seonah Moon
Current Affiliation: Engineer, I Corporation

Kasra Nowrouzi
Current Affiliation: Postdoctoral Scholar, Advanced Quantum Testbed at Lawrence Berkeley National Lab

Zack Phillips
Current Affiliation: Photonics Engineer, Apple

Christina Porter
Current Affiliation: Design Engineer, ASML Research

AJ Pryor
Current Affiliation: Principal Data Scientist, American Tire Distributors

Elisabeth Shanblatt

Marta Sulima
Current Affiliation: Research Scientist, Chromatic Technologies, Inc.

Tina Tran
Current Affiliation: System Integration Engineer, ASML

Omer Tzang
Current Affiliation: Research Scientist, 3i Denver

Li-Hao Yeh
Current Affiliation: R&D Engineer, Chan Zuckerberg Biohub

Dmitry Zusin
Current Affiliation: Research Scientist, KLA

Jennifer Ellis
Current Affiliation: NRC Postdoctoral Fellow, NIST

Bjoern Enders
Current Affiliation: Data Science Workflows Architect, National Energy Research Scientific Computing Center, LBNL

Travis Frazer
Current Affiliation: Argonne National Laboratory

Dennis Gardner, Jr.
Current Affiliation: Research Physicist, U.S. Naval Research Laboratory

William Peters
Current Affiliation: Postdoc, Los Alamos National Lab

Xiyu Yi
Current Affiliation: Postdoctoral Research Staff, Lawrence Livermore National Laboratory

STROBE Best Practices based on APS CSWP, NAS, SMART, COACH, team experience

- Community building
- Mentor training
- Team projects: academe, industry, natnl labs
- Exchanges, engagement
- Professional respectful environment
- Role models at all levels
- Alumni network
- New curricula prepare for 21st century careers
- Soft skills development
- Well-designed, meaningful, undergraduate research
- Outreach training
- Expert evaluation

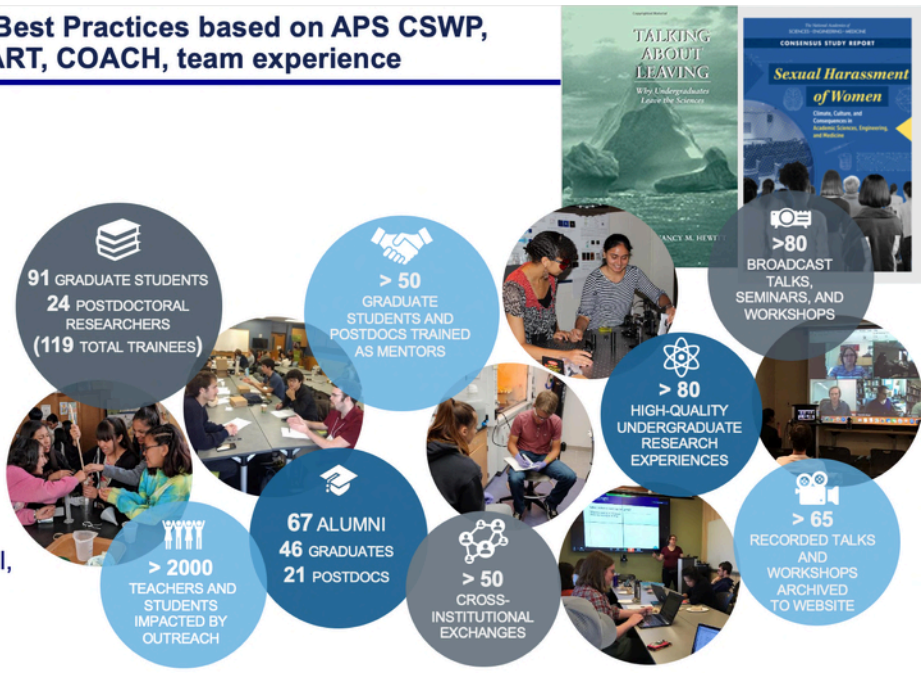

STROBE creates a rich, attractive, diverse and inclusive STEM environment by developing and using Best Practices

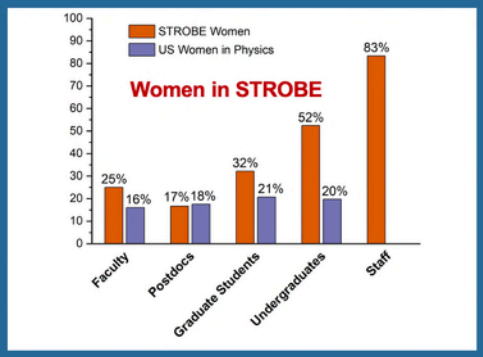

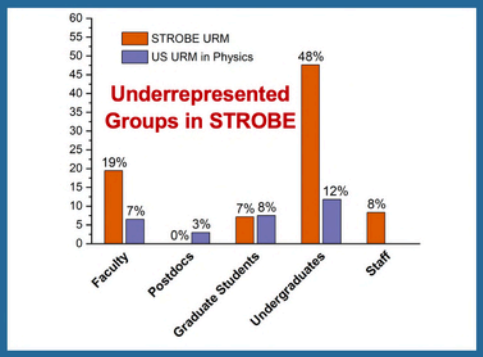

STROBE NSF SCIENCE AND TECHNOLOGY CENTER — PREM PEAQS Partnership for Functional Nanomaterials - Integrated research, education, outreach & broadening participation

PEAQS

- **Jeff Jessing**, Kay Phelps, Fort Lewis College (highest # Native American & Alaskan Native US phys/eng students)
- **Doyle Temple**, Norfolk State University (HBCU)
- Full STROBE team – see PEAQS talks
- Opportunities for collaboration, mentoring

FORT LEWIS COLLEGE

NORFOLK STATE UNIVERSITY

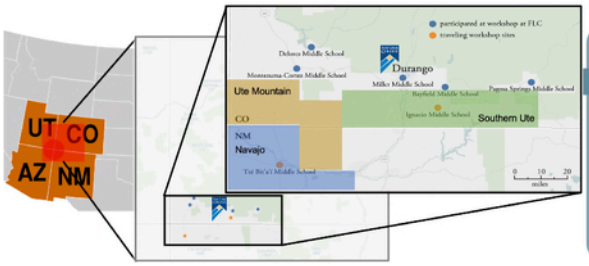

Recruitment

- Outreach to High School Students in Diverse Communities
- High School Research Experiences at FLC and NSU
- Active PREM Student Groups to Attract the Best and Brightest
- Leverage STROBE Undergraduate Imaging Science Curricula to Recruit Freshman/Sophomores
- Undergraduate Recruitment to Graduate School

RESEARCH + COMMUNITY

Retention

- Faculty & Student Exchange to Build Community & Collaborations
- Annual Retreat and Social Activities
- Support for PREM Undergraduate Researchers at all Nodes
- Access to Infrastructure & Experts
- Diverse Role Models & Careers
- Leverage STROBE Advanced Undergraduate Imaging Science Labs
- Empower ACCESS Student Groups & Mentoring Training Program

RESEARCH + COMMUNITY

Graduation & Careers

- Undergraduate Professional Development & Career Readiness
- Professional Networks with Role Models in Industry, Federal Labs, and Academic Careers in Research & Teaching
- Undergraduate Recruitment to Graduate School
- Ensure the Best and Brightest Rise and Thrive in STEM

STROBE NSF SCIENCE AND TECHNOLOGY CENTER — Impact of covid-19 – big thank you to the STROBE team!

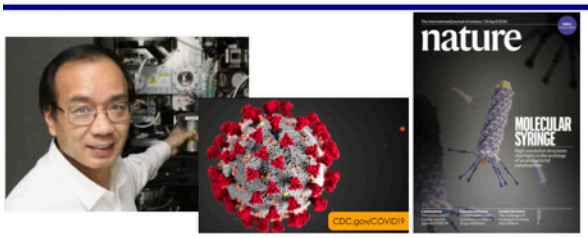

Hong Zhou lab at UCLA worked with Moderna on vaccine and drug development

Trainees worked hard on papers, designs, theses, seminars, codes, analysis, during stay-at-home

Lewandowski, Werth and Phillips worked on best practices for remote learning

25 undergraduates remote summer of 2020, thanks to Ellen, Sarah, faculty and trainees!

Returned to low-density safe research environment looking forward to vaccines!

Full name of the funded project: Collaborative Research:

MRI Consortium: Development of Fiber-coupled stimulated emission depletion microscopy (STED)

First and last name of the primary investigator (PI) for this project (or PI's):

Juliet Gopinath (PI), Emily Gibson (PI)

Enter a short description or abstract of the project:

The goal is to develop a unique miniature optical fiber-coupled microscope that will enable flexible imaging at unprecedented spatial resolution. Developed with a diverse team that includes engineers, physicists, and neuroscientists, this cutting-edge microscope will not only provide new fundamental and practical insights across research areas, but will also yield far-reaching impacts through intellectual property development and future commercialization and deployment in industry. The research team will use the new instrument to expand ongoing efforts to mentor and inspire young students from groups underrepresented in Science Technology Engineering and Mathematics (STEM) fields.

Real-time in-brain imaging has made tremendous advances in the past few years, allowing unprecedented inquiry into how dynamic structures such as dendritic spines enable brain functions such as learning, memory, cognition, and behavior. However, future advances in observation-based understanding of the function and response of these cellular structures are limited by the blur inherent to light's fundamental properties that obscures these features. Based on the established and Nobel Prize-winning principle of Stimulated Emission Depletion (STED) microscopy, the instrument developed in this collaborative project will be capable of a 5X increase in spatial resolution. This miniature microscope will enable, for the first time, imaging of small structures such as synaptic spine dynamics and changes in myelination underlying behaviors and social interactions in behaving animals. It will also enable lithography in 3D materials at unprecedented spatial scale aimed towards the next generation of electronic devices.

Summarize progress made over the last year, focusing on key objectives or milestone reached, challenges encountered, and/or other particularly noteworthy highlights (limit answer to 1/2 page).

Development of miniature fiber-coupled STED microscope We demonstrated a two photon (2P) fiber STED microscope in which the excitation and STED light are delivered to the sample in polarization maintaining (PM) fiber. The 2P excitation source for our fiber STED microscope is a homebuilt Ti:Sapph laser oscillator with a rep rate of 81 MHz, mode locked at a wavelength of 910 nm. The excitation beam passes through a grating stretcher in order to compensate for dispersion in the fiber and microscope optics. Using a dichroic mirror, we couple the beam in to 1 m of PM fiber with a core diameter of 4.5 μm. A photodiode monitoring the Ti:Sapph pulse train triggers the STED laser (NKT Katana HP-06) so that the two lasers are synced. The STED beam (wavelength of 592 nm) is shaped into a Hermite-Gaussian (HG) beam with an SLM in order to couple to the higher order modes of the fiber. It passes through a half wave plate, and a polarizing cube beam splitter breaks the beam into two arms of a Mach-Zehnder interferometer. In one arm, a dove prism rotates the beam shape by 90o so that the combined HG beams create the doughnut shape, as shown in **Fig. 1**. This also provides a delay so that at the end of the interferometer, the two halves of the doughnut no longer interfere. The composite STED beam is combined with the 2P excitation light using a dichroic mirror and then carefully coupled into the PM fiber: the STED doughnut is coupled into the higher-order fiber modes, while the 2P excitation light is coupled into the fundamental mode. An apochromatic 20x objective collimates the excitation and depletion beams at the output of the fiber. The beams then impinge on a MEMS mirror (Mirrorcle A7B2.1-3600AL-TINY20.4-A/TP) that steers them through a scan and tube lens. We use a 100x 1.4 NA oil immersion objective for imaging. The fluorescence is de-scanned through the system and split from the beam path using a low-pass dichroic mirror. It is coupled to a multimode fiber and detected with a PMT (Hamamatsu H7422P-40). The voltage signal from the PMT is discretized using a photon counting unit (Hamamatsu C9744). The microscope is controlled using a customized program written in MATLAB.

Images from our microscope are presented in **Fig. 2**. The imaged specimen is a 500 μm coronal slice of the brain of a Plp1-eGFP mouse, where the myelin is labeled with eGFP [7]. While there is clearly an improvement in the sharpness of the image when acquired with STED (Fig. 2 b), a more quantitative measure is made by taking column averaged line cuts (Fig. 2 c and d). To extract a column averaged line cut, a rectangular region of interest is found (shown in Fig. 2 a and b) and pixels spanning the short distance of the rectangle are averaged as columns. These line cuts confirm that features in our sample are resolved more clearly when using STED. A 180 nm structure is shown in Fig. 2c, which is roughly half of its apparent size without using STED. However, it is not possible to extract the resolution of the system from these images alone, as the sizes of the features themselves are not known.

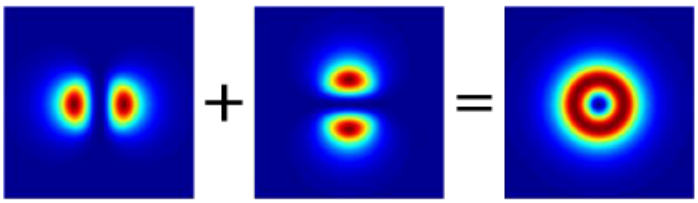

Fig. 1. Simulated intensity distributions of the two higher-order modes of PM fiber that are combined to create the doughnut-shaped depletion beam. Prior to being coupled into fiber, the depletion beam is split into two arms of a Mach-Zehnder interferometer. The path length difference between the two arms is much greater than the coherence length of the STED laser, so there is no interference between the two modes during fiber propagation. This makes our fiber STED microscope robust against fiber bending.

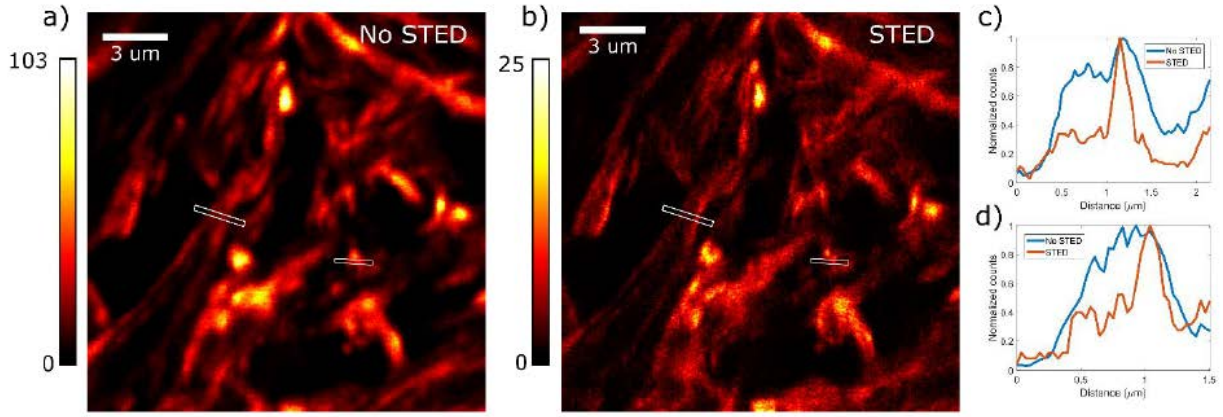

Fig. 2. Images of a Plp1-eGFP mouse brain with eGFP labeled myelin [7] taken on our 2P fiber microscope a) without STED light and b) with 40 mW of STED light, measured before the objective. Images have a pixel size of 35 nm and the dwell time for each pixel is 50 microseconds. A Gaussian blur filter with a sub-pixel waist of 25 nm is applied to both images to smooth pixel shot noise. The STED image appears sharper, with features that are not evident in a). As a more quantitative measure, column averaged line cuts are taken at two locations, with the leftmost presented in c) and the rightmost in d). Both the STED and no STED have been normalized by their largest count to facilitate comparison. A description of the column averaged line cuts is available in the text.

Provide outcomes/benefits of this project over the past year, including both scientific advancements as well as other benefits. Examples of the latter include contributing to graduate and undergraduate education; K-12 or other outreach; technology commercialization and/or spin-off companies; collaboration with others.

The project has provided opportunities for two graduate students (Brendan Heffenan and Omkar Supekar) at the University of Colorado Boulder, one undergraduate at the University of Denver (Drew Voitiv) and one research scientist at the University of Colorado Denver Anschutz Medical Campus (Dr. Stephanie Meyer). Dr. Meyer taught a lab section and gave a lecture on STED for a combined undergraduate/graduate course (BIOE4053/5053) with 15 students composed of neuroscience students and bioengineers. We have submitted a conference paper on our two-photon STED to the Conference on Lasers and Electro-Optics 2021.

Teaching **In January 2020, PI Gopinath also launched a for-credit online Coursera course titled Active Optical Devices, which includes light emitting diodes, semiconductor lasers, integrated photonic detectors, including avalanche photodiodes, and displays. The course content can be viewed free of charge. The class covers important topics that are critical to understand for researchers building devices and lasers to implement practical quantum technology. Additionally, the course will allow working professionals and those in third-world countries without the opportunity to attend a University in person, an opportunity to learn high-quality technical material.**

Dr. Stephanie Meyer continues to organize an Advanced Microscopy Techniques Journal Club on the CU Denver, Anschutz Medical Campus that includes participation by students/faculty at CU Boulder and University of Denver. The Journal Club meets monthly to disseminate STED microscopy and other recent microscopy advancements to the campus microscopy community. These types of dissemination efforts will be ongoing

and have already been extremely successful in encouraging more users and interest in STED microscopy.

Improving the Climate for Undergraduate and Graduate Students **PI Gopinath is currently chairing the Climate Committee for her department, tasked with improving relations between students, faculty and staff. Isolation and imposter syndrome have been identified as primary problems for both undergraduate and graduate students. To combat this, she is arranging a series of seminars on the topics.**

Commitment to Diversity **PI Gopinath's climate committee also rewritten the inclusive excellence statement for her department along with a code of conduct and reporting to make sure that there is a culture of inclusion, diversity and respect. Also, Professor Gopinath served as the faculty advisor for the Women in ECEE student group, recruiting and hosting guest speakers and social hours. The group is hosting an African American professor emeritus, Brenda Allen, who will speak on diversity.**

Outreach **Before COVID-19 disrupted summer plans, PI Gopinath had committed to teaching part of a high school summer electromagnetics course for under-represented students. She has served as the faculty advisor for the course over the past decade. Additionally, the Gopinath group recently produced a video that can be found here (http://ecee.colorado.edu/~julietg/outreach.html), about light and color for a workshop with two third-grade Boulder school district science classes. Her group also participates in the CU Science Discovery Engineering Family Day, attended by over 2500. She brings demos of orbital angular momentum to expo.**

Professor Siemens incorporated light science outreach into his fall 2020 freshman seminar course, culminating in students making their own STEM-themed videos that were distributed to K-5 students at a Denver Public Schools elementary. Each student built their own hands-on demonstration and designed a curriculum to engage with the first-graders and build their curiosity and interest in science. These demonstrations featured fluorescence, imaging, and optical fiber. Additionally, Professor Siemens is the faculty advisor of the University of Denver's Society of Physics Students (SPS) group, and he provides encouragement, training, resources, and organization to support the SPS's outreach efforts. Before covid-19 disrupted the last year's outreach plans, he was working with SPS students to develop new hands-on demonstrations to highlight optical fiber and imaging science for use in K-12 and general public demos (including a scheduled event at Elitch Gardens, Denver's premiere amusement park).

Additional documentation:
(Additional documentation may include additional artifacts, reports, or content that should be included as an appendix or addendum to the content supplied in this form.)

None

University of Colorado – Boulder

Project Name: QLCI - CI: NSF Quantum Leap Challenge Institute for Enhanced Sensing and Distribution Using Correlated Quantum States
Primary Investigator: Jun Ye
Description and Progress in 2020:

Quantum Sensing and Measurement both underlie the ultimate success of, and leverage advances in, quantum simulation, quantum computing, and quantum networking. The proposed NSF Quantum Leap Challenge Institute, led by the University of Colorado Boulder, includes extensive collaborations with leaders from other academic institutions in the US and Europe, NIST, National Laboratories, and industry to make broad, fundamental advances in quantum science and engineering. The aim is to demonstrate and leverage quantum advantages in state-of-the-art quantum sensing across the field. The Institute is designed for core integration of research with education and workforce development. It will explore multiple outstanding problems in science and technology, create new quantum platforms and insights, and translate novel technology into transportable systems engineered for practical application. A workforce development component includes designing and establishing quantum science and engineering programs for faculty at community colleges, industry professionals, and academic trainees at multiple levels.

The Institute will strengthen and expand collaborations in quantum science and engineering among world-leading national laboratories and academic institutions in the US and Europe to attack grand challenges at the quantum frontier and build a quantum infrastructure so important nationally. This was awarded and just began ramping up in the last quarter of 2020. Although progress on the award is moving forward, the anticipated expenses covered by the first year CHECRA funds will take place after this reporting period.

Appendix D

Engineering Research Center Reinvention of the Nation's Urban Water Infrastructure (ReNUWIt)
Colorado School of Mines
CHECRA Grant: $400,000 (per year for 10 years, renewed)
Reporting Period: January 1 - December 31, 2020

Summary: The Engineering Research Center (ERC) for Reinventing the Nation's Urban Water Infrastructure (ReNUWIt) at the Colorado School of Mines, under the leadership of Dr. John E. McCray, is a collaborative effort among four research universities: CSM, Stanford University, University of California at Berkeley, and New Mexico State University. The ERC was established on August 1, 2011 and is the first center to focus on civil infrastructure ever funded by the National Science Foundation.

Cities are facing a mounting water crisis from population expansion, ecosystem demands, climate change, and deteriorating infrastructure that threatens economic development, social welfare, and environmental sustainability. ReNUWIt's vision is to facilitate the transition of existing water supply systems, urban flood control, and wastewater treatment to a new state that will enhance the security and economic vitality of the nation's cities. Accordingly, the goal of this ERC is to advance new strategies for water/wastewater treatment and distribution, develop modular technologies and concepts, and prepare students to lead efforts to reinvent urban water infrastructure.

Description of the project, the principal persons or entities involved in the project, and the amount of funding allocated to each principal person or entity

To meet the challenges of reinventing urban water infrastructure, ReNUWIt has three research thrust areas defined as follows:
(1) **Urban Systems Integration and Institutions:** Support the reinvention and restoration of urban water systems through the development of decision-making tools that enable sound decision making about future investments in urban water infrastructure;
(2) **Efficient Engineered Water Systems:** Develop new, modular technologies to overcome barriers that prevent wider application of existing by underutilized technologies and collecting data on technical performance;
(3) **Natural Water Infrastructure Systems:** Develop technologies for managing natural systems to treat and store water while simultaneously improving urban aesthetics, with focus areas in stormwater treatment for beneficial use and groundwater recharge.

Water resource planners are hesitant to integrate new types of engineered treatment systems into their water portfolio due to uncertainties about cost, reliability, public health risks, and overall impacts on system performance. Thus, a mechanism for technology assessment is needed at scales ranging from the laboratory to the full-scale service area. Such capabilities do not exist and as a result, many good ideas are not brought into practice. To facilitate the integration of new technologies into urban water systems,

tools like life-cycle assessment for decision-making are being advanced as well as conducting research and implementation of engineered systems. The strategic research plan continues to evolve in response to research outcomes, supplemental funding opportunities, and new information related to achieving ReNUWIt's overarching goals.

Within the *Urban Systems Integration and Institutions* thrust, research focuses on the development of integrated regional water models. The goals of the thrust area are to: (i) develop integrated decision support systems for utility planning; (ii) develop integrated visioning, assessment, and implementation tools for regional and municipal water planning; and (iii) identifying "technology diffusion pathways" to increase the likelihood of technology implementation. Mines is examining the legal, economic and technical feasibility of beneficial use of stormwater in a redeveloping neighborhood in northwest Denver (Berkeley neighborhood) including a method to project increases in impervious areas and the subsequent impact to stormwater flows and quality.

The goal of the *Efficient Engineered Systems* research thrust is to characterize the viability of existing but underutilized technologies at different scales by assessing their economic, environmental, and social costs and benefits. The specific aims of this thrust are: (i) develop improvements to energy and resource recovery from existing municipal wastewater systems; (ii) develop or asses new processes, approaches, and practices that support direct potable reuse of municipal wastewater; and (iii) advance (i) and (ii) to pilot-scale and full-scale demonstration and adoption. Research at Mines has incorporated smart system controls to monitor/ model/ optimize the hybrid sequencing batch-membrane bioreactor (SB-MBR) system operation for nutrient management (e.g., tailored water management).

The thrust area on the use of *Natural Water Infrastructure Systems* brings a much-needed quantitative approach to an area that has not previously been subjected to rigorous engineering analysis. The realigned goals of the thrust area are to: (i) develop novel approaches for manipulating subsurface natural system unit processes to predictably enhance stormwater and treated wastewater qualities; (ii) identify new ways of designing and operating unit process to maximize water quality and flood protection while enhancing function and aesthetics; and (iii) deploying sensors and actuators for real-time control and management of processes. Research at Mines is advancing passive treatment of stormwater through bioinfiltration systems and the hyporheic zone in streams.

Within the ReNUWIt framework described above, twelve projects were funded in part by CHECRA in 201:

- Feasibility for Beneficial Use of Stormwater in Denver (U2.5);
- Long-term Sustainability of Stormwater Technologies (U2.13), joint with Colorado State University;
- Predicting Urban Water Demand for Infill and Redevelopment in Denver (U2.15);
- Reclaiming Energy from Wastewater using Anaerboic Digestion (E2.4);
- Tailoring Water Reclamation for Specific Purposes (E2.9, formerly E1.1);
- Chemical valorization of Energy from BioWaste (E2.12);
- Phosphorus Recovery in Existing Wastewater Treatment Facility Infrastructure (E2.16);

- Alternative Potable Reuse Treatment Trains (E3.4);
- Smart Engineered Wetlands (N1.2);
- Stormwater Infrastructure for Water Quality (N3.3); and
- Engineering Streambeds for Water Quality Improvement (N3.4).

The table below lists project funding per project by the primary lead for each project, although several projects are co-led, as annotated below**.**

Principal Investigators	Funding from CHECRA
John McCray, CSM Principal Investigator, ReNUWIt Center Lead Project Lead, Feasibility of Beneficial Stormwater Use in Denver, U2.5 (Terri Hogue is co-lead), Collaboration with City of Denver Project Lead, Long-term Feasibility of Stormwater Technologies, U2.13, collaboration with CSU and City of Fort Collins Project Lead, Engineering Streambeds for Water Quality Improvement, N.3.4 (Chris Higgins is co-lead)	**$61,758** **$70,022** **$79,617**
Tzahi Cath Project Lead, Tailoring Water Reclamation for Specific Purposes, E2.9	**$30,795**
Linda Figueroa Project Leads, (Figueroa) Novel Phosphorus Extraction/Recovery in WWTF, E2.16, Collaboration with Metro Wastewater Reclamation Authority	**$21,884**
Linda Figueroa and Junko Munakata Marr Project Leads: Reclaiming Energy from Wastewater using Anaerboic Digestion, E2.4, Collaboration with South Platte Renew, a wastewater treatment facility in southwest Denver metro area.	**$94,680**
Timm Strathmann, Hydrothermal Technologies to Valorize Biologically Tailored Wastewater Solids, E.2.12, Collaboration with NREL	**$22,363**
Christopher Higgins Project Lead, Stormwater Infrastructure for Water Quality, N3.3, Collaboration with Colorado School of Mines and Geosyntech, Inc.	**$89,454**
Terri Hogue Project Lead, Predicting Urban Water Demand in Denver, U2.15, Collaboration with Denver Water	**$44,767**
Jonathan Sharp Project Lead, Smart Engineered Wetlands, N1.2, Collaboration with CSU and Orange County CA.	**$43,564**
Christopher Bellona, E3.4, Innovative Potable ReUse	**$19,530**
TOTAL SPENDING (Jan-Dec 2019)	***$582,468***

Within the ReNUWIt projects (2019), full or partial support was provided to:

- 3 Post-doctoral Researchers
- 7 Doctoral students
- 5 Master's of Science Thesis students
- 16 Hourly Undergraduate and Non-thesis MS students
- 8 REUs ~ Mines undergraduates conducting research
- 2 Research Staff
- 9 Faculty ~ 1 Assistant Professor; 2 Associate Professors; and 6 Professors

The manner in which each principal person applied the CHECRA funding in connection with project results

John McCray, Professor: Discretionary center funding for supporting new research directions. In support of the Denver Beneficial Stormwater Use project (U2.5) CHECRA funding supported partial salary support for Dr. McCray, partial support for one post-doctoral researcher, tuition, stipend and nominal materials for one M.S. student, three undergraduate and one non-thesis MS student to assist with frameworks and technical research for the following purposes: (a) promote data-based decision making with regarding to stormwater quality control for urban development, and (2) to overcome policy and legal barriers to allow stormwater beneficial use . This work lead to a separate research directive focused on the evaluation of the long-term feasibility and sustainability of stormwater technologies (U2.13), which is a collaboration with the NSF UWIN center at Colorado State University and the City of Fort Collins. In support of U2.13, CHECRA funding supported tuition and stipend for one PhD student.

One PhD student was supported for field scale testing and implementation of engineered urban streambeds for water quality enhancement thru BEST (N3.4). As an outcome of this work, Dr. McCray secured a partnership with the City of Golden, to engineer streambeds in stormwater channels to improve water quality. Mines and Golden jointly received a Proof of Concept (POC) Innovation grant, awarded by an external technical advisory board of Colorado business entrepreneurs.

Tzahi Cath, Associate Professor: Funding for one PhD student focused on SB-MBR energy optimization and tailored non-potable reuse of treated wastewater (E2.9). The goal is to use treatment systems that are tailored to provide specific water quality needed for specific non-potable tasks, which should be more cost efficient than treating to near drinking water standards, the traditional approach for traditional urban treatment plants. This research is leveraged with a PhD student and materials supported by NSF funds.

Linda Figueroa and Junko Munakata Marr, Professors: CHECRA funds supported one graduate student and one hourly undergraduate student on E.2.4, working on novel energy and nutrient recovery from wastewater using anaerobic digestion techniques in collaboration with South Platte Renew, a wastewater treatment utility for cities in southwest Denver metro area CHECRA funds supported tuition for two graduate students and one hourly undergraduate student working on novel phosphorus recovery within existing wastewater treatment facility infrastructure (E2.16) at Metro Water Reclamation District (MWRD). Both graduate students on E.2.16 are currently employed with MWRD and are expected to directly implement research findings at the District. Outcomes from this work have transformational changed in the current wastewater treatment paradigm. Partial salary was provided for Drs. Marr and Figueroa for research oversight.

Christopher Higgins, Associate Professor: Partial salary support for Dr Higgins for his leadership role as N-Thrust Leader and leader of N3.3. One undergraduate student supported work with the City of Denver to develop of a field site in partnership with the City of Fort Collins and also on Colorado School of Mines campus for pilot scale testing of BioCHARGE (N3.3). A post-doctoral researcher was also partially supported (20%) to help with the BIOCHARGE system in the City of Fort Collins.

Terri Hogue, Professor: One PhD student was fully supported for remote sensing to help understand factors affecting urban water use and projecting changes to water demand in Denver (U2.15) in collaboration with Denver Water. The broad goals this effort is to develop high-resolution remote sensing methodologies to help predict water use and manage water conservation.

Chris Bellona, Assistant Professor, received partial funding to support one PhD student and some undergraduate researchers for his project on direct potable reuse (E.3.4).

Jonathan Sharp, Associate Professor: Partial faculty salary support was provided for Dr. Sharp for his leadership roll as the Diversity and Inclusion co-Director for ReNUWIt across all partner institutions, as well as for implementing an engineered treatment wetland at the Mines Park Test site on Mines Campus. CHECRA funds also supported undergraduate researchers working on an hourly basis. NSF supports a graduate student on this project.

Timm Strathmann, Professor, received general center support for ReNUWIt project E2.12 (Application of hydrothermal technologies to valorize biologically tailored wastewater biosolids). This project focuses on advancing hybrid biological-thermochemical technologies for recovering economically valuable products from wastewater biosolids (i.e., valorizing the waste). Working closely with collaborators at the National Renewable Energy Laboratory (NREL), located in Golden, CO, we are examining multiple process pathways for producing propylene, a billion dollar chemical intermediate, from biosolids. This product has much greater financial potential than the conventional biogas product from anaerobic digestion of wastewater sludge. Two Mines PhD students, funded by non-CHECRA sources, work in laboratories at both Mines and NREL to identify stable solid acid catalyst formulations that are active for breaking down microbial products and upconverting the resulting acid monomers into propylene. The work also serves as a vehicle for inclusion of undergraduate student researchers in the state of Colorado (2 participated this past year). This work supports both the missions of ReNUWIt (Transforming the way we manage urban water infrastructure systems) and NREL (advancing the science and engineering of energy efficiency, sustainable transportation, and renewable power technologies).

Results Achieved

Results are summarized in this section. Publications and other research products are summarized near the end of this report.

Results from the *Urban Systems Integration and Institutions* thrust continued to focus on stormwater planning, management and treatment. In partnership with the City and County of Denver (U2.5), the technical, legal, policy and social barriers are being evaluated to enable beneficial use of stormwater runoff in the rapidly re-developing aeras. Modeling and stormwater quality sampling is being conducted for Denver to inform proposed new regulations for infill redevelopment in the City to promote and enable data-based decision making. This work involves monitoring water quality during storm flows and dry weather flows in Denver. The goal is to help the city to understand whether real data, and subsequent data-based decision making, is better than traditional decision-making processes related to urban water quality and potential new regulations for new infill development. For the State of Colorado, we worked with the Colorado Water Conservation Board (CWCB) and the State Engineer's office (SEO) to

develop new policy to enable increased stormwater runoff from infill development to be utilized for beneficial use. Mines received a $50,000 grant from the National Science Foundation (NSF) to provide an internship for PhD student Ryan Gilliom with the CWCB and Colorado SEO to work on innovative policy to enable stormwater beneficial use. This work was recently codified into law by the Colorado legislature. In addition, Professor McCray received a $60,000 grant from NSF to fund stakeholder workshops in the front range to brainstorm overcoming barriers to implementing beneficial stormwater use in the Front Range. A new grant from City and County of Denver ($40,000) on urban stormwater quality is in the works. McCray received a $50,000 grant from NSF to look at urban water quality during COVID-19 with a goal of understanding how future sustainable living strategies, that involve much less traffic, impact water quality. McCray and a Mines graduate student are also working with a graduate student and professor at the UWIN Sustainability Center at Colorado State University, evaluating the sustainability of innovative new green stormwater infrastructure developed by ReNUWIt and CHECRA funding relative to traditional stormwater infrastructure. Work by professor Hogue in U.2.15 aims to use remote sensing techniques to better understand greening (largely from urban irrigation) across the city, and to elucidate the technical and socio-economic factors that impact outdoor water use. This project was in collaboration with Denver Water. Results from this project should be useful in developing remote sensing techniques to predict water use for various development scenarios, and also to implement and track new water conservation programs. Ultimately, work in this Thrust area resulted in an EPA STAR grant of $2MM to create decision support tools for stormwater green infrastructure.

Results from the *Efficient Engineered Systems* research thrust continued to rely on field research on the Mines campus utilizing sequencing batch membrane bioreactor treatment of wastewater from housing at Mines (~7,000 gal/day), as well as pilot scale projects at the Metro Water Reclamation District utility in the Front Range (described in more detail below) and with the South Platte Renew, a wastewater utility in southwest metro Denver area (see below). The demonstration-scale treatment unit at Mines Park allows effluent qualities to be tailored to various reuse applications (i.e., urban landscape irrigation; streamflow augmentation; groundwater recharge) and continues to be supported through collaborations with manufacturers and start-up companies within Colorado. Identifying mechanisms (E2.9) by which Phosphorus recovery can efficiently be achieved while lowering energy consumption is beneficial both from an energy resource standpoint and an economic perspective. Alternatively, E2.9 also investigates strategies for optimization of generating on-demand effluent qualities with elevated levels of nitrogen while simultaneously optimizing energy demands continue.

Our demonstration scale project titled “Coupled Hybrid Anaerobic Reactors for Generation of Energy (CHARGE)” have been operating at the Plume Creek Water Reclamation Authority (PCWRA) in Castle Rock for 7 years to evaluate the long-term viability of generating energy from wastewater. The Mines team is now working with South Platte Renew, a wastewater utility in southwest metro Denver area. The project has a focus on enabling small utilities to make use of an anaerobic treatment process to generate methane that can be used for energy while eliminating the need for aeration.

The results from primary anaerobic treatment have led to additional investment by NSF ($329K) and Water Environment Research Foundation (106K).

A project to evaluate phosphorus extraction/recovery schemes and pilot scale implementation within existing wastewater treatment facility infrastructure was started in 2017 (E2.16). This project is part of an overall goal to recover valuable resources of energy and nutrients, particularly phosphorus, from wastewater. Metro Wastewater Reclamation District (District) is currently undergoing extensive upgrades to the Robert W. Hite Facility (RWHTF) to meet increasingly stringent nutrient regulations, particularly focused on effluent discharge phosphorus concentrations. Enhanced biological phosphorus removal (EBPR) is a sustainable and cost effective means to remove phosphorus from the liquid stream, however the process has been shown to negatively impact other process areas in both performance and cost. As a result, the District has continued developing near-term and potential long-term phosphorus management options, harnessing the experience of industry leaders and university expertise to make informed infrastructure and operating strategy decisions that best serve the 1.8 million Denver Metro area ratepayers. This project research will evaluate EBPR for improvements and optimization to maintain low effluent phosphorus concentrations while improving the effectiveness and efficiency of the RWHTF in other areas.

Our research on novel and efficient direct potable reuse (E.3.4) is geared toward more efficient treatment of wastewater that can be delivered directly as potable water has potential to change our current water paradigm, resulting in more localized water use, and reducing energy required to deliver water. This project has resulted in additional funding from U.S. Bureau of Reclamation and WateReuse Foundation.

Results from the *Natural Water Infrastructure Systems* thrust continued to focus on treating polluted stormwater or wastewater from urban settings using smart, engineered natural systems. For example, upscaling for field testing at the field scale of modules termed “Biohydrochemical Stream Water Treatment (BEST)” continued (N3.4). We received the final Patent for the BEST in 2020. The BEST system was employed at a site by the City of Golden to mitigate stormwater runoff pollution. We are working with Golden to implement a second site. Mines received funding from the State of Colorado Innovation program to work with Golden. To our knowledge, this was the first such grant given to an environmental-water project. A BEST system was also installed in the City of Aurora by a private contractor. Researchers from University Cork in Cork Ireland are interested in conducting research on BEST systems for improvement of agricultural runoff water. A geomedia stormwater infiltration system (BioCHARGE) was installed by the City of Denver at Cuernavaca Park for removal of dry-weather urban drool pollutants (N3.3). Systems were also installed by the City of Fort Collins and by Colorado School of Mines An outcome from this work was the successful DoD SERDP award ($491K; 2018 - 2020) to improve BMP stormwater treatment designs to prevent sediment recontamination. A new BIOCHARGE system has been installed in the streets of Fort Collins, in collaboration with the City of Fort Collins and the Colorado State University Stormwater Center.

Summary of Benefits to the State of Colorado

- Received $171,880 NSF core funds in 2020. These funds in combination with CHECRA funds ($400,000) and $82,500 CSM matching funds supported projects as stated above. The total funding from NSF and CHECRA has funded:
    - 46 graduate students (MS thesis and PHD tuition and stipend) in the first 9.5 years of ReNUWIt (2011-2019) with degrees in Civil & Environmental Engineering, Environmental Engineering Science, and Hydrologic Science and Engineering. Women comprised ~40% of these graduate students.
    - Research experiences for 52 Mines undergraduates where 55% of these students are female and 22% are other under-represented minorities.
- Continued collaboration with the City and County of Denver, the Urban Drainage and Flood Control District (UDFCD) to predict changes in stormwater management due to urban infill and development.
- A new collaboration has been approved working with the City and County of Denver's Department of Environment and Public Health and with Geosyntech engineering to install innovative infrastructure in the city to remove stormwater quality effluent to streams.
- Continued collaboration with Southeast Metro Stormwater Authority (SEMSWA) to develop methods to recovery energy from wastewater using anaerobic digestion, while at the same time saving energy by removing a need for aeration. This focuses on smaller utilities that need more help with cost-saving in their engineered design, and could eventually be adopted by numerous small utilities across the state.
- Continued collaboration with Metro Wastewater Reclamation District and Carollo Engineers investigating potential energy savings and treatment efficiencies associated with alterations in treatment plant operation for Phosphorus removal. Given new phoshorus controls implemented by the state of Colorado in response to concerns over lead in aging water-delivery pipes, we expect this project to have a significant impact on all water and wastewater treatment plants in Colorado.
- A second biohydrochemical enhancements for streamwater treatment (aka, BEST) pilot channel is being constructed with support from the City of Golden as well as from the State of Colorado Innovation Fund through a competitive grant process. In addition, BEST modules were installed in the City of Aurora CO.
- A new BIOCHARGE stormwater quality enhancement technology was installed near the intersection of Mountain and Walnut streets in Fort Collins. This work is s a collaborative effort between Mines, CSU, and the City of Fort Collins.
- A new Biocharge unit was installed in a parking garage on Colorado School of Mines parking garage.
- Research to valorize waste biosolids into valuable plastic-like products has shown promising results. This is a joint effort between Mines and NREL.
- Continued success obtaining new research grants at Mines to broaden the design and implementation of ReNUWIt developed treatment systems and approaches. These grants will support graduate and undergraduate students, many of which are expected to enter or remain in the Colorado workforce.
- Bi-monthly seminars organized and sponsored by the ReNUWIt students. Seminar speakers and topics include a range of student research, industry partners, and experts.
- The collaboration continues between ReNUWIt at Mines and the Urban Water Innovation Network (UWIN), an NSF Sustainability Research Network (SRN), at Colorado State University continues. A student and a faculty member at Mines is working with a student and two faculty members at CSU to evaluate sustainability of

ReNUWIt water green infrastructure (GI) technologies compared to traditional GI technologies.

- An engineered treatment wetland was installed on Mines campus to test effictiveness in Colorado climates.
- A new water treatment technology research Hub called WE^2ST, operated by Colorado School of Mines, was opened off campus, in Denver near I-70 and Quebec Street. This center was largely conceptualized and made possible by ReNUWIT and CHECRA research and funding.
- Numerous front range water professionals came to Mines to give talks and workshop at the invitation of ReNUWIt, particularly in the Environmental Engineering Seminar Series and the ReNUWIt student group (SUWIR) seminar series.
- Several outreach efforts are ongoing, including with Shelton Elementary in Golden, Lakewood High School, and numerous children's camps. Highlights include the Shelton Elementary (K-5) Math and Science Fair, Rocky Mountain Summer Camp for Dyslexic Kids.

Publications in 2020 (funded wholly or in part with CHECRA funds) not on last report:

Thesis and Dissertations:

Still waiting for faculty to report.

Publications:

Bell, C.D., Wolfand, J. M., Hogue, T.S. 2020 Regionalization of Default Parameters for Urban Stormwater Quality Models, *JAWRA Journal of the American Water Resources Association* 56 (6), 995-1009

Blount, K., Ruybal, C.J., Franz, K.J., Hogue, T.S. 2020. Increased water yield and altered water partitioning follow wildfire in a forested catchment in the western United States*, Ecohydrology* 13 (1), e2170

Boehm, A., C.D. Bell, C.D., N.J. M. Fitzgerald, E. Gallo , C. P. Higgins , T.S. Hogue, R.G. Luthy , A. C. Portmann, B.A. Ulrich, J.M. Wolfand, 2020. Environ. Sci.: Water Res. Technol.**6**, 1520-1537; DOI: 10.1039/D0EW00027B (Critical Review)

Fang, Y., Vanzin, G., Cupples, A.M., Strathmann, T.J. Influence of terminal electron-accepting conditions on the soil microbial community and degradation of organic contaminants of emerging concern, *Science of The Total Environment* 706, 135327

Gallo, E.M., Bell, C.D., Panos, C.L., Smith, S.M., Hogue, T.S. 2020. Investigating tradeoffs of green to grey stormwater infrastructure using a planning-level decision support tool, Water 12 (7), 2005

Gallo, E., Bell, C., Mika, K., Gold, M., Hogue, T.S. Stormwater Management Options and Decision-Making in Urbanized Watersheds of Los Angeles, California, *Journal of Sustainable Water in the Built Environment* 6 (2), 04020003

Garcia-Chevesich, P., García, V., Martínez, G., Zea, J., Ticona, J., Alejo, J., Vanneste, J., Acker, S., Vanzin, G., Malone, A., Smith, N., Bellona, C., Sharp, J.O. Inexpensive Organic Materials and Their Applications towards Heavy Metal Attenuation in Waters from Southern Peru, Water 12 (10), 2948

Garcia-Chevesich, P., García, V., Martínez, G., Zea, J., Ticona, J., Alejo, F. Inexpensive Organic Materials and Their Applications towards Heavy Metal Attenuation in Waters from Southern Peru, Water 12 (10), 2948

Gilliom, R., Bell, C., Hogue, T.S., McCray, J.E., 2020. Adequacy of Linear Models for Estimating Stormwater Best Management Practice Treatment Performance, ASCE J. Sustainable Water in the Built Environment, 6(4), https://doi.org/10.1061/JSWBAY.0000921

Huo, X., Vanneste, J., Cath, T.Y., Strathmann, T.J., A hybrid catalytic hydrogenation/membrane distillation process for nitrogen resource recovery from nitrate-contaminated waste ion exchange brine, *Water Research*, *175* (2020) 115688.

Huo, X., Vanneste, J., Cath, T.Y., Strathmann, T.J. A hybrid catalytic hydrogenation/membrane distillation process for nitrogen resource recovery from nitrate-contaminated waste ion exchange brine, Water research 175, 115688

Klanderman, M.C., Newhart, K.B., Cath, T.Y., Hering, A.S., Case studies in real-time fault isolation in a decentralized wastewater treatment facility, *Journal of Water Process Engineering*, 38 (2020) 101556.

Klanderman, M., Newhart, K.B., Cath, T.Y., Hering, A.S., Fault isolation for a complex decentralized wastewater treatment facility, *Journal of the Royal Statistical Society,* 69 (2020) 931-951.

Lucio, D., Pfluger, A., Callahan, J., Van Houghton, B., Munakata-Marr, J., Figueroa, L. From poop to gold: an examination of energy-positive wastewater treatment in an anaerobic reactor system, Mountain Scholar.org, Colorado School of Mines. Arthur Lakes Library

Maltos, R.A., Holloway, R.W., Cath, T.Y., Enhancement of activated sludge wastewater treatment with hydraulic selection, *Separation and Purification Technology*, 250 (2020) 117214.

McCray, J.E., 2020. Pollutant transformations and residence times in engineered hyporheic zones of urban waterways, Keynote Lecture at Conferencia de Especialidad en Recursos Hídricos en el Valle Central de Chile, Universidad Catolica Del Maule, Talca Chile, 5 March

Newhart, K.B., Marks, C.A., Rauch-Williams, T., Cath, T.Y., Hering, A.S., Hybrid statistical-machine learning ammonia forecasting in continuous activated sludge treatment for improved process control, *Journal of Water Process Engineering*, 37 (2020) 101389.

Panos, C.L., Wolfand, J.M., Hogue, T.S. 2020. SWMM Sensitivity to LID Siting and Routing Parameters: Implications for Stormwater Regulatory Compliance, *JAWRA Journal of the American Water Resources Association* 56 (5), 790-809

Phanwilai, S., Kangwannarakul, N., Noophan, P.L., Kasahara, T., Terada, A., Munakata-Marr, J., Figueroa, L. Nitrogen removal efficiencies and microbial communities in full-scale IFAS and MBBR municipal wastewater treatment plants at high COD: N ratio, *Frontiers of Environmental Science & Engineering* 14 (6), 1-13

Regnery, J., Li, D., Lee, J., Smits, K.M, Sharp, J.O. Hydrogeochemical and microbiological effects of simulated recharge and drying within a 2D meso-scale aquifer, *Chemosphere 241, 125116*

Sedlacko, E.M., Chaparro, J.M., Heuberger, A.L., Cath, T.Y., Higgins, C.P., Effect of produced water treatment technologies on irrigation-induced metal and salt accumulation in wheat (Triticum aestivum) and sunflower (Helianthus annus), Science of the Total Environment, 740 (2020) 140003.

Spahr, K.M, Bell, C.D, McCray J.E., Hogue, T.S., 2020. Greening up stormwater infrastructure: Measuring vegetation to establish context and promote co-benefits in a diverse set of US cities, Urban Forestry & Urban Greening, 48, https://doi.org/10.1016/j.ufug.2019.126548

Wu, B., Hao, S., Choi, Y., Higgins, C.P., Deeb, R., Strathmann, T.J. Rapid destruction and defluorination of perfluorooctanesulfonate by alkaline hydrothermal reaction*, Environmental Science & Technology* Letters 6 (10), 630-636

Sorting and Impurity Removal to Improve the Recycling of Steel Scrap from Auto Shredders

Final Report for REMADE Project: 18-01-RR-16

Prepared by: Patrick R. Taylor, Colorado School of Mines

August, 2020

Appendix E

*Acknowledgment: "*This material is based upon work supported by the U.S. Department of Energy's Office of Energy Efficiency and Renewable Energy (EERE) under the Advanced Manufacturing Office Award Number DE-EE0007897."

This document does not contain any proprietary information.

The REMADE Institute Statement

This report documents research that was conducted by Colorado School of Mines under a cost-shared subrecipient contract with the REMADE Institute.

The objective of this project is to overcome the barriers that currently limit the use of recycled steel (as recovered from scrap streams) in new steel products, including i) the inability to identify and sort steel scrap in an automated way, ii) the inability to efficiently separate Cu from steel scrap using post-shredder technologies.

Principal Investigator: Patrick R. Taylor, Colorado School of Mines

REMADE Project Manager: Ed Daniels

The REMADE Institute project number is 18-01-RR-16

The REMADE Institute—a $140 million Manufacturing USA Institute co-funded by the U.S. Department of Energy—was launched in January 2017.

In partnership with industry, academia, trade associations, and national laboratories, REMADE will enable early-stage applied research and development of technologies that could dramatically reduce the embodied energy and carbon emissions associated with industrial-scale materials production and processing. The REMADE Institute is particularly focused on increasing the recovery, reuse, remanufacturing, and recycling (collectively referred to as Re-X) of metals, fibers, polymers, and electronic waste (e-waste).

By focusing our efforts on addressing knowledge gaps that will eliminate and/or mitigate the technical and economic barriers that prevent greater material recycling, recovery, remanufacturing and reuse, REMADE seeks to motivate the subsequent industry investments required to advance technology development that will support the U.S. manufacturing eco-system.

The REMADE Institute is committed to accelerating the adoption of sustainable innovations that will expand the circular economy.

The REMADE Institute - Accelerating the Circular Economy

www.remadeinstitute.org

Colorado School of Mines Statement

The Colorado School of Mines conducted cost-shared research to overcome the barriers that currently limit the use of recycled steel (as recovered from scrap streams) in new steel products, including i) the inability to identify and sort steel scrap in an automated way, ii) the inability to efficiently separate Cu from steel scrap using post-shredder technologies.

The Principal Investigator for the project is: Patrick R. Taylor, Colorado School of Mines

The Project Team included: Sridhar Seetharaman, Colorado School of Mines

Erik Spiller, Colorado School of Mines

Zhijiang Gao (Ph.D. Student), Colorado School of Mines

Funding for this project was provided by the REMADE Institute with cost-share provided by the State of Colorado

Our industrial partners that provided samples are: Western Metals recycling, Englewood, Colorado and SSAB-USA, Muscatine, Iowa

Acknowledgement:

Table of Contents

List of Tables

List of Figures

Acronyms, Abbreviations, and Definitions

EAF - Electric Arc Furnace

GJ - GigaJoule

PJ - PetaJoule

LIBS - Laser-induced Breakdown Spectroscopy

XRT - X-ray Transmittance

XRF - X-ray Fluorescence

PGNAA - Prompt Gamma Neutron Activation Analysis

WMR - Western Metals Recycling

AAS - Atomic Absorption Spectrometry

CNNs - Convolutional Neural Networks

$W_{Fe\ Shreds}$ - Weight of Fe Shreds from Sample 1

$C_{Background\ Cu}$ - Background (Alloyed) Cu Content (wt%) of Sample 1

$W_{Cu\ Sources}$ - Weight of Identified Cu Sources from Sample 1

VGG - Visual Geometry Group

ReSNet - Residual Neural Network

IF Steel - Interstitial Free Steel

Executive Summary

Understanding steel scrap recycling and Cu impurities

The 1-year exploratory research is aimed at carrying out a preliminary study to pursue research to overcome the existed technical gaps that would weaken the use of recycled steel due to contaminants that downgrade the value of the steel by limiting the range of products in which the recycled steel can be used. It is linked to the use of scrap in EAF steelmaking, but with the intention to enable more value-added products. This is because contaminants such as Cu, accumulated in the scrap through wires and motors in cars and tin-plate, cause surface cracking when the produced steel is processed in hot and oxidizing conditions, during secondary cooling from the continuous caster or reheating for thermo-mechanical processing. The cracking phenomenon is referred to as surface hot shortness and occurs at 0.1wt% Cu content or greater. The mechanism for this detrimental effect is the enrichment of Cu leading to a separate liquid Cu-enriched phase which penetrates the austenite grain boundaries. Worldwide speaking, about 75% of metal in the charge of an EAF is comprised of steel scrap, while the remaining is typically virgin pig iron, DRI/HBI and other hot metal.

The occurrence of Cu impurities such as motors and wires in steel scrap charged to EAF could be attributed to the upstreaming liberation. Conventional hammer mill shredding followed by magnetic separation is commonly implemented in most automobile recycling plants. Dismantling of Cu motors and wires would be just confined to units with larger sizes considering the costs and benefits. During hammer mill shredding, smaller copper motors and wires become enmeshed and entangled within Fe shreds, resulting in a decreased separation efficiency in the subsequent magnetic separation. Based on discussions with EAF based steelmakers (e.g. SSAB, Evraz, Nucor, Timken, Hyundai Steel and others) in the US, Europe and South Korea, there is no current industrially implemented technology for removing impurities from auto shredder steel scrap to the levels required for manufacturing value added products such as automotive sheet steel.

Technical effectiveness and economic feasibility of identified potential removal technologies

Through literature review, and engagements with the scrap sorting industry, potential physical and chemical removal technologies have been identified and further investigated for their feasibility.

Methods		Technical Effectiveness	Economic Feasibility
Physical Removal Technologies	Optical recognition improved by machine learning	Based on the completed machine learning experiments, the improved optical recognition could be used to reduce the Cu impurities, especially for Cu motors and wires within magnetically cleaned shredded steel scrap, achieving the 0.1wt% limitation for Cu content.	As analyzed in the literature review and industrial survey, low cost requirement could be satisfied by camera-based sorting sensor for optical recognition, compared to other types of sensor, including LIBS, XRT&XRF, PGNAA, with the use of industrial laser, X-ray, and gamma source, which all need high capital and maintenance cost.
	Blue laser sensor	Laboratory tests demonstrate that Cu and Fe sheets have different performance referring to the thermal conductivity and adsorption.	Compared to LIBS, no ablation is needed for blue laser. The cost would likely be acceptable because of lower beam intensity, though there is

		Cu sheet sample showed a rapid temperature increase and drop compared with the Fe sheet sample. The temperature response for the composite sample was faster than for the single Fe sheet, due to the heat distribution through underlying Cu sheet.	no existing product that applies blue laser as a type of sensor and could be used for comparative cost analysis.
Chemical Removal Technologies	Chlorination with Cl_2-O_2 gas at 800 ^oC	Experimental results demonstrate better effectiveness to remove isolated pieces of Cu impurities, while potential for removing alloyed Cu from steel scrap could still need to be discussed.	Considering the corrosive quality of chlorine gas and flowrate controlling of mixture gas, recycling the unreacted chlorine gas must be required. Also, the oxidation of Fe could not be avoided, leading to the loss of Fe.
	Slagging with FeO-SiO_2-$CaCl_2$ at 1600 ^oC	Experimental results demonstrate better effectiveness to reduce Cu content, no matter what kind of Cu impurities, since this method has been conducted in the molten state.	It is highly desirable with economic feasibility if this technology could be conducted in ladle furnace in order to incorporate into the well-developed steelmaking process.

Benefit to public

EAF-based scrap re-melting would eliminate a large fraction of energy consumption and CO_2 production. Over 80% of energy and CO_2 emissions, 14GJ (and 1560 kg of emitted CO_2) per metric ton of steel, can be eliminated if carbon-based reduction in large integrated steel plants via the blast furnace route are replaced with scrap recycling. A further 2GJ reduction is in-directly achieved outside of the steel plant since the carbon-free process eliminates coke-making and agglomeration, giving in total a 90% reduction in energy (and CO_2) usage. Currently, approximately 34 million metric tons of steel are landfilled in the US. A modest increase (20%) in the recovery of this landfilled steel could result in the replacement of 6.8 million metric tons of primary steel with secondary feedstock. This modest increase would also result in a total savings of 131 PJ.

As a result, the chief industrial beneficiaries are the steel industries through the identification of process and chemistry windows to allow low energy (and CO_2) production of high value steel components using recycled steel scrap. The automotive and construction sectors will benefit since commercially viable sources of metal components / assemblies that could be re-designed to support the principles of the circular economy and have the right technical characteristics for recycling at end of life will be identified. These sectors will also benefit from lower cost steel supply with increased speed of delivery and reduced time to market for new grades. Society will benefit from reduced energy consumptions, lower CO_2 emissions and the manufacture of high-value products from a scrap route in the US and the safeguarding of high value jobs in the steel sector in the United States.

Sorting and Impurity Removal to Improve the Recycling of Steel Scrap from Auto Shredders

REMADE Project: 18-01-RR-16

Introduction

Project Objectives and Benefits

The objective of this project is to overcome the barriers that currently limit the use of recycled steel (as recovered from scrap streams) in new steel products. Currently, the use of recycled steel is limited due to contaminants that downgrade the value of the steel by limiting the range of products in which the recycled steel can be used. These limitations are due to technical gaps which are to be addressed in this exploratory project.

- The inability to identify and sort steel scrap from auto shredders, in an automated way: We will study the composition of steel scrap to determine the amount of copper (Cu) and tin (Sn) that end up in secondary steel that passes onward to steel production. Once identified we will determine the potential for sorting the scrap to reject these metals.

- The inability to efficiently separate Cu and Sn from steel scrap from auto shredders using post-shredder technologies: We will review, identify and evaluate metallurgical ways of removing the impurities, downstream, in the molten state.

The chief industrial beneficiaries are the steel industries through the identification of process and chemistry windows to allow low energy (and CO_2) production of high value steel components using recycled steel scrap. Increases in capacity through increased tolerance to the presence of impurities from recycled scrap will benefit the low energy steel producers in opening new markets. The automotive and construction sectors will benefit since commercially viable sources of metal components / assemblies that could be re-designed to support the principles of the circular economy and have the right technical characteristics for recycling at end of life will be identified. These sectors will also benefit from lower cost steel supply with increased speed of delivery and reduced time to market for new grades. Society will benefit from reduced energy consumptions, lower CO_2 emissions and the manufacture of high-value products from a scrap route in the US and the safeguarding of high value jobs in the steel sector in the United States.

Project Approach

1. Commercially available options and processes in development for sortation of automobile steel scrap will be evaluated to determine if there may be a viable method to remove some of the undesirable impurities prior to feeding to an electric arc furnace. This evaluation will include industry surveys of current practice and literature, patent and vendor surveys. The issues with sortation relate to the size of the material and the mode of occurrence of the impurities in the scrap. If this method for the reduction of impurities is possible, then the amount of primary iron (along with energy use) could be reduced.

2. For the treatment of molten steel containing Cu, and Sn, several alternatives (chemical and metallurgical) will be assessed: a) vacuum distillation b) treatment by reaction with sulfur containing slag and c) other treatment methods. For example, tin sulfide could be precipitated by treating liquid tin-plate with reducing, sulfur containing gases. Coke oven gas could be considered for this, but while Sn could be removed, carburization of the steel might occur. Producing a high carbon melt for recycle to an electric arc furnace could have significant benefits including lower energy consumption. Theoretical concepts and methods of steel scrap purification will be investigated along with details regarding the practical applicability and energy and emissions impacts. This will allow control of alloy composition to closer limits, with the benefit of improving the properties and simultaneously reducing the need for degassing and grain refinement additives.

Project Accomplishments

<table>
<tr><th colspan="2">Goals and Objectives</th><th>Actual Accomplishments</th></tr>
<tr><td rowspan="2">Inability to identify and sort steel scrap from auto shredders</td><td>Study the composition of steel scrap</td><td>(1) Two scrap samples were collected from WMR and SSAB-USA.
(2) Visual Inspection for Cu impurities has accomplished for the scrap sample from WMR and SSAB-USA.
(3) Melting of scrap sample from WMR has accomplished for further AAS analysis.
(4) Detailed characterization of Cu content, including isolated pieces and alloyed Cu, in the scrap sample from WMR has accomplished.
Note:
(1) Since scrap sample from WMR could be more representative after visual inspection, so further experiments just target to scrap sample from WMR.
(2) Sn impurities was not explored in our work.</td></tr>
<tr><td>Determine the potential for sorting the scrap</td><td>(1) Two potential physical sorting technologies have been identified, including: optical recognition improved by machine learning and blue laser sensor.
(2) Initial laboratory tests for blue laser have been conducted and accomplished with pure Cu and Fe sheets to understand its sorting mechanism and feasibility.
(3) Experiments and further optimization for machine learning using CNNs have accomplished with photographs from Cu impurities and Fe shreds, demonstrating good sorting feasibility.</td></tr>
<tr><td rowspan="2">Inability to efficiently remove the impurities using post-shredder technologies</td><td rowspan="2">Review, identify and evaluate metallurgical ways of removing the impurities</td><td>Review: Literature review has accomplished to understand the mechanism of various metallurgical methods of removing the impurities, including Cu, Sn and Zn.</td></tr>
<tr><td>Identify: Since surface hot shortness induced by Cu impurities would be the major problem, so cost analysis of chosen metallurgical methods to reduce Cu content has accomplished based on the standard composition requirement of common steel product. Two</td></tr>
</table>

		potential methods with lower costs, including chlorination with Cl_2-O_2 gas at 800 °C and slagging with FeO-SiO_2-$CaCl_2$ at 1600 °C, have been identified for further experimental evaluation.
		Evaluate: Experiments have accomplished for the identified two methods. (1) Chlorination with Cl_2-O_2 gas at 800 °C: Initial experiments with pure Cu and Fe sheets have accomplished, demonstrating good feasibility to remove isolated pieces of Cu impurities. Initial experiments with Fe-Cu alloy collected from the previous melting experiment have accomplished, demonstrating less potential to remove alloyed Cu. (2) Slagging with FeO-SiO_2-$CaCl_2$ at 1600 °C: Initial experiment with Fe-Cu alloy collected from the previous melting experiment has accomplished, demonstrating good feasibility to reduce Cu content, no matter what kind of Cu impurities, since this method has been conducted in the molten state.

Project Results

Task 1. Review of technologies to remove impurities and characterization of shredder steel scrap

Task 1. Objective

CSM will perform a review of past work and current state of the art by conducting an industry survey and by carrying out a literature and patent search. CSM will then review the results with the aim of identifying viable physical and chemical separations technology. The most promising technologies will be identified for further investigations. Two shredder steel samples will be obtained and characterized. The outputs of this task are 1) a summary of results from an industry survey (Subtask 1.1), 2) a list of academic, trade and patent literature references covering the most promising methods for removal of contaminant metals from steel (Subtask 1.1), 3) a summary of characterization results for two shredded steel samples (size distribution, visual inspection, and compositional analysis using hand held XRF, hand held LIBS and melting of a sample for chemical analysis) (Subtask 1.2), and 3) the results of preliminary experiments with potential physical sorting technologies (Subtask 1.3).

Task 1. Results

Task 1.1 Survey industry and perform a technical literature and patent review to identify technologies for physical and chemical removal of contaminants from steel

The literature search (Appendix A) has been prepared combined with the Industry Survey (Appendix B) and Cost Analysis of Chemical Removal Methods (Appendix C). Then based on these fundamental studies, two physical removal technologies and two chemical removal technologies that appear to be economically viable and technically suitable have been identified separately.

For physical removal of Cu, the Industry Survey (Appendix B) demonstrates that optical recognition is potentially economically viable, especially when compared to other types of sensor. So, camera-based optical sorting and blue laser sensing, which both could be classified as optical recognition, have been

identified and focused for further research. Among them, camera-based sorting could possibly be applied to recognize Cu due to the differences in color, shape and other characteristics. Although the cleanness of steel scrap may influence the identification, new image classification technologies using machine learning could potentially be involved to eliminate this effect. For blue laser, due to its properties, which could be specifically related to Cu, it is highly desirable to conduct initial laboratory tests for deep understanding its feasibility. Also, compared to LIBS, no ablation is needed for blue laser. The cost would likely be acceptable because of lower beam intensity, though there is no existing product that applies blue laser as a type of sensor.

For chemical removal of Cu, Cost Analysis (Appendix C) shows the energy consumption and materials cost of six possible methods. These possible methods were chosen based upon the mechanism analysis in Literature review (Appendix A). The calculation is based on the composition requirement for different types of steel product, including commercial and IF steel. As a result, chlorination with Cl_2-O_2 gas at 800 ^oC and slagging with FeO-SiO_2-$CaCl_2$ at 1600 ^oC are respectively focused for further exploration, referring to the energy consumption and materials cost. For chlorination with Cl_2-O_2 gas, unreacted Cl_2 gas can be recycled back to the furnace. Slagging FeO-SiO_2-$CaCl_2$ could likely be done in the ladle-furnace as compared to other methods using reduced pressure.

Task 1.2 Characterization of two samples of steel scrap from auto shredders

Two samples of steel scrap were collected from WMR (Sample 1) and SSAB-USA (Sample 2). Characterizations for shredded steel scrap samples, including size distribution test, visual inspection, compositional analysis using handheld XRF, portable LIBS and AAS analysis, and blue laser test, have been carried out to figure out the Cu composition in steel scrap.

(1) Particle Size Distribution

Table 1. Results of size distribution test

Particle Size, inches	Sample 1, wt %	Sample 2, wt%
+3	3.9	14.7
-3 + 2	28.9	35.0
-2 + 1½	24.5	20.3
-1½ + ½	39.9	26.6
-½	2.8	3.4
Total Weight	1,337.96 kg	434.68kg

Most of the apparent Cu motor material appears in the -1½ + ½ inch size fractions and Cu wire appears in the -½ inch size fraction. Preferential removal of the less than ½ inch size fraction may lower the Cu content of the scrap without material loss of iron values.

(2) Visual Inspection

Table 2. Results of visual inspection

	Sample 1	Sample 2
Identified Cu Source	Cu Motors and Wire	Wire (no motors)
Measured Mass (kg)	2.831	0.791
Mass Percent (%)	0.212	0.182

As shown in Figure 1, 2 and 3, Sample 1 was collected directly from auto shredder without additional handpicking or sorting and also didn't contain white goods material (kitchen appliances and similar) as feed stock to the auto shredder. For Sample 2, in addition to shredded automobile scrap, it appeared to also

contain “new” scrap and home white-goods scrap. SSAB-USA also informed that Sample 2 had already been handpicked for copper reduction before being shipped to our laboratory.

Based on the data in Table 2, Sample 1 could be more representative considering the definition of contaminated steel in the project. So, for the following compositional analysis and further exploration of proposed removal methods, pieces from Sample 1 have been mainly adopted as experimental materials.

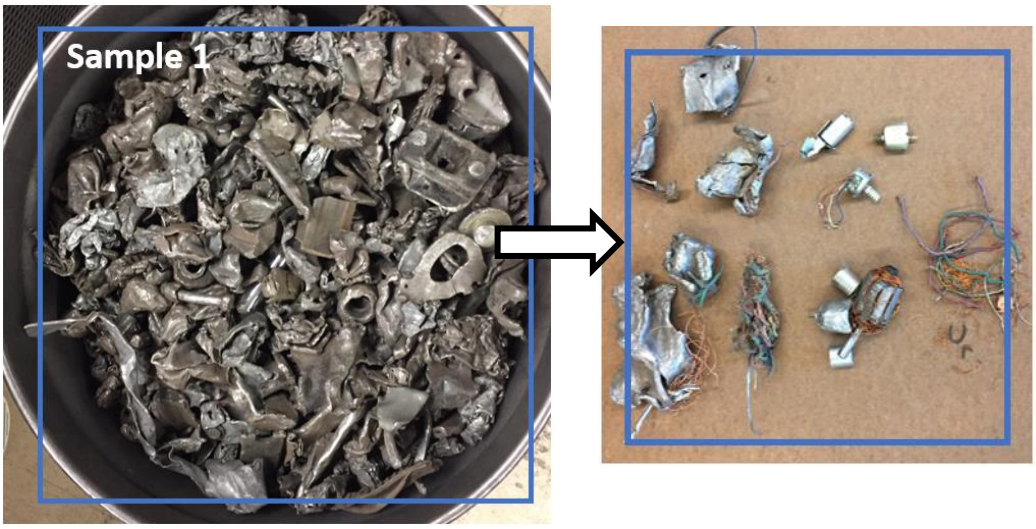

Figure 1. Steel scrap of Sample 1 and identified Cu source

Figure 2. Details of identified Cu source from Sample 1

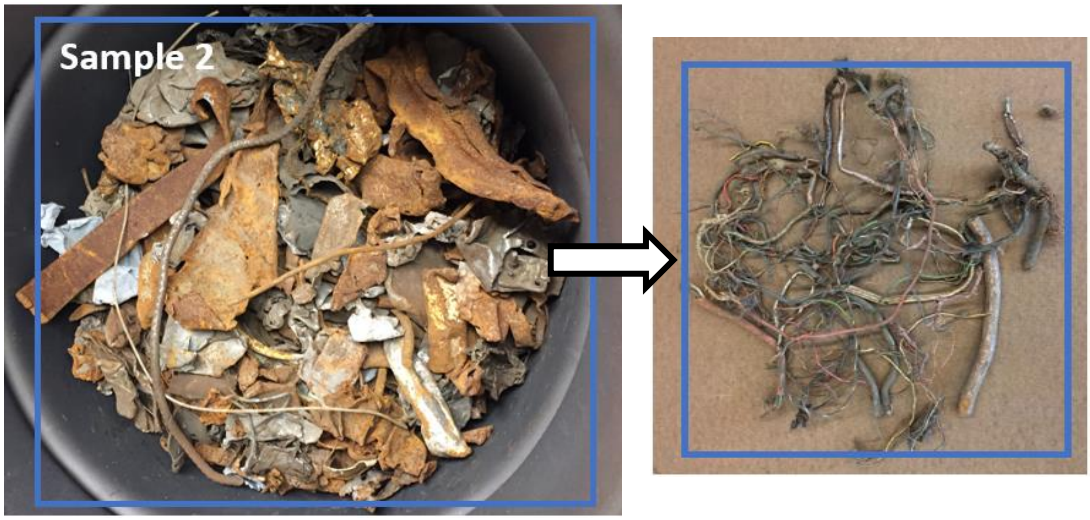

Figure 3. Steel scrap of Sample 2 and identified Cu source

(3) Handheld XRF Analysis

Identified Cu source from Samples 1 and 2 have been subjected to scanning by handheld XRF. Remnant copper motors with a metal shell could be difficult for copper detection. Copper wire was more easily detected by the scanning.

Each one hundred iron shreds from different size distributions of Sample 1 and 2, including individual mass weights, have been analyzed. Then the average Fe and Cu content of each 100 pieces can be calculated and shown in Table 3.

Table 3. Results of handheld XRF analysis

	Total Weight of 100 Pieces	Fe		Cu	
		Weight	Percent	Weight	Percent
Sample 1	27,595.5g	22,238.7g	80.59%	19.453g	0.0705%
Sample 2	21,474.1g	16,206.15g	75.47%	36.195g	0.168%

The overall Cu content of two samples could be estimated with the combination of results from Visual Inspection and Handheld XRF analysis. Cu content of sample 1 and 2 were 0.2825% and 0.35% respectively. Although these data might not be so accurate, it could offer some basic information for understanding the Cu composition of steel scrap.

(4) Trial of Melting Scrap for Chemical Analysis

A sample (1249.6g), assembled from randomly selected minus 0.5inch Sample 1 shreds without visual Cu source, was prepared for the melting procedure. The trial was conducted at 1600 ºC in a resistance furnace with oxidation protecting gas (Ar-5%H_2). After melting, the solidified metal (1016.3g) was sawed into blocks and sheets to facilitate AAS and LIBS analysis.

For portable LIBS analyzer, with calibration on the intensity of specific wavelength for Cu (324.75 nm), sheet sample was struck by laser 10 times and then the average Cu content was calculated, as shown in Table 4.

Table 4. Results of portable LIBS analysis for the trail of melting scrap

Piece No.	Weight (g)	Cu wt%

		Handheld XRF Analysis	LIBS Analysis
1	2.5647	0.11%	0.109%
2	0.9837	0.10%	0.109%
3	1.9220	0.15%	0.092%
4	1.0981	0.11%	0.102%
5	1.6224	0.13%	0.102%
6	1.7339	0.22%	0.105%
Estimated background Cu wt% for the Solidified Melt			0.103%

For AAS analysis, sawed pieces of the solidified metal from the above trial melting were dissolved in aqua regia to prepare the solution. Then corresponding Cu content was calculated, as shown in Table 5.

Table 5. Results of AAS analysis for the trial of melting scrap

Piece No.	Weight (g)	Cu wt%	
		Handheld XRF Analysis	AAS Analysis
1	0.5265	0.09%	0.103%
2	0.1562	0.07%	0.120%
3	0.3243	0.08%	0.103%
4	0.1598	0.13%	0.116%
5	0.0904	0.08%	0.142%
Estimated background Cu wt% for the Solidified Melt			0.110%

Since the sample was only prepared from Fe shreds within minus 0.5inch size fraction, the result of chemical analysis would be not representative.

(5). Experiments of Melting Scrap for Chemical Analysis

As mentioned before, Sample 1 came directly from an auto shredder, whereas Sample 2 had already incurred hand sorting when it was shipped to our laboratory; hence, Sample 1 could be better representative for purposes of melting experiment. So randomly pieces from Sample 1 for each size distribution without visual Cu source have been prepared for the melting and following AAS analysis. Detailed results of AAS analysis are shown in Table 6.

Table 6. Detailed results of AAS analysis for different size distribution

Particle Size, inches	Size Distribution (wt%)	Cu wt% (AAS Analysis)
+3”	3.9%	0.033%
-3” +2”	28.9%	0.037%
-2” +1½”	24.5%	0.049%
-1½” +½”	39.9%	0.043% - 0.133%
-½”	2.8%	0.069%
Background Cu Content (wt%)		0.043% - 0.079%

Considering the four pieces in the -1½”+½” fraction, as shown in Figure 4, contained significantly more copper, the estimated Cu content (wt%) of this fraction is about 0.133%. So, the total background Cu content of Sample 1 could be estimated about 0.061%. As a result, the total Cu content of Sample 1 could be calculated as shown in Table 7.

Figure 4. Identified high Cu containing pieces for -1½"+½" fraction

Table 7. Overall Cu content of Sample 1

Total Weight	1,337.96 kg
Weight of Fe Shreds ($W_{\text{Fe Shreds}}$)	1,335.129 kg
Background (Alloyed) Cu Content (wt%) ($C_{\text{Background Cu}}$)	0.061%
Identified Cu Sources	Cu Motors and Wires
Weight of Identified Cu Sources ($W_{\text{Cu Sources}}$)	2.831 kg
Weight Percent of Identified Cu Sources (wt%)	0.212%
Total Cu Content (wt%)	0.272%

(6) Blue Laser Study

Considering the known difference of thermal conductivity and adsorption of Cu and Fe within the wavelength of an excited blue laser, initial laboratory experiments, as shown in Figure 5, were conducted. A 150W blue laser source provided a nominal 2mm diameter laser impact-spot for 500ms on the surface of pure Cu and Fe sheets, fixed on a platform. Real-time data from thermocouples fixed to the sheets and a FLIR (Forward Looking Infrared Radar) camera were collected for 60 seconds after initiation of the laser. Due to the higher thermal conductivity and absorption for Cu, the Cu sheet showed a rapid temperature increase and drop compared with the Fe sheet. A third sample called a composite, Fe sheet overlaid on a Cu sheet, was similarly tested, as shown in Figure 6. The temperature response for the composite sample was faster than for the single Fe sheet. These thermocouple-based data observation were consistent with data from the FLIR videos, which show immediate differences in heat generation and dissipation.

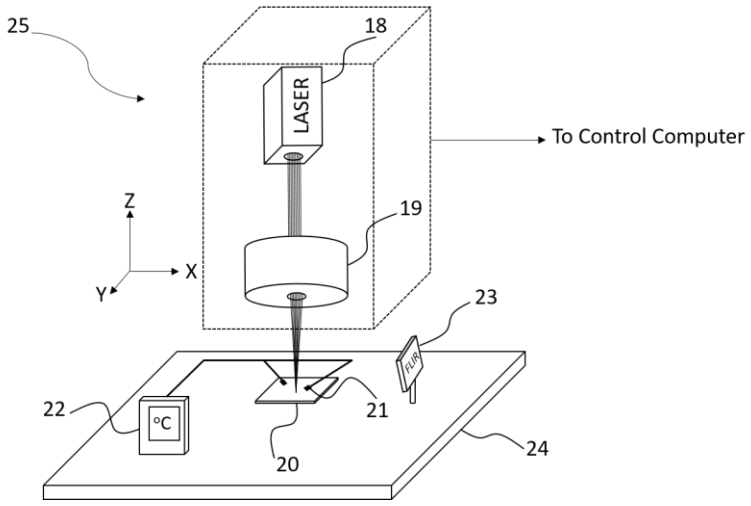

Figure 5. Schematic overall view of blue laser testing system

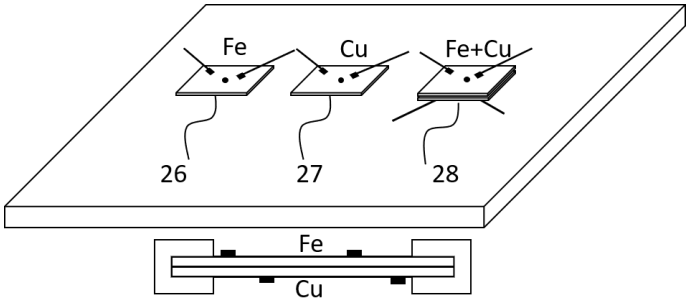

Figure 6. Diagrammatic illustration of the prepared samples for blue laser test

Task 1.3 Assess current limits of sensor-based sorting technologies

Optical Recognition Improved by Machine Learning

With further understanding, the essence of optical recognition is the designed program for analyzing images and distinguishing different color values. It shares the same mechanism of image classification using CNNs, which have become a common application for machine learning. So the purpose of this method is to investigate and determine the feasibility of eliminating errors related to surface heterogeneities through applying machine learning to improve optical recognition of steel scrap for a better sorting efficiency of Cu impurities.

An average of 2000 photographs for identified Cu sources and Fe shreds, which were placed on a black conveyor belt to simulate the real working condition for sorting system, have been collected, as shown in Figure 7. Considering the small amount of identified Cu sources, random rotations were manually operated to each piece of identified Cu sources during acquiring the photographs as a way of data augmentation, in order to maintain a balance with the number of acquired photographs for Fe shreds.

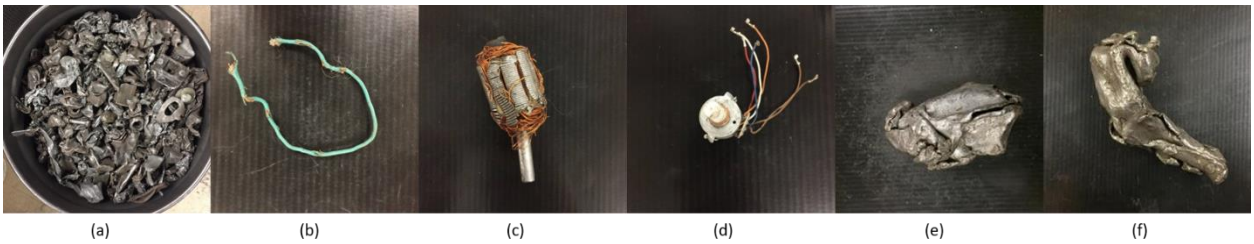

Figure 7. Acquired Photographs for shredded steel scrap: (a) Shredded steel scrap from Sample 1 in container; (b) Cu wire; (c) Cu motor rotor; (d) Cu motor with wire; (e) and (f) Fe shreds

As shown in Figure 8, the whole process of experiments was spilt into 3 major parts: inputting dataset, training and testing. Also the detailed distribution of photographs to the training and testing parts as the dataset is shown in Figure 9. For the training process, 80% of the dataset was chosen for training, while the rest 20% was applied for validation, which could provide an unbiased evaluation of the model fit on the training dataset for each training epoch.

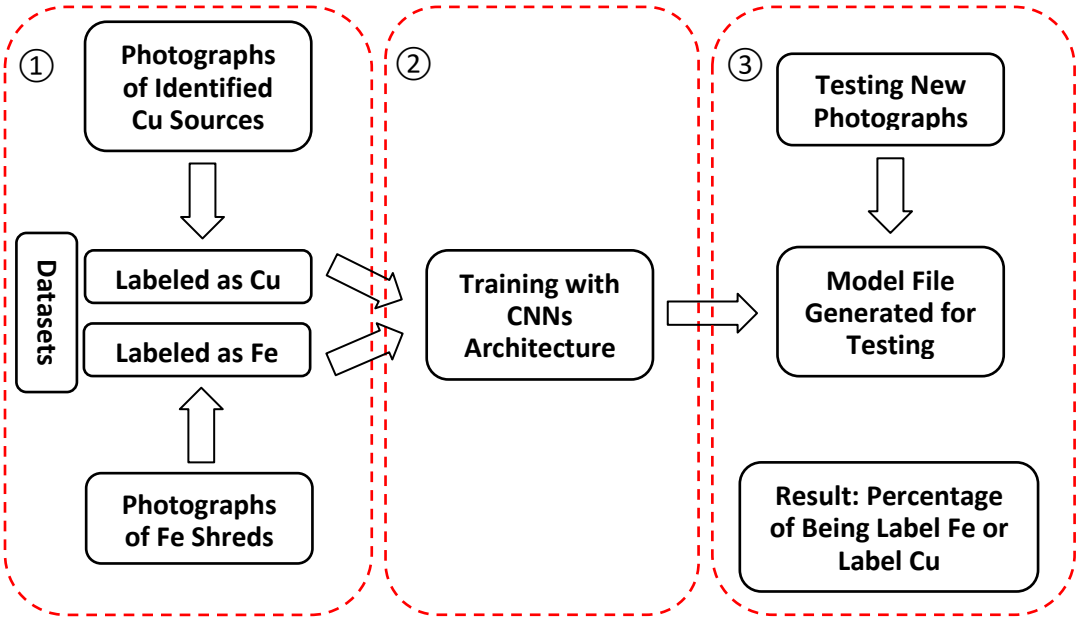

Figure 8. Implementation of machine learning experiment

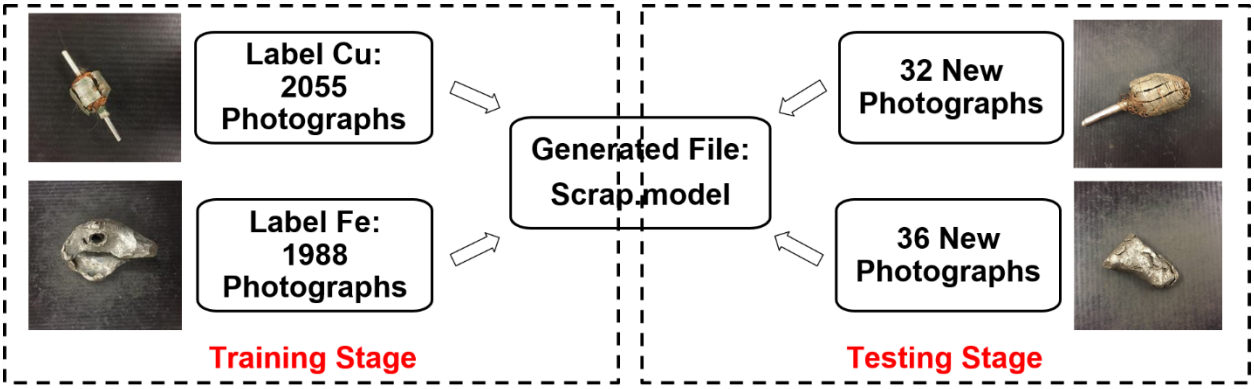

Figure 9. Dataset distribution for training and testing process

In the initial trial, architecture VGGNet[1] was used to enable deep learning to be achieved with a relatively simple and linear structure. As shown in Figure 10, the accuracy of training and validating could be approximate 99% and the corresponding loss could be as low as 0.01 for the final epoch.

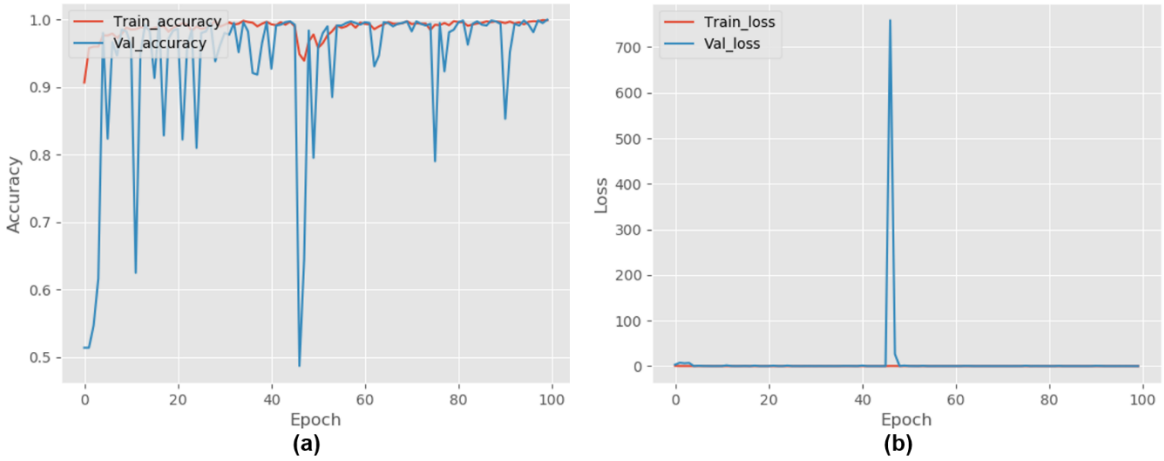

Figure 10. Training with VGGNet and original dataset: (a) Accuracy of training and validating; (b) Loss of training and validating

However, during testing stage, shredded Fe parts in 27 of 36 photographs were recognized correctly, while 17 pieces among 32 photographs of identified Cu sources were recognized correctly. Thus the accuracy for recognizing Cu impurities could be estimated as 53.1%. Compared with the high training and validating accuracy, overfitting could be the major concern for further optimization.

Overfitting[2] happens when a model learns the detail and noise in the training data to the extent that it negatively impacts the performance of the model on new data, as shown in Figure 11.

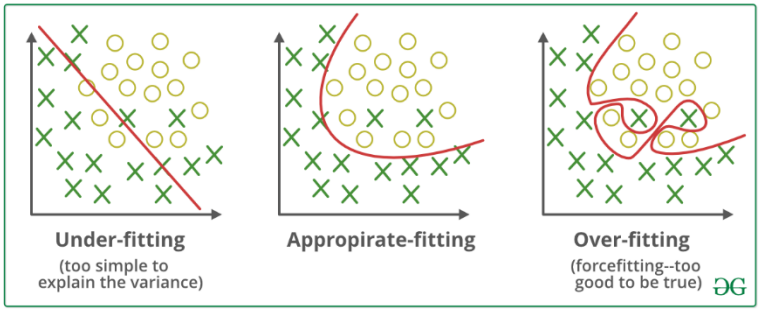

Figure 11. Explanation of overfitting

One possible reason for the low Cu recognizing accuracy and overfitting could be the interference from black background, which was dominant in most of the photographs compared to the shredded objects. During the training, this dominated area might be analyzed as the feature information, weakening the weight of other distinct colors, such as the reddish-brown of Cu metal in the motor rotor, the bright white of the motor shell, and the red or blue insulation of Cu wire. With this concern, photographs had been cropped by programming to remove the background as much as possible and applied as new dataset, as shown in Figure 12.

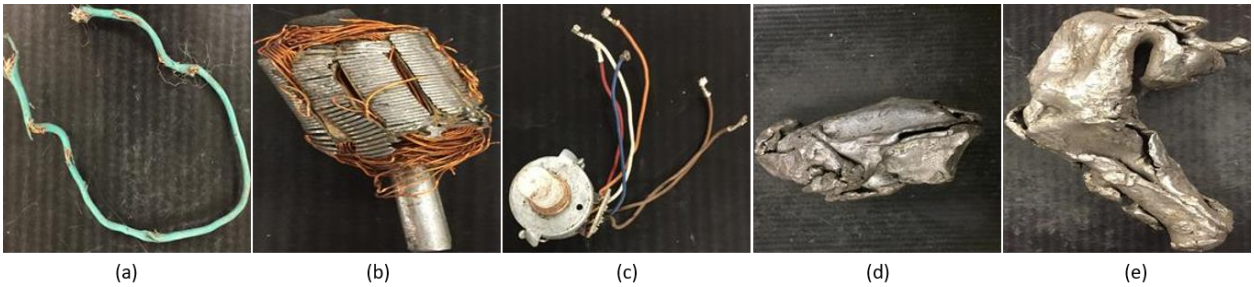

Figure 12. Cropped dataset: (a) Cu wire; (b) Cu motor rotor; (c) Cu motor with wire; (d) and (e) Fe shreds

The same process utilizing VGGNet architecture was applied to the new cropped dataset. As a result, 20 pieces among 32 photographs of identified Cu sources were recognized correctly, while 22 pieces among 36 photographs of Fe shreds were recognized correctly. Thus the accuracy for recognizing Cu impurities could be estimated as 62.5%, while the accuracy for Fe shreds could be 61.1%. As shown in Figure 13, overfitting could be still a problem, nonetheless, dataset with cropped photographs is worth pursuing.

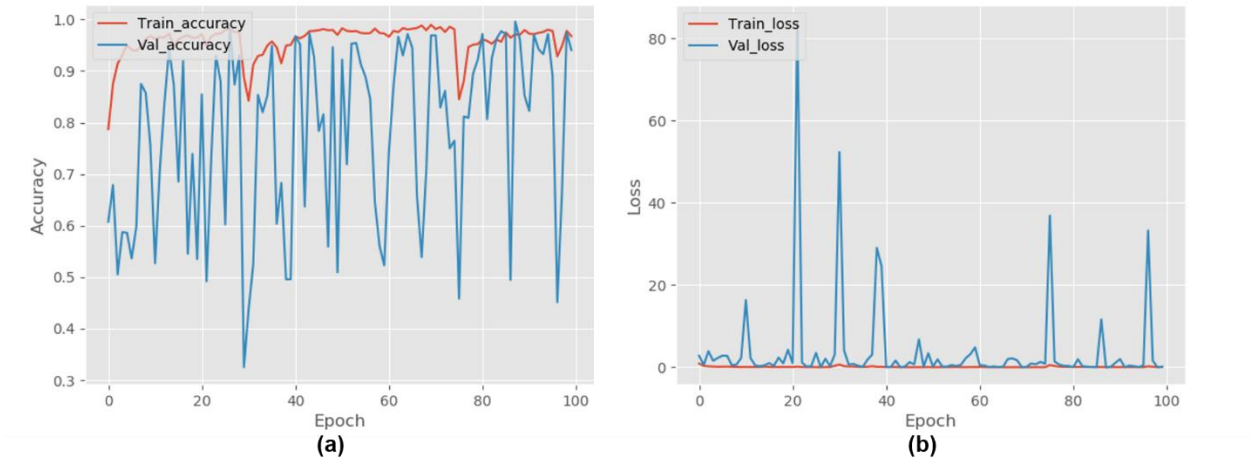

Figure 13. Training with VGGNet and cropped photographs: (a) Accuracy of training and validating; (b) Loss of training and validating

Based on above investigation and further analysis, it seems that initial VGGNet architecture might not be the suitable architecture, referring to the specific dataset. Other architectures, such as ReSNet[3], InceptionV3[4], Xception[5] and Inception_ReSNet[6], have been tried with cropped photographs as dataset. The testing results of applying these architectures are shown in Table 8.

Table 8. Detailed testing results for training with different architectures

No. of Training with Cropped Dataset	Testing Results	Recognizing Accuracy	Testing Results	Recognizing Accuracy	Testing Results	Recognizing Accuracy	Testing Results	Recognizing Accuracy
	Architecture: ReSNet		Architecture: InceptionV3		Architecture: Xception		Architecture: Inception_ReSNet	
#1	Fe: 28/36	77.8%	Fe: 30/36	83.3%	Fe: 35/36	97.2%	Fe: 32/36	88.9%

	Cu: 26/32	81.3%	Cu: 17/32	53.1%	Cu: 24/32	75.0%	Cu: 21/32	65.6%
#2	Fe: 19/36	52.8%	Fe: 22/36	61.1%	Fe: 34/36	94.4%	Fe: 34/36	94.4%
	Cu: 19/32	59.4%	Cu: 27/32	84.4%	Cu: 26/32	81.3%	Cu: 25/32	78.1%
#3	Fe: 23/36	63.9%	Fe: 28/36	77.8%	Fe: 35/36	97.2%	Fe: 32/36	88.9%
	Cu: 25/32	78.1%	Cu: 26/32	81.3%	Cu: 25/32	78.1%	Cu: 23/32	71.9%
#4	Fe: 33/36	91.7%	Fe: 29/36	80.6%	Fe: 28/36	77.8%	Fe: 32/36	88.9%
	Cu: 16/32	50.0%	Cu: 31/32	96.9%	Cu: 29/32	90.6%	Cu: 21/32	65.6%
#5	Fe: 30/36	83.3%	Fe: 26/36	72.2%	Fe: 21/36	58.3%	Fe: 27/36	75.0%
	Cu: 19/32	59.4%	Cu: 26/32	81.3%	Cu: 29/32	90.6%	Cu: 22/32	68.9%

The testing accuracy for Cu impurities and Fe shreds both got improved compared to the initial trials, especially for #4 training with InceptionV3 and Xception architecture. Meantime, to a certain extent, overfitting problem could be regarded as mitigation, though the accuracy of training and validating remained high, for example, as shown in Figure 14 for #4 training with architecture Xception.

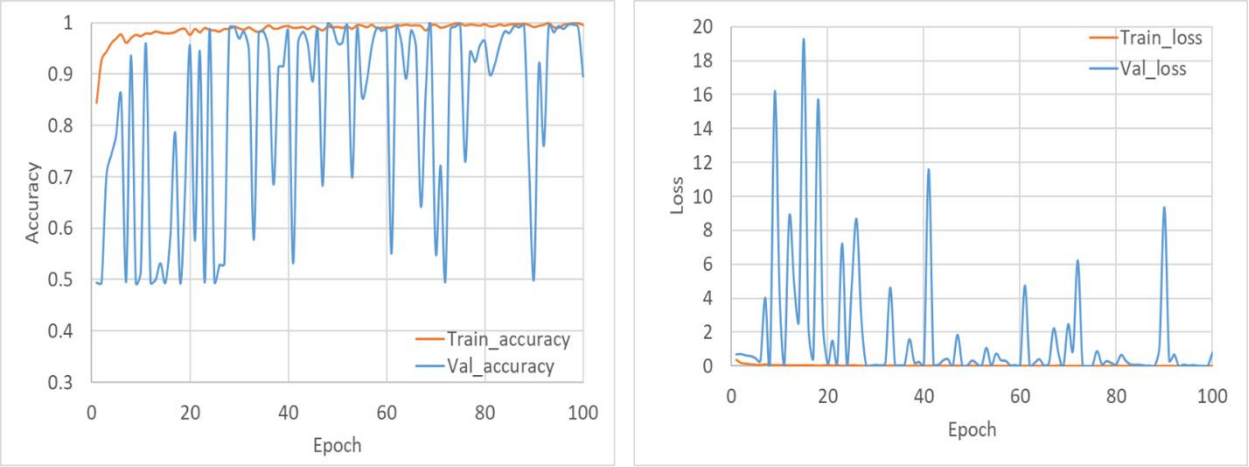

(a) (b)

Figure 14. Training with Xception and cropped photographs: (a) Accuracy of training and validating; (b) Loss of training and validating

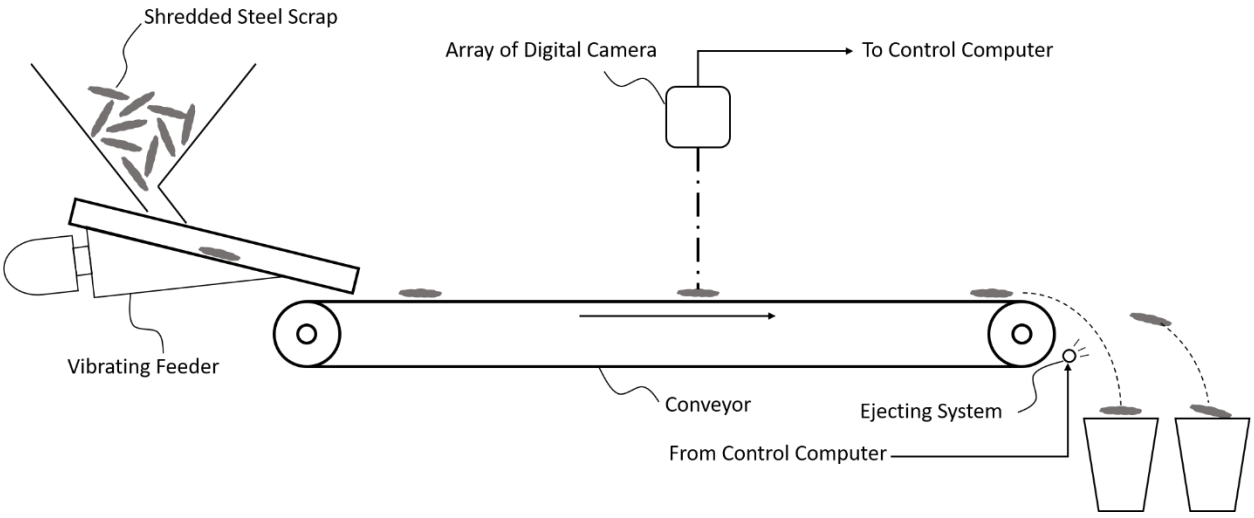

Figure 15. Schematic view for optical recognition system

By focusing on the essence of optical recognition, the testing process based on the generated model in above experiments could be incorporated into the sensor-based sorting system as the designed program shown in Figure 15, assuming the same recognizing accuracy could be achieved for the system. Therefore the Cu content (wt%) after optical recognition could be calculated with the equation (1):

$$\frac{W_{\text{Cu Sources}} \times \frac{(100 - \text{Cu Recognizing Accuracy})}{100} + W_{\text{Fe Shreds}} \times (\text{Fe Recognizing Accuracy})/100 \times C_{\text{Background Cu}}/100}{W_{\text{Cu Sources}} \times \frac{(100 - \text{Cu Recognizing Accuracy})}{100} + W_{\text{Fe Shreds}} \times (\text{Fe Recognizing Accuracy})/100} \times 100\% \quad (\mathbf{1})$$

and the results are shown in Table 9.

Table 9. Estimated Cu removal for improved optical recognition with machine learning

Experiments		Testing Results	Recognizing Accuracy	Estimated Cu wt% before Optical Recognition	Estimated Cu wt% after Optical Recognition
Initial Trial with VGGNet and Original Photographs		Fe: 27/36	75.0%	0.272%	0.193%
		Cu: 17/32	53.1%		
Optimization	Trial with VGGNet and Cropped Photographs	Fe: 22/36	61.1%		0.191%
		Cu: 20/32	62.5%		
	#4 Trial with Xception and Cropped Photographs	Fe: 28/36	77.8%		0.087%
		Cu: 29/32	90.6%		
	#4 Trial with InceptionV3 and Cropped Photographs	Fe: 29/36	80.6%		0.069%
		Cu: 31/32	96.9%		

It is evident that applying this improved optical recognition could be used to reduce the Cu content of shredded steel scrap, achieving the 0.1wt% limitation for Cu content. Considering that scrap is currently blended with virgin iron, to dilute the impurity concentration, when manufacturing value-added steel products, such as coated strips, the improvement shown in Table 9, would reduce the needed level of virgin iron, corresponding to the energy saving, when accounting for the embedded energy in coal used to produce virgin iron, as shown in Table 10.

Table 10. Detailed reduction of virgin iron and energy consumption

Experiments		Cu wt% Before Sorting	Cu wt% After Sorting	Cu Removal Rate	Reduction of Virgin Iron per tonne of sorted steel scrap	Energy-saving per tonne of sorted steel scrap [7]
Initial Trial with VGGNet and Original Photographs		0.272%	0.193%	0.079wt%	0.428t	5.4GJ
Optimization	Trial with VGGNet and Cropped Photographs		0.191%	0.081wt%	0.443t	5.6GJ
	#4 Trial with Xception and Cropped Photographs		0.087%	0.185wt%	2.222t	28.2GJ
	#4 Trial with InceptionV3 and Cropped Photographs		0.069%	0.203wt%	3.074t	39.04GJ

Task 2. Chemical Processing for Impurity Removal

Task 2. Objective

For the treatment of molten steel containing Cu and Sn, several alternatives (chemical and metallurgical) will be assessed: a) vacuum distillation b) treatment by reaction with sulfur containing slag and c) other treatment methods (e.g. chemical and metallurgical methods from the literature search in Subtask 1.1). Theoretical concepts and methods of steel scrap purification will be investigated along with details regarding the practical applicability and energy and emissions impacts. The research findings in this task will answer the simple question: how long does it take to treat a certain volume of liquid iron containing Cu and Sn (to derive Cu and Sn removal rates) with these methods for minimum energy input, cost and complexity? This will allow control of alloy composition to closer limits, with the benefit of improving the properties while simultaneously reducing the need for degassing and grain refinement additives, and reducing energy and emissions. The outputs of this task will be 1) a brief description of preparation and composition of sample of contaminated steel (Subtask 2.1), 2) results of a theoretical analysis that will be used to guide the selection of impurity removal methods for economic evaluation in Subtask 2.4 and lab testing in Subtask 2.5 (Subtask 2.2), 3) a matrix of industrial steel sources to blend with scrap steel to produce various steel grades (Subtask 2.3), 4) results of economic analysis of available chemical technologies and identification of the most likely candidate technology based on the economics and technical performance, and 5) results of proof of concept trials, including test results to confirm that the level of combined impurities (Cu and Sn) is below a target level of 0.1% (i.e. so that the steel may be used in an electric arc furnace) (Subtask 2.5).

Task 2. Results

Task 2.1 Brief description of preparation and composition of sample of contaminated steel

Due to the limiting capacity of the resistance furnace in our lab, it is not feasible to produce a molten mixture of Fe shreds and identified Cu source together from Sample 1 with maintaining the particle size distribution in Table 1. So pieces of Fe shreds from different size distribution and identified Cu source, such as Cu motor and wire-entangled piece, were melted separately for further chemical analysis. Collected molten

melts are shown in Figure 16 and 17. Considering Cu content would be the priority of sample chemistry, AAS analysis could be the suitable and convenient choice compared to ICP-MS. Detailed results of AAS analysis are shown in Table 11.

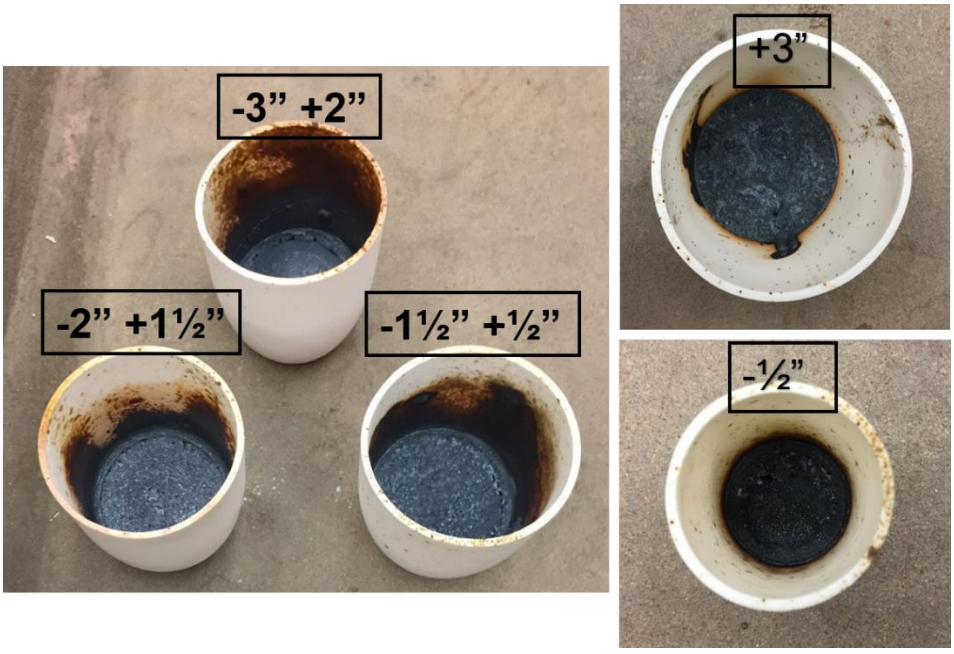

Figure 16. Collected molten melt for Fe shred from different size distribution of Sample 1

Figure 17. Collected molten melt for identified Cu source of Sample 1

Table 11. Detailed results of AAS analysis for collected molten melts

Sample	Before Melting		After Melting			
	Weight (g)	Weight Distributions	Weight (g)	Metal Loss (g)	Cu wt% (AAS Analysis)	Cu wt%[(3)] (Calibrated)
+3”	1084.4	3.9%	850.4	234	0.042%	0.033%
-3”+2”	894.3	28.9%	743.7	150.6	0.045%	0.037%
-2”+1½”	758	24.5%	621.2	136.8	0.060%	0.049%
-1½”+½”	1234.2	39.9%	1013.6	220.6	0.152%	0.133%
-½”	93	2.8%	50.8	42.2	0.127%	0.069%
Wire-entangled Piece	240.2 (Fe: 233.6g + Cu wire: 6.6g)	/	113.6	126.6	4.272%	2.020%
Cu Motor	150.8	/	104.7	46.1	55.25%	38.36%

Although the protecting gas was used during the melting process, it could not purge the air out the furnace sufficiently due to the large space and furnace seal issues, which could contribute to the oxidization of Fe, leading to metal loss. So, Cu content could be calibrated considering the loss of Fe.

Task 2.2 Fundamental evaluation of chemical processing routes

As shown in Appendix C, six chemical processing methods have been evaluated based on fundamental thermodynamic and kinetic analysis for the energy and materials consumption to reduce Cu content to standard composition requirement of common steel product, such as commercial steel and IF steel.

Task 2.3 Develop model to identify the blending requirements for scrap sources and virgin ferrous materials

As shown in Appendix D, a matrix of industrial steel sources to blend with scrap steel to produce various steel grades has been prepared to understand what scrap sources are appropriate and minimum iron dilutions necessary for producing distinctly different steel products.

Task 2.4 Review of economics of methods for removing Cu and Sn impurities from the melt

As shown in Table 12, based on the evaluation of chemical processing methods in Task 2.2, two potential methods with lower costs, including chlorination with Cl_2-O_2 gas at 800 ^oC and slagging with FeO-SiO_2-$CaCl_2$ at 1600 ^oC, have been identified for further experimental evaluation.

Table 12. Cost analysis and comparison of chemical removal methods

Method		T(°C)	$[Cu_I]$ (wt%)	$[Cu_F]$ (wt%)		Time		Extra Energy Consumption* (kWh/tonne)		Extra Materials Cost($/tonne)		Secondary Effects
				Comm-ercial	IF steel	Comm-ercial	IF steel	Comm-ercial	IF steel	Comm-ercial	IF steel	
Solid Scrap (before melting)	Fluxing with matte: FeS and Na_2S	1000	0.4	0.1	0.03	30 min (heating) + 15 min (reaction)	30 min (heating) +18 min (reaction)	169.28	198.78	2227.735		(1) Sulfur contamination (2)SO_2 in the exhausted gas
	Fluxing with Cl_2-O_2 gas	800	0.4	0.1	0.03	60 min (heating) + 4 min (reaction)	60 min (heating) + 6 min (reaction)	78.4	89.18	934.614		(1)Fe partially oxidization (2)Cl_2 in the exhausted gas
Melting Scrap (ladle furnace)	Vacuum Evaporation (50Pa)	1600	0.4	0.1	0.03	2.5 h (heating) + 25.67 h (removing)	2.5 h (heating) + 47.97 h (removing)	3952.84	7342.44	None directly		Difficult to maintain lower pressure
	Blowing NH_3 under 2000 Pa	1600	0.4	0.1	0.03	2.5 h (heating) + 145 min (removing)	2.5 h (heating) + 270 min (removing)	597.73	1101.4	0.111	0.207	Additional degassing due to nitrogen dissolution
										(NH_3 522$/tonne)		
	Blowing Weak Oxidizing Powder under Reduced Pressure(130Pa)	1650	0.4	0.1	0.03	2.5 h (heating) + 325 min (removing)	2.5 h (heating) + 10 h (removing)	1529.07	2825.84	9100	16800	Adding carbon and following decarburization
	Using FeO-Cu_2O-SiO_2-$CaCl_2$ Slag to Remove Cu in Ladle Furnace	1600	0.4	0.1	0.03	3 h (heating) + 50 min (removing)	3 h (heating) + 87 min (removing)	204.55	298.95	1474.76 + price for FeO (couldn't find the bulk price)		(1)Unclear mechanism (2)May need decarburization

Task 2.5 Conduct proof-of-concept trials to identify suitable chemical processing method

(1) Chlorination with Cl_2-O_2 gas at 800 ºC

Cu and Fe sheet were adopted as sample for the initial experiments with the configuration in Figure 18&19. Multitube rotameter was used to control the flowrate of chlorine and oxygen gas. Argon gas was used to purge the air out of the furnace before the experiment and maintain protective atmosphere after the reaction with inputting gas.

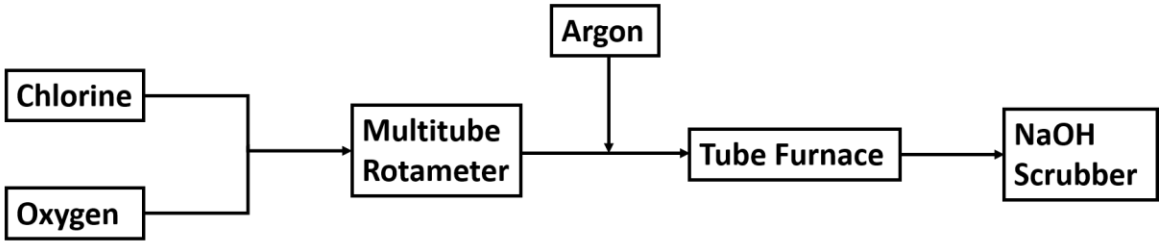

Figure 18. Schematic view of chlorination experiment

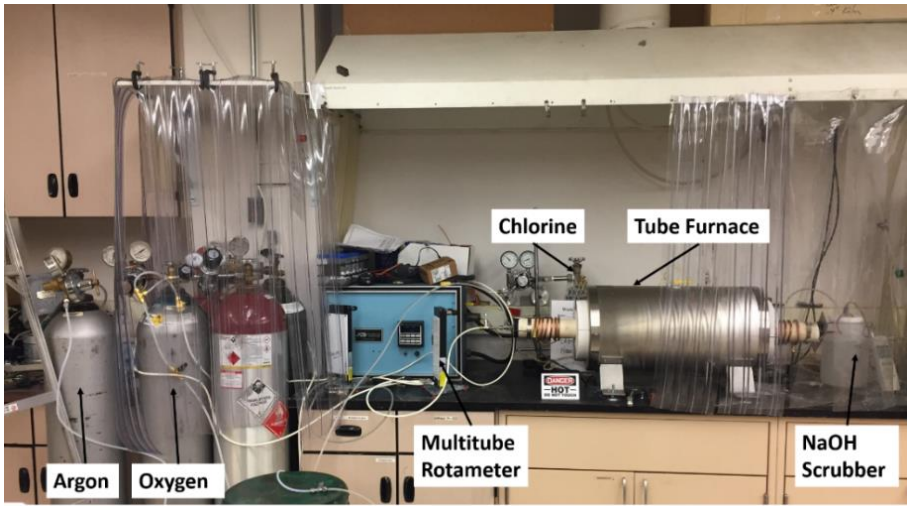

Figure 19. Practical configuration of chlorination experiment

<u>Initial experiment with chlorine gas at 800 ºC:</u>

To understand the reaction between metal sheet and chlorine gas, only chlorine gas was introduced to the tube furnace after heating up to the designed temperature without controlling its flowrate. Based on the observation of bubbles in the NaOH scrubber, the whole reaction finished quickly in about 5 minutes after introducing chlorine gas. As shown in Figure 20, Cu and Fe sheet were both totally volatilized. Most of the volatile product was collected from the output end of tube furnace. A very small amount of solid is found in the scrubber after filtration, which might be the precipitate of $Fe(OH)_3$.

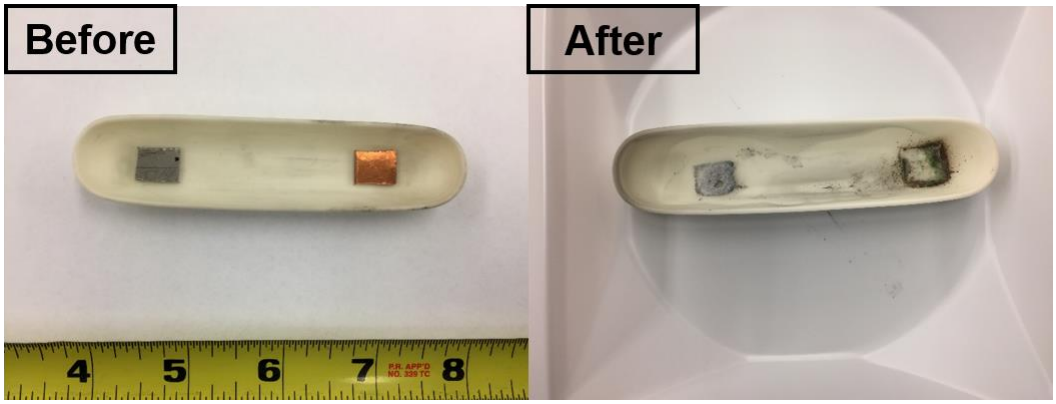

Figure 20. Cu and Fe sheet sample before and after experiment with chlorine gas

<u>Initial experiment with the mixture of chlorine and oxygen gas at 800 ºC</u>: Based on thermodynamic analysis, with the increasing ratio of oxygen and chlorine gas, Fe_2O_3 will be gradually formed to stop the further reaction with gas phase for Fe sheet, while volatile copper chloride will be formed for Cu sheet. So the flowrate ratio of chlorine and oxygen gas was maintained at 1:10 according to thermodynamic calculation. Trial experiment has been tried with introducing the mixture gas about 60 minutes. Oxidation of Fe sheet could be observed, while 0.95g Cu sheet got totally volatilized after the experiment, as shown in Figure 21.

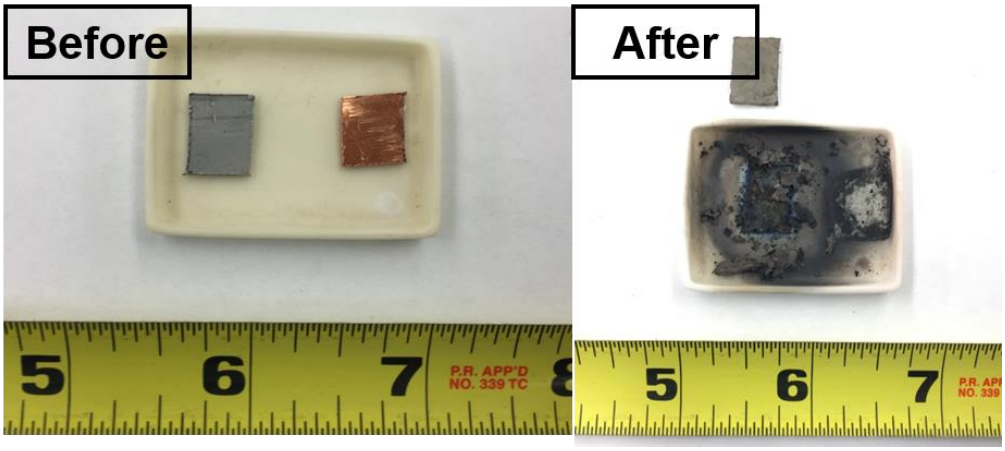

Figure 21. Cu and Fe sheet sample before and after experiment with mixture of chlorine and oxygen gas

After dissolving the solid collected from the output end of tube furnace and the rubber tube between furnace and scrubber in water, blue solution could be observed with the adding of NaOH, as shown in Figure 22. Considering the small weight of original Cu sheet, though precipitate was difficult to observe, we can still confirm that volatile copper chloride was collected as product.

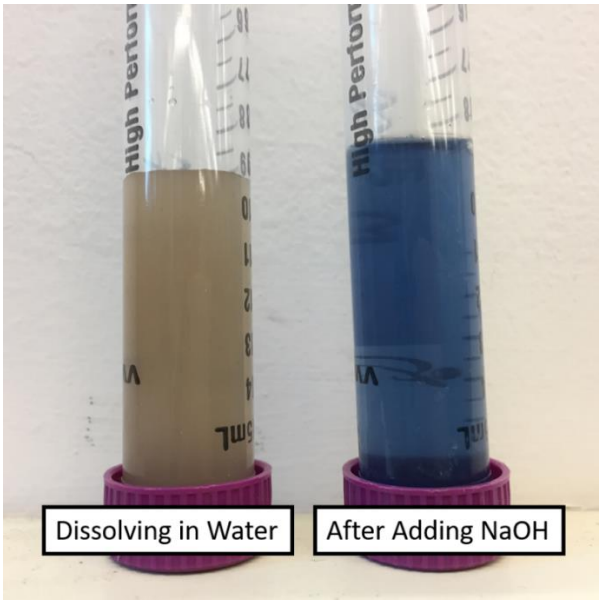

Figure 22. Solution: dissolving collected solid in Water & adding NaOH

For Fe sheet, its weight changed from 1.10g to 0.9g after the experiment. Besides of the oxidation, part of the weight loss could be attributed to the reaction with chlorine gas. This can also be proved by the reddish brown precipitate in the water dissolved solution with enough standing time, as shown in Figure 23. The possible reason could be attributed to the controlling of flowrate, which fluctuated during the whole experiment and was hard to maintain the designed ratio.

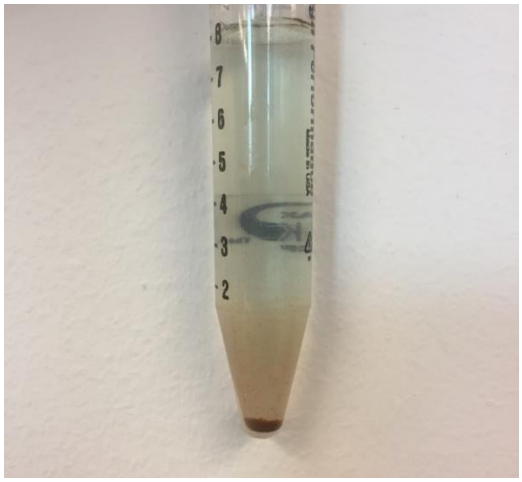

Figure 23. Water dissolved solution of collected solid after enough standing time

<u>Initial experiment with Fe-Cu alloy collected from the completed melting experiment</u>: Similar as the previous experiment with the mixture of chlorine and oxygen gas, Fe-Cu alloy collected from the melting experiment for Cu motor and wire-entangled piece, as shown in Figure 17, has been adopted as sample. After experiment, oxidation layer could be observed, as shown in Figure 24. Detailed result of AAS analysis is shown in Table 13. It is highly possible that the loss of Cu could be just attributed to the reaction on the surface.

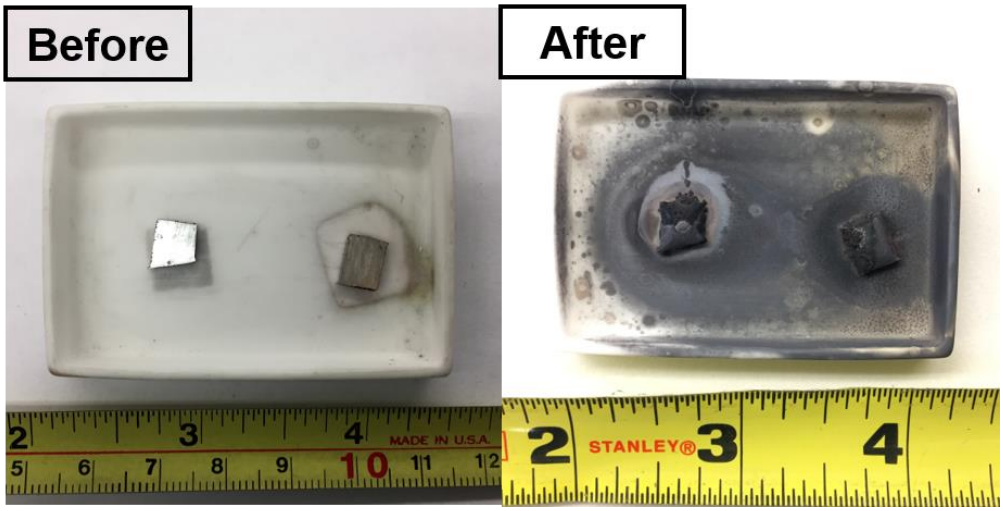

Figure 24. Fe-Cu alloy sample before and after experiment with mixture of chlorine and oxygen gas

Table 13. Detailed result of AAS analysis for experiment with Fe-Cu alloy sample

Sample	Before Experiment			After Experiment			Weight Loss of Cu/g	Weight Loss of Fe/g
	Weight/g	Cu Content /wt%	Cu weight /g	Weight /g	Cu Content /wt%	Cu weight /g		
#1	0.5g	4.44wt%	0.0222g	0.3g	4.71wt%	0.01413g	0.00808g	0.18587g
#2	0.7g	29.01wt%	0.20307g	0.5g	30.1wt%	0.1505g	0.05257g	0.147g

Based on above experimental results and further analysis, this method demonstrates good feasibility to remove isolated pieces of Cu impurities, while potential for removing alloyed Cu from steel scrap could still need to be discussed.

(2) Slagging with $FeO\text{-}SiO_2\text{-}CaCl_2$ at 1600 °C

As shown in Figure 25 for the mechanism of this method, reaction (1) and (2) are supposed to happen during the whole process. Also more details can be found in the Appendix C for method #6.

$$2[Cu]_{steel} + FeO = Cu_2O + Fe(l) \quad \textbf{(1)}$$

$$Cu_2O + CaCl_2 = 2CuCl(g) + CaO \quad \textbf{(2)}$$

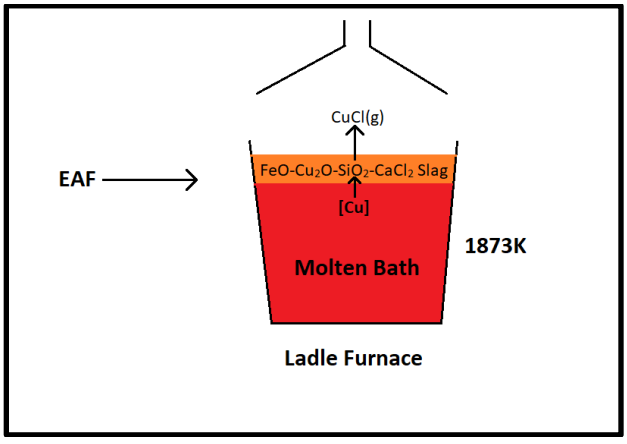

Figure 25. Schematic view of slagging experiment

Fe-Cu alloy collected from the melting experiment for Cu motor and wire-entangled piece, as shown in Figure 17, has been adopted as sample. Slag was prepared in accordance with the molar ratio of FeO, SiO_2 and $CaCl_2$ as 1:1.5:1.5, maintaining excess FeO for reaction (1). Detailed weights of metal sample and slag are shown in Table 14.

Table 14. Detailed weights of metal sample and slag

Sample	Metal	Slag Composition		
		FeO	$CaCl_2$	SiO_2
#1	14.1g	1.0191g	2.3556g	1.2782g
#2	9.9g	2.0140g	4.6568g	2.5354g

The furnace was heated up to 1600 ºC and dwelled at this temperature for about 40 minutes. After experiment, metal with oxidation layer could be collected from the crucible, as shown in Figure 26.

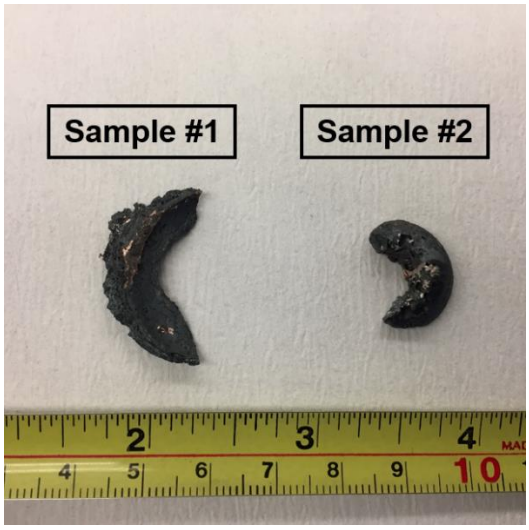

Figure 26. Collected metal after slagging experiment

Then whole piece of collected metal was dissolved by aqua regia for AAS analysis. Detailed results are shown in Table 15.

Table 15. Detailed results of AAS analysis for the collected metal

Sample	Before Experiment			After Experiment			Weight Loss of Cu/g	Cu Removal Rate
	Weight /g	Cu Content/wt %	Cu weight/ g	Weight/ g	Cu Content/wt %	Cu weight /g		
#1	14.1g	4.41wt%	0.622g	3.6g	11.24wt%	0.405g	0.217g	34.89%
#2	9.9g	29.82wt%	2.952g	3.4g	65.49wt%	2.227g	0.725g	24.56%

Based on above calculation, this method demonstrates good feasibility to remove Cu impurities. Meanwhile a large amount of Fe has been oxidized due to the insufficient sealing of the furnace, though Ar gas was inputted during the whole process. Also, as shown in Figure 27, alumina crucible reacted with FeO before the melting of alloy sample, considering the longer heating up time (13 hours). Both factors could affect the proceeding of reactions, leading to a lower removal rate of Cu. So we believe this result could be further improved with good atmosphere control, suitable crucible and furnace for sampling.

Figure 27. Broken alumina crucible after slagging experiment

Other Project Products

a. A patent disclosure has been written on the new sensor and was submitted to the CSM Technology Transfer Office for review.
b. Manuscript on the machine learning work has been written and submitted after revision.
c. A review paper has been written on alternatives and submitted for peer review.
d. Presentation at TMS 2020 - Sorting and Impurity Removal to Improve the Recycling of Steel Scrap from Auto Shredders

Project Conclusions and Recommendations

Conclusions:

- The presentation of Cu impurities in steel scrap can be classified as isolated pieces, such as Cu motors and wires, and alloyed Cu in Fe shreds.
- Characterization of collected steel scrap offers fundamental understanding for the composition of identified Cu source (0.212wt%) and background Cu (0.061wt%).
- For blue laser sensor, as one of identified physical removal technologies, initial laboratory tests conducted with pure Cu and Fe sheets have confirmed its sorting mechanism related to the difference of thermal conductivity and adsorption, demonstrating good sorting potential for Cu impurities.
- For optical recognition, as another identified physical removal technology, experiments conducted with different architectures of CNNs and cropped dataset have proved that it is highly possible to reduce Cu content to the 0.1wt% limitation with the improvement of machine learning, resulting in the reducing of needed virgin iron for blending and corresponding embedded energy in coal used to produce virgin iron.
- Chlorination experiments, as one of identified chemical removal technologies, demonstrate good feasibility to remove isolated pieces of Cu impurities, while potential for removing alloyed Cu from steel scrap could still need to be discussed. But its economic feasibility could be subject to the corrosive quality of chlorine gas and flowrate controlling of mixture gas.
- Slagging experiment, as another identified chemical removal technology, demonstrates good feasibility to reduce Cu content, no matter what kind of Cu impurities, since this method has been conducted in the molten state.

Recommendation:

- Potentially discussion with industrial partners, which focus on sensor sorting, should be planned for utilization of the two physical removal methods, especially for optical recognition.
- Further experiments for blue laser sensor should be planned with scrap sample combined with identified Cu source.
- For the applied different architectures of CNNs, more experiments should be planned to identify the one with best performance to further optimize the accuracy.
- The feasibility of slagging method should be further investigated considering its application to the industrial ladle furnace.

References

1. Rosebrock, Adrian (2017) "Imagenet: Vggnet, resnet, inception, and xception with keras."

2. https://www.geeksforgeeks.org/underfitting-and-overfitting-in-machine-learning/

3. He, Kaiming, et al. "Deep residual learning for image recognition." Proceedings of the IEEE conference on computer vision and pattern recognition. 2016.

4. Milton-Barker, Adam. "Inception V3 Deep Convolutional Architecture for Classifying Acute Myeloid/Lymphoblastic Leukemia". intel.com. Intel. Retrieved 2 February 2019.

5. Chollet, François. "Xception: Deep learning with depth wise separable convolutions." Proceedings of the IEEE conference on computer vision and pattern recognition. 2017.

6. Szegedy, Christian, et al. "Inception-v4, inception-resnet and the impact of residual connections on learning." Thirty-first AAAI conference on artificial intelligence. 2017.

7. Fruehan, R. J., et al. (2000) Theoretical minimum energies to produce steel for selected conditions. Carnegie Mellon University, Pittsburgh, PA (US); Energetics, Inc., Columbia, MD (US).

Appendix – A: Literature Review

This page left BLANK intentionally

Review of Impurity Removal Methods in Steel Scrap Recycling

Abstract

Impurities in steel scraps, such as copper and tin, have been identified as barriers limiting the use of recycled steel for producing certain grades of steel. Their accumulation during the whole recycling process could induce detrimental effects on the surface quality of downstream steel products, resulting from the penetration of Cu-enrich phase into grain boundaries during hot working would appear at 0.1wt% Cu content or above. In order to eliminate such detrimental effects, impurity removal methods have been researched considering the physical separation and chemical treatment at different stages of steel scrap recycling. For physical separation, apart from regular shredding and magnetic separation, different types of sensor-based sorting can be introduced. For chemical treatment, different technologies are introduced and classified according to the existent state of steel scrap. In this review, possibilities and limitations of these methods have been presented and discussed based on their removal mechanism to weigh their applicability. It becomes evident that sensor-based sortation would be feasible if specific physical or chemical characteristics of steel scrap can be identified. Considering chemical treatment, most of the technologies were just demonstrated with laboratory scale and limited industrial applicability due to the involving either high temperature or vacuum or chemicals.

Key words: Scrap recycling, impurities, hot shortness, physical separation, chemical separation

1. Introduction

Steel recycling can be treated as a full-developed industry in the world, including scrap collecting, processing and utilizing [1]. Due to the energy and raw materials intensive nature of the industry and strict environmental policies, steel practitioners must take energy costs and environment protection into consideration during steelmaking, promoting the recycling of waste and by-products. When considering the industry beyond primary steelmaking, steel scrap has become indispensable as a valuable secondary resource. Traditional large integrated steel plants mainly use coke as a reductant. The major source of energy in iron and steelmaking is the embedded energy in coal, used for reducing iron ore. Of the 17 GJ it takes to produce 1,000 kg of steel strip, (and corresponding emission of 2000 kg CO_2), 14 GJ (and 1560 kg of emitted CO_2) can be eliminated if this C-based reducing process can be replaced with scrap via recycling [2]. A further reduction is indirectly achieved outside of the steel plant since the C-free process eliminates coke-making and agglomeration. That means a lower energy consuming and raw-material flexible steelmaking process can be formalized by incorporating steel recycling. These obvious advantages urge steel practitioners and researchers to enlarge the utilization of steel scraps. However, the quality of steel scraps from different sources could severely hinder this desirability.

Generally, scrap collectors gather steel scraps from steelmaking plants, manufacturing plants, and consumers at end-of-life. Based on these origins, steel scraps can be subdivided into three categories, home, process and old scrap. In steelmaking plants, metal can be collected from the surrounding of furnaces, ladles and slags, and casting molds as home scrap. In manufacturing plants, process scrap can be produced during cutting, drawing, rolling, or shaping [3]. Both of these sources have high purity and can be directly recycled to the BOF or EAF units. Old scrap, also called obsolete scrap, mainly comes from discarded consumer (end-of-life) products. Due to the complicated assembly and integration, this type of scrap contains components or materials that make up the major source of impurities and can downgrade the recycling value [4]. According to the up-to-date statistics from U.S. Geological Survey [5], old scrap can account for 58% of recycled steel scrap in United State, along with 24% process scrap and 18% home scrap.

As estimated by Hiroki Hatayama [6], steel stock consumed by three major end uses could rise from 25,000 billion kg in 2020 to 55,000 billion kg in 2050, which consists of approximately 55% building, 33% civil engineering and 12% vehicles. However, in United States, the lifetime duration of civil engineering and building could be 67 years, comparing to 17 years for vehicles, which is crucial for the recycling of old scrap [7]. Thus, all these factors contribute to the increasing of automotive scrap as the primary source of steel scrap.

The commonly mentioned impurities in steel scraps include Cu, Sn and Zn. Among these contaminating elements, Cu and Sn are the primary concern relating to “hot shortness”. Volume 5 of the Metals handbook [8] gives the following definition of hot shortness: “Hot brittleness in metal in the hot forging range”. It is a phenomenon that occurs commonly on the surface of steel, whenever it is exposed to oxidizing conditions and some form of mechanical deformation, e.g. cooling from the continuous casting and re-heating followed by hot-rolling. Preferential oxidation of iron in Fe-alloys containing residuals, leaves the more noble elements, Cu and Sn as a separate molten phase which causes embrittlement in the underlying steel [9]. At 0.1wt% Cu content and 0.04wt% Sn content or above [10], a Cu-enriched phase can be found which will penetrate into grain boundaries under the forging force, causing cracking. The role of Sn in this phenomenon is to lower the solubility of Cu in the γ-Fe austenite phase and the melting point of the Cu-rich phase. Studies on the use of high Zn content scrap shows no adverse effect on the mechanical properties of the produced steel, however dust emissions are problematic relative to environment control.

For further understanding, the composition of different types of scrap and allowable limits of scrap residuals in the manufacture of steel products are demonstrated in Table 1-1 and Table 1-2 [11]. As shown in Table 1-1, comparing to Table 1-2, only reinforcing bar, which has a higher tolerance, can be produced using old scrap directly. For interstitial free (IF) steel, which is mainly sourced into automotive production, the use of only common scrap is unacceptable. As a result, dilution with virgin iron in EAF has been the most practical method. The required virgin iron for diluting Cu content to achieve the allowable limit is also shown in Table 1-2, according to the equation (1-1). Apparently, impurities have been an important barrier limiting the use of recycled scrap. Therefore, various technologies have been investigated to overcome the impurity problem, as will be described in the following sections.

Table 1-1: Composition of different types of steel scrap

Scrap Category		Chemical composition, wt%				
		Cu	Sn	Ni	Cr	Zn
Obsolete	Shredded car scrap	0.230	0.052	0.069	0.123	0.05
	Heavy scrap	0.234	0.017	0.070	0.130	0.210
	Can scrap	0.050	0.128	0.032	0.061	0.000
Process	Factory bundle	0.027	0.002	0.020	0.031	0.700
Home	Steel	0.021	0.010	0.020	0.030	0.010
	Pig iron	0.010	0.002	0.020	0.020	0.002

Table 1-2: Allowable limits (wt%) of scrap residuals in the manufacture of steel product and required virgin iron for dilution

Steel Product	Allowable Limit of Cu wt%	Estimated Cu wt% of Steel Product	Average Fe wt% of Virgin Iron	Blending Virgin Iron per tonne of Steel Scrap (kg)
IF	0.03wt%	0.25wt% [12]	94wt% (95.7wt% for pig iron, 93wt% for HBI, and 94wt% for DRI) [13]	7,801 kg
DDQ	0.04wt%			5,585 kg
Drawing	0.06wt%			3,369 kg
Commercial	0.1wt%			1,596 kg
Structural	0.12wt%			1,152 kg
Fine-wire	0.07wt%			2,736 kg
Rebar	0.4wt%			No need for dilution

$$Required\ virgin\ iron = \frac{\frac{Cuwt\%\ of\ steel\ scrap - Cuwt\%\ of\ steel\ product}{Cuwt\%\ of\ steel\ product} \times Weight\ of\ Steel\ Scrap}{Average\ Fe\ wt\%\ of\ virgin\ iron} \times 100 \quad (1-1)$$

2. Physical Separation

Physical separation is the primary method of impurity removal in shredding plant facilities. Whether this process is efficient and useful, or not, depends on the nature of feed materials and the extent of liberation, such as dismantling and size reduction (shredding). For certain materials, for example to liberate metallic Sn and Zn from tinplate and galvanized steel scrap, normal shredding is ineffective, since these elements are either dissolved inside or strongly bonded to the steel. Therefore, chemical treatment is preferred for Sn and Zn removal.

Obsolete automobiles occupy the majority of steel recycled processed materials. Other post-consumer products, such as refrigerators, washers, municipal wastes and industrial wastes, are also recycled in significant proportions. For these scrap sources, the dismantling of Cu motors and wires, as the major source of Cu contamination, would be limited to those units of larger sizes when considering the costs and benefits. The problem is compounded during hammer shredding when smaller copper motors and wires become enmeshed and tangled within the steel shreds. Therefore, during the subsequent magnetic separation this lack of practical liberation results in a reduced separation efficiency, perhaps 80% or less, for the Cu contaminants [10]. This situation is also the obstacle to the application of eddy current separation. As a result, shredded pieces containing metallic Cu separate to the Fe shred stream.

Generally, shredding plants can maintain the final Cu content in steel scraps between 0.2-0.3wt% with 70-80% Cu removal rate [12]. If handpicking was incorporated after shredding and magnetic separating, the final Cu content could reach 0.1wt% [14]. However, handpicking is labor intensive and can

only be cost-balanced if the copper price is high. Also, expensive sophisticated shredding, such as high density shredding and cryogenic shredding, could be applied to obtain a better liberation, improving the efficiency of subsequent magnetic separation. Sicon [15], a recycling company, focuses on high density shredding, which can reduce the size of shredded scrap to 40-50 mm, contributing to the effective removal of Cu to nominally about 0.1wt% [10]. However, lower processing rates and high cost would be a concern. Cryogenic shredding, via cooling the feed in liquid nitrogen, results in improved liberation at <10mm particle size. This cryogenic shredding has been shown to produce a magnetic separation product containing a lowered Cu content of 0.04-0.06wt%. However, 500-1,000 kg liquid nitrogen is consumed for cooling 1,000 kg of scraps, resulting in high capital and operating costs [16].

Due to the limitations of shredding and magnetic separation, more and more sensor-based technologies have been investigated to support sortation as a method for Cu rejection from Fe shreds. With the capability of detecting and examining each individual shred-piece based on different mechanisms, corresponding signals might be generated by the sensor and transmitted to the analysis system, i.e., the computer. Through analyzing signals with customized sorting standards, this system can derive a yes/no decision for actuating the ejection system positioned at the end of the conveyor. As a result, the unwanted pieces can be ejected by an amplified mechanical, hydraulic or pneumatic equipment. Identifying the difference in physical and/or chemical properties between Cu and Fe can be the key factor to build a suitable sorting standard. The most obvious characteristics of Cu are its excellent electric conductivity and the reddish brown color. There are other spectrums unique to Cu such as X-ray, gamma ray and lasers that may present feasible technologies to distinguish Cu pieces mixed in Fe sheds. The basic configuration of sensor-based sorting methods is showed in Figure 2-1 [17]. More details will be discussed in the following sections with reference to different types of sensors.

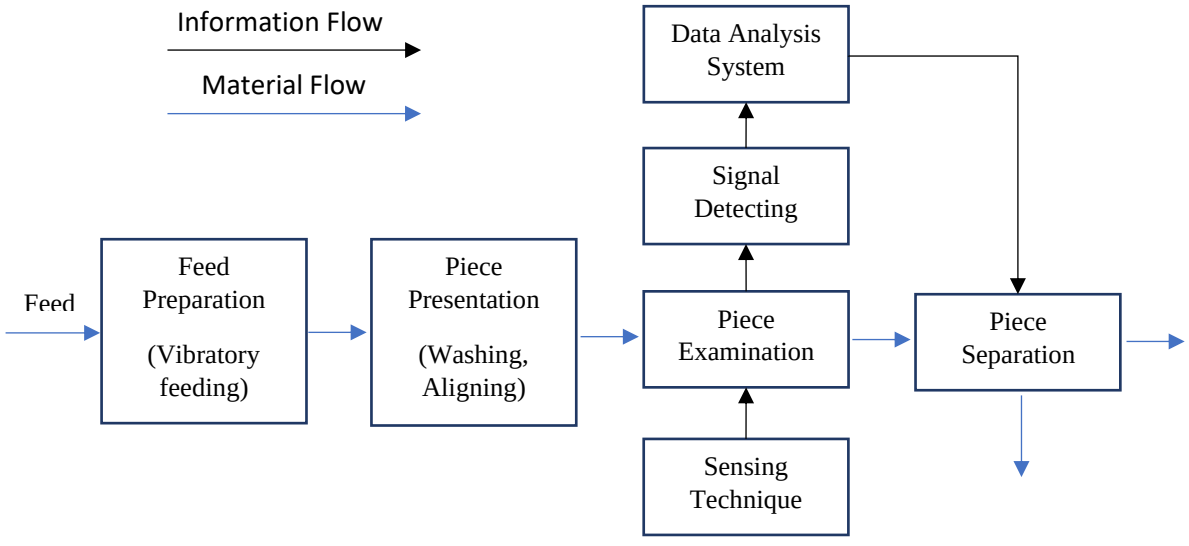

Figure 2-1 Basic configuration of sensor-based sorting

(1) Color Sensor

RGB (red green blue) line scan cameras are commonly equipped as a color sensor to distinguish different color values. Many researchers also combine 3D detection with RGB data to produce shape information. After analyzing and integrating using a design program, topographical color images of each shredded piece on the conveyor can be generated. Based on customized sorting criteria, an individual object, which has a certain percent of specific color in the image, such as reddish brown, can be recognized, classified and ejected. High resolution cameras can efficiently increase the quality of images and decrease the analysis time. However, a high level of surface cleanliness would be required to obtain efficient scanning, posing an obvious problem for steel scraps. Additional washing and cleaning might be needed before sortation. But the development and application of machine learning for image classification can improve the result of sortation and might eliminate this disadvantage, since the analysis program can be trained ahead with the same condition of cleanliness as sorting.

Fumio Tanaka et al. [18] applied the TV camera to image individual pieces of shredded scrap, including their position data, and analyzed the hue angle and saturation value of every point in the image. Then Cu was labeled and discriminated with the range of saturation value ($0.3 \leq S \leq 1.0$) and hue angle ($0^o \leq H \leq 52^o$ and $329^o \leq H \leq 360^o$). Calculating the ratio of the area discriminated to be Cu to the total area in each piece as a standard, pieces identified as copper-containing were separated at the end of the conveyor. The speed of conveyor was 1 m/s due to the processing time of images. The removal rate could be 100% for the scale of 1,000 kg scraps.

(2) XRT & XRF

X-ray, as a type of electromagnetic radiation with a wavelength between 0.001 nm and 80 nm, is widely used in the laboratory and industry. Based on different working mechanisms, X-ray fluorescence (XRF) and X-ray transmittance (XRT) can both be applied as a type of sensor.

When the incident primary X-ray radiation from the X-ray tube above the conveyor penetrates into shredded pieces of steel scrap, excitation and emission of electrons can be detected due to high radiation energy. Vacancies created by this process can be refilled by the electron from the outer shell. The refilling and transferring of electrons will lead to energy emitting as secondary fluorescence radiation, which is a key characteristic for each element. Detectors, positioned around the conveyor, can capture the second radiation as a transmitted signal, which can be analyzed into the elemental composition of each piece. Then

ejection criteria for one element Cu or a ratio of Cu and Fe can be set to achieve the sortation. This is the mechanism of XRF sorting.

Another commercial sensor is based on X-ray transmission (XRT) where the excitation and emission of electrons can be understood as energy absorption of primary radiation. This absorption information, which is distinct for each element relating to the element's atomic weight, is collected by detectors under the conveyor and then processed into a detailed "density image". The density area of Cu reflects a deeper color than the density area of Fe in the "density image" due to their differences in atomic weight. Moreover, dual energy XRT system comprising two channels has been adopted to eliminate the deviation through capturing the absorption information in different X-ray energy level. The produced "density image" demonstrates different shades of gray with higher accuracy.

Attributing to the ability of non-destructive penetration, applying X-ray technologies shows good performance without considering the color, or the presence of labels or other impurities. However, XRT sorting can be complicated by the thickness of shredded pieces, i.e., absorption information could also vary with different shreds/particle thickness. As a result, the deeper color area in the "density image" may be effected by thickness and not the higher atomic weight. So appropriate shredding must be achieved to obtain a uniform shape. This would mean that a sophisticated feeding system is required, such as a vibrating feeder, to facilitate placement of a single layer of shreds (no overlapping) on the conveyor, upstream of the sensors.

Günter Buzanich [19] studied a new XRF sorting system from LLA Instruments GnbH with more complicated algorithms to distinguish the copper-containing particles. Composition data could be obtained using measurement times of 0.001 s and 25 mm resolution corresponding to 2.5 m/s belt velocity.

(3) PGNAA

Another type of electromagnetic radiation, Gamma rays, can also be used to simultaneously indicate the presence and amount of different elements. As shown in Figure 2-2, neutrons emitted by the source can penetrate into the target medium of materials and interact with the nuclei of elements present. During this interaction, nuclei will be excited to a high energy level by consuming the energy of neutron. Subsequent return to the original level will rapidly produce gamma rays that can be recognized as a key characteristic of the elements present in the target material.

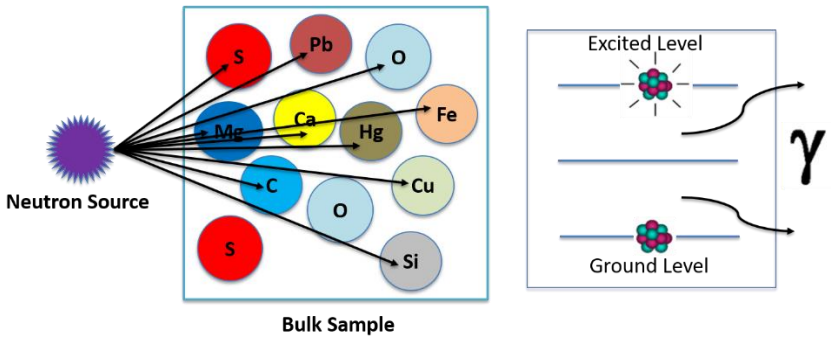

Figure 2-2 Mechanism of gamma ray generation

Based on this mechanism, Prompt Gamma Neutron Activation Analysis (PGNAA) has been applied to measure the elemental composition of bulk materials. During the analysis, Californium-252 (Cf-252) is adopted as a reliable neutron source with lower cost and higher safety than other sources. The emitted gamma rays are captured by detectors and then analyzed by a multi-channel system in the form of spectral energy peaks. Gamma rays of a certain energy are used for qualitative analysis and their intensity is used for quantitative analysis. After a complex calculation, the elemental composition of materials can be determined.

Like X-ray, PGNAA can adapted to achieve a real-time analysis without being influenced by the surface cleanliness of steel scraps. Because of the complex spectrum, which may contain hundreds of energy peaks, a calibration must be performed to eliminate the significant unwanted “noise/disturbance” from the environment. Meanwhile safety factors and maintenance costs must be considered for use of the selected radioisotope.

More importantly, PGNAA is not suitable for piece-by-piece analysis. Alvin D, Shulman [20] proposed that shredded scrap stream could be divided into increments and then analyzed by PGNAA to obtain the composition of the bulk. He suggested PGNAA should be used as a real-time composition analyzer combined with a bulk sorting system. The bulk, which did not conform to the composition standard, such as 0.2wt% Cu, would be diverted to a stockpile.

(4) LIBS

With respect to compositional analysis, Laser Induced Breakdown Spectroscopy (LIBS) has become an applicable method to quickly identify the elemental composition of materials. A pulsed laser beam with high energy is generated to spot the surface of shredded pieces. When this irradiated laser reaches a certain threshold level, optical breakdown will happen as laser ablation. Ablated atoms from different elements on the surface interact with the pulsed laser to generate a highly energetic plasma, including

released electrons, excited atoms and ions. After the laser pulse, the excited electrons return to a neutral state which results in emitting light with different frequencies. Then the emitted light can be detected by optical emission spectrograph detectors and analyzed by the supporting analysis system to produce a diagram with characteristic spectral peaks. With identification and interpretation, the elemental composition of the target is determined. Similar to PGNAA, calibration is also required in order to obtain high accuracy. Shunsuke Kashiwakura [21] et al. applied JISF FXS 350-352, which were a series of Fe-Cu binary alloy with certified Cu content, as standard reference materials to optimize calibration lines. Parameters of the pulse laser, such as energy and duration, were 80 MJ/pulse and 16-18 ns, respectively. They found Cu-I with the wavelength of 327.396 nm worked better as the calibration line, due to less spectral interference. In addition, multiple pulsed laser shots (200) offered a precise detection of 0.004wt% Cu.

The most significant restriction of LIBS is that the produced analysis results only demonstrate the condition of the surface. This could lead to deviation in heterogeneous materials, especially for steel scraps with inappropriate liberation and surface condition. This could, however, be mitigated by repeatedly spotting the laser in the same position to measure the depth profile of materials.

(5) Discussion

Although the incorporating of sensor-based sorting can improve the impurity removal in steel scrap recycling, the decision whether this new technology could be accepted by shredding plants or not mainly depends on the economic consideration, especially the capital and operating cost. For LIBS, PGNAA, XRF and XRT, capital investment would be very high for large capacity plants. Accessory equipment, such as multi-channel conveyors and washing and ejection systems, will be a major part of the cost. Except for electricity and labor, the majority of the operating cost is the consumption of compressed air, which is widely used as a method to blast the unwanted piece. Generally, in USA, the cost of compressed air is about $ 0.3-0.7 per tonne of feed [17]. Maintenance costs depends on the techniques used for sorting, such as LIBS and PGNAA, which would be treated as high maintenance-intensive.

3. Chemical Treatment

It is evident that the efficiency of physical separation is subject to the geometry features and properties of shredded steel scraps, i.e., liberation. One way to overcome the physical liberation issue is to consider chemical treatment in the melt using diffusion or reaction of impurities without the loss of Fe. Chemical treatment can be considered in two categories, either as a pretreatment or during smelting.

(1) Impurities removal during pretreatment in the melt

Impurities, such as Cu, Sn and Zn, all have a lower melting point compared to Fe. But from a thermodynamic point of view, Cu and Sn are nobler than Fe. Under this circumstance, with proper chemistry and temperature there is a possibility of preferential dissolution or reaction with impurities, while Fe (steel) could be maintained in a solid state. Technologies under this category are classified according to the use of chemical additions/control, in solution, slag, metal, and gas states.

A. Aqueous solution

The process involved can be treated as a hydrometallurgical method, including leaching and electrochemical extracting. The most widely used reagent to leach Cu is ammonia solution, which has a competitive advantage that it doesn't react with Fe. Hirokazu Konishi [22] et al. studied the dissolution of Cu in an ammonia solution and found that a copper sheet with the size of $20\times20\times10$ mm^3 totally dissolved after 12 min at 353 K. Different acid solutions, such as HCl and H_2SO_4, could also be used to leach Cu, Sn and Zn from steel scraps. However, one significant restriction of this process is that the acid would also be corrosive to Fe. Sedar Aktas [23] et al. stripped and recovered Zn from galvanized scraps using sulfuric acid with a pH value of 0.2 and found that the obtained solution contained 0.2 g/l Fe. Although a 100% removal rate of impurities could be obtained, the leaching processes was time-consuming, which would make them not suitable for industrial scale up.

Reversing the electroplating process for tinplate and galvanized steel is a possibility for removing Sn and Zn. It might be applied to remove Cu, even if Cu is not presented as a coating material. Scrap, conceivably bundles from shredding plants, are used as the anode and immersed into the electrolyte to achieve this reversed process. Der-Tau Chin [24] studied different electrolytes, such as ammoniacal carbonate and alkaline cyanide solution, to dissolve Cu anodically from steel scrap at room temperature. He found using an alkaline cyanide solution, the Cu content of anode (60 g of scrap) could be reduced to 0.06wt% in 7 hours with a cell current of 200 mA. As studied by D. Janke et al. [4], electrolytic detinning has already been applied at industrial scale. Tinplate scrap bundles, as the anode, were immersed into a hot caustic soda bath (358 K). This process could reduce the tin content to 0.02wt%, and be economically efficient with an annual capacity of 3×10^7 kg. Also immersing tinplate bundles, $40\times60\times60$ cm (about 160 kg), into 11% NaOH bath at 353 K, Hendrik Giezen et al. [25] reached the same tin content by maintaining 1800 A current about 8 hours. The same electrolytic process of detinning can be adopted to dezinc. Frederick J. Dudek et al. [26] investigated this process in hot NaOH solution (343-363 K) and scaled up to 1×10^6 kg pilot test. The zinc content could be reduced to below 0.01wt% with an estimated cost in the \$0.025-0.050/kg range, over 6-24 hours.

Based on above analysis, higher impurity removal rate could be achieved with the use of aqueous solution. However, this hydrometallurgical process could be impacted by the extent of impurity exposure to the solution, becoming time-consuming.

B. Slag

Under specific temperatures with iron scrap (steel) in solid state, molten slag could be used as a flux to induce a surface reaction with impurities. The diffusion of impurities to the surface could be a restriction on the reacting speed and removal rate. R. J. Fruehan et al. [27] investigated Cu removal using sulfur matte containing FeS and Na_2S. His investigation was based on adding 15-20% Na_2S to decrease the melting point of the matte and the activity coefficient of Cu_2S. Reaction (3-1) was carried out at 1273 K in a rotary kiln with 6kg of matte per ton of scrap. This reaction could be rapid (5 min) compared to the forming time of molten matte (30-40 min).

$$FeS + 2Cu = Cu_2S + Fe \quad \Delta G^o = -13.64 \text{ kJ/mol} \tag{3-1}$$

For this process, the removal rate of Cu could reach 90%. However, there are limitations. Firstly, in order to avoid SO_2 off gas and the oxidation of Fe, the atmosphere in the rotary kiln must be controlled. Secondly, an additional cleaning step would be required before delivering the pretreated scrap into an EAF because of the adhesion of molten matte. Also during the reaction, dissolution of [S] from molten matte might be possible to induce sulfur contamination in the downstream steelmaking.

Based on the thermodynamic data, Reaction 3-3 does not have the potential to move forward at this temperature, while Reaction 3-2 shows a good potential. No detailed papers relating to Zn can be found. A possible reason is that Zn will evaporate quickly before Reaction 3-2 can proceed.

$$FeS + Zn = ZnS + Fe \quad \Delta G^o = -59.40 \text{ kJ/mol (T=1273 K)} \tag{3-2}$$

$$FeS + Sn = SnS + Fe \quad \Delta G^o = 20.82 \text{ kJ/mol (T=1273 K)} \tag{3-3}$$

C. Metal

There is no chemical reaction involved in this process. The mechanism is simply based on the thermodynamic activity of impurities behaving differently in the Fe scrap in the presence a chosen metal solvent, such as Al, Mg, or their alloys. Normally, Cu, Sn and Zn all have lower activity in molten aluminum compared to the unit activity in Fe. Therefore, diffusion into molten aluminum was predicted at the interface. Masanori Iwse et al. [28] carried out diffusion in a rotary kiln at 1073 K, mainly focusing on Cu removal. As a result, the Cu content of 1kg of scrap fluxed with 100 g of alloy, which contained 20-30wt% Al/Mg, could be reduced from 0.6 to 0.1wt%. A higher removal rate could be reached by repeating this

process. However, repeating could lead to unacceptable levels of Fe in the molten aluminum. Due to the diffusion and dissolution of Cu and Fe with higher melting point, maintaining molten state of aluminum at 1073 K could be so affected that it would be difficult to peel the metal solvent from scrap after the whole process.

D. Gas

Although Cu and Sn have a lower oxygen affinity than Fe, oxidation could still be a possible way for their removal at a certain temperature, especially for Zn with lower melting point and higher oxidation potential. The main reason is that the formed oxidation layer of Fe can be dense and prevent a further reaction between Fe and oxygen. For Cu, continuous oxidation could be observed due to the spallation of formed oxidation layer. However, this method could be only applied to Cu impurities exposed to the surface or existed independently. Otherwise, the formed oxidation layer of Fe could also inhibit the further oxidation of Cu impurities existed as alloying element or inclusion. In Weol Dong Cho's study [29], this process was carried out at 673-973 K with an atmosphere of 40% oxygen and 60% Ar. As described in the research, copper in the ferrous scrap sample was presented independently. After about 4-6 hours of oxidation, most of the copper oxide could be removed by simple impacting. In addition, a CaO/Na_2O-SiO_2-B_2O_3-based slag was used to flux the oxidized scrap at a temperature of 1000-1473 K. During this fluxing, copper oxide could be totally dissolved into the molten slag in about 100 minutes. Therefore, the removal rate approached 99% in his laboratory test. K. Ogawa and H. Matsumoto [16] studied the oxidation of tin coating at 1223 K in a rotary furnace containing tungsten balls. The removal rate approached 40% for 2 kg scrap in about 15 minutes.

Based on the thermodynamic data at 773 K, it is evident that

$$2Cu + S(g) = Cu_2S \qquad \Delta G^o = -277.49 \text{ kJ/mol} \tag{3-4}$$

$$Sn + S(g) = SnS \qquad \Delta G^o = -273.30 \text{ kJ/mol} \tag{3-5}$$

$$Zn + S(g) = ZnS \qquad \Delta G^o = -362.42 \text{ kJ/mol} \tag{3-6}$$

Copper, Sn and Zn all have a good potential to react with sulfur gas, as well as Fe. Similar to oxidation, the formed iron sulfide layer could not only stop the further reaction between Fe and sulfur gas, but also limit the impurity removal. K. Onuki and T. Tokumitsu [16] investigated the removal of tin coating using sulfur-containing gas at 773 K. The formed brittle stannous sulfide (SnS) could be peeled by impacting with about 70% removal efficiency. In addition, due to the toxicity of sulfur, careful atmosphere control was required during the reaction step. These limitations would increase the difficulty during any industrial application.

Researchers have speculated that ASR combustion gas from an EAF could be recycled and used as the source of sulfur-containing gas to pretreat the steel scrap.

Chlorine gas is another possibility for removal of Cu, Sn and Zn. This gas is inexpensive and readily available, as compared to sulfur gas. Additionally, the use of PVC combustion gas as the source of chlorine has been investigated to increase energy efficiency and decrease costs. Based on the phase stability diagram of Fe-O_2-Cl_2, Cu-O_2-Cl_2 and Zn-O_2-Cl_2 systems, for Cu and Zn, the prevailing phase is chloride. Ferric oxide can also be used for removal as shown in Figure 3-1 and Figure 3-2. Temperature applied in these diagrams are referenced from related literatures. With this thermodynamic understanding, the gaseous mixture of air and chlorine may be a better choice because the chloride of Cu and Zn becomes volatile with the increasing of temperature. In addition, a protective layer, mostly Fe_2O_3, is formed to prevent the steel body from corrosion by chlorine.

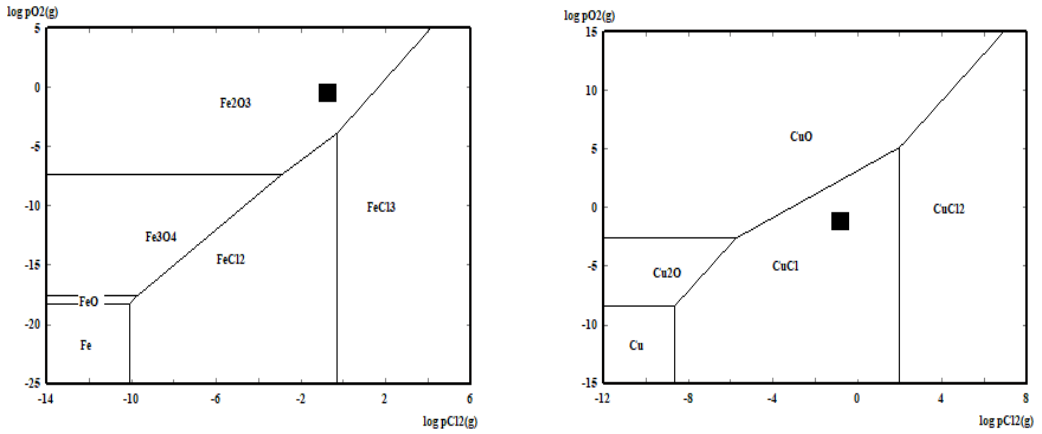

Figure 3-1 Phase stability diagram for Fe-O_2-Cl_2 and Cu-O_2-Cl_2 at 1100 K

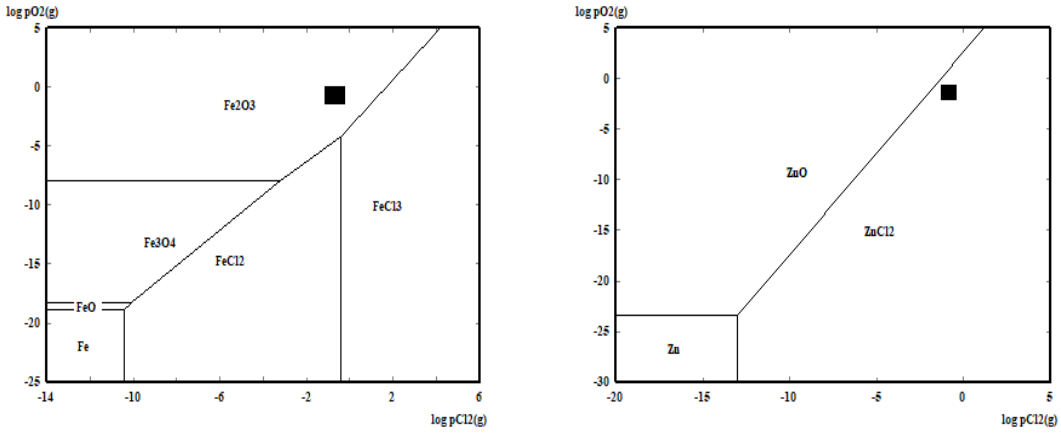

Figure 3-2 Phase stability diagram for Fe-O_2-Cl_2 and Zn-O_2-Cl_2 at 1073 K

Koji Matsumaru et al. [30] applied this process to an iron sheet (10mm×10mm×1mm) twined with copper wire (1mm diameter) at 1100 K with the gas composition of O_2-10%Cl_2. They found that the copper wire could be totally volatilized in 30 minutes. A. D. Hartman, et al. [31] used chlorine, hydrogen and air to remove Cu. For 3.5 kg scraps, the removal rate could be 74% within 90 mins.

F. Tailoka, R. V. Kumar & D. J. Fray [32] applied this process to remove Sn from tinplate at 403-473 K with the volume ratio of air and chlorine maintaining 10:1. Large scale test with 1kg baled tinplate scraps was carried out. The tin content could be reduced from 0.25wt% to 0.078wt% in 41 hours and to 0.039wt% in 81 hours. According to the phase stability diagram of Sn-O_2-Cl_2 system, as shown in Figure 3-3, tin oxide should be the prevailing phase at this range of temperature. But stannic chloride could be collected as $SnCl_4 \cdot 5H_2O$ in their research. More analysis would be conducted refer to the equilibrium composition and thermodynamic data of related reactions.

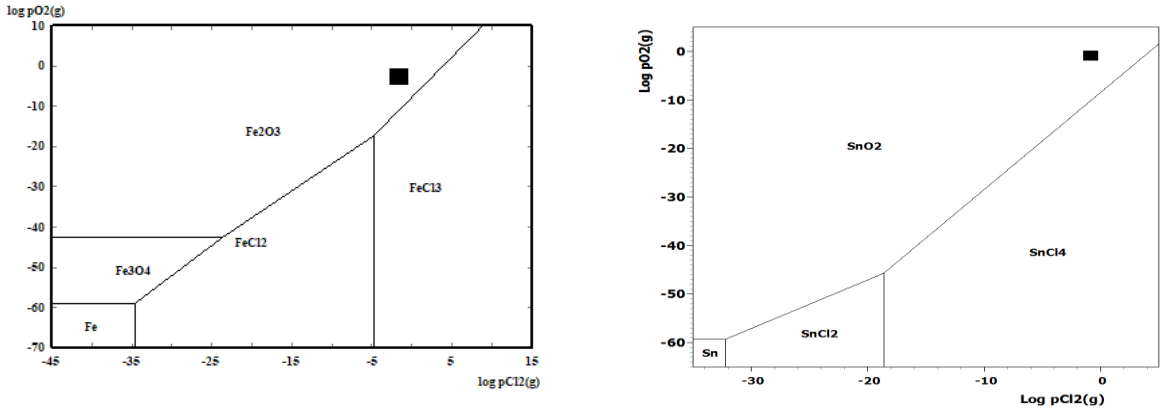

Figure 3-3 Phase stability diagram for Fe-O_2-Cl_2 and Sn-O_2-Cl_2 at 430 K

J. K. S. Tee and D. J. Fray [33,34] also investigated this process to remove Cu and Zn at 1073 K with an air/chlorine flowrate of 400/40 cm^3min^{-1}. The Cu content could be reduced from about 1wt% to 0.05wt% after 10 minutes, using an iron sheet (23 g) wound with copper windings (225 mg) as sample. Also the removal rate of Zn could be 97% in 10 minutes, using galvanized steel sheet (10 mm×5 mm) as sample.

For Zn, the increasing of temperature can easily enhance its evaporation. Bahri ozturk and R. J. Fruehan [35] studied zinc vaporization of galvanized scraps under different atmospheres. At 1123 K, they found that under N_2 atmosphere the removal rate of Zn could be 70% in the first 3 minutes and reach 97% in 50 minutes. Under CO atmosphere, the same removal rate could be reached in 10 minutes at the same temperature.

We can conclude that pretreatment with different types of reagent is subject to the extent of impurities exposure or their diffusion rate to the surface, correlating with the removal rate and time. Especially for the use of gas, the formed protective layer could not only reduce the loss of Fe, but also hinder the further impurity removal reactions. As a result, pretreatment involving solid steel scrap could be a diffusion controlled process and may not be the most appropriate option to remove impurities.

(2) Impurities removal during smelting

Whether the applied technologies for physical separation and pretreatment demonstrate good removal performance or not, the smelting of steel scraps is an essential step in its recycling. In steelmaking plants, the electric arc furnace (EAF) is commonly used. During the transferring of molten steel scrap in ladles, degassing, decarbonizing, and desulfurizing is controlled for the preparation of final steel products. In order to better understand the distribution of element occurrence in the process of steelmaking, Kenichi Nakajima et al. [36] applied thermodynamic analysis to illustrate the distribution tendency of elements among the metal, slag and gas phases. Based on their methodology, the distribution ratio can be calculated with thermodynamic data from published literature and following assumptions: x_m=0.01(mol fraction), P_{O2}=1.9×10^{-5} Pa, P_{Fe}=8.5 Pa and T=1873 K.

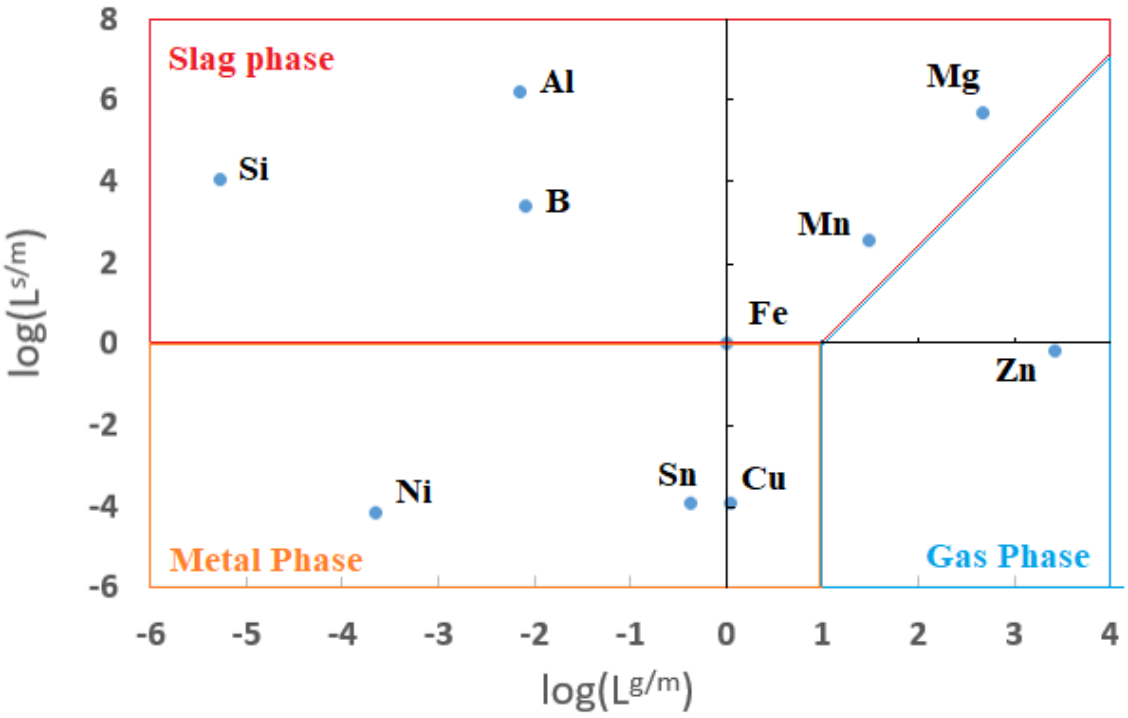

Figure 3-4 Distribution chart of elements among metal, slag and gas phase

As shown in Figure 3-4, Zn can be easily vaporized into the gas phase during smelting and removed as fume. The only concern is its recovery. Due to the constraining environmental regulations, landfill cannot be used to dispose of the fume. In addition, the Zn content in the dust may not be high enough to promote effective recovery. Certainly, Cu and Sn remain stable in the metal phase during smelting. Therefore, the target for different technologies in this category is to facilitate the volatilization or diffusion of Cu and Sn, either directly into gas phase or through reacting with slag to form volatile compounds.

A. Separation into a gas phase

According to the thermochemical database, the vapor pressures for pure Cu and Sn are 123 and 121 Pa, respectively, at a temperature of 1873 K, while the pure Fe vapor pressure is 80 Pa. Thusly, the higher vapor pressure could facilitate the diffusion of Cu and Sn into the gas phase, through volatilization. However, the pressure difference between impurities and Fe is not significant enough to achieve significant differential separation. Alternative atmospheres have been investigated to promote and improve the volatilization of Cu and Sn, such as vacuum, blowing NH_3 and Ar-H_2 plasma.

Luben Savov and Dieter Janke [37] investigated the evaporation of Cu and Sn from 20kg iron-based molten bath at reduced pressure in a laboratory-scale vacuum induction melting furnace. They confirmed that the evaporation of Cu and Sn could be classified as a first order reaction at1873 K. The rate of evaporation increased with a decrease of pressure, especially at 10Pa. However, the removal rate of Cu and Sn were only 75% and 43% in 60 minutes, respectively, which could be insufficient for a commercial scale. Sung-hoon Jung and Youn-bae Kang [38] found that the evaporation of Cu and Sn from molten Fe could be accelerated with high S content at 1873 K, due to the formation of CuS and SnS.

Meanwhile, Janke [37] mentioned that higher temperatures could improve the volatilization rate of Cu and Sn. So plasma could be a way to provide sufficient temperature. Tohru Matsuo [39] adopted Ar-H_2 plasma at 10^5 Pa to remove Cu and Sn from 1.5 kg of molten Fe. The temperature at the hot spot could be 2323 K. Maximum removal rate of Cu and Sn were about 90% and 60%, respectively, in 2 hours. Also reduced pressure, such as 1.3×10^4 - 2.0×10^4 Pa, and higher H_2 content and gas flow rate could increase the removal rate. One significant disadvantage of this technology is the high cost of plasma generation, especially for industrial capacity.

Other than pressure and temperature, another factor that could control the volatilization rate of Cu and Sn from Fe is the specific surface area of the molten bath, described as the ratio of surface area to the volume. Blowing gas could induce turbulence in the molten bath to increase the surface area. R.O. Suzuki and K. Ono [40] improved the volatilization of Cu by blowing NH_3 gas in a laboratory test at 1900 K. Under a 2000 Pa pressure, the Cu content of 1kg molten Fe was reduced from 0.2wt% to 0.0002wt% in about 100

minutes. They suggested that the formation of unstable and volatile compounds, CuN_x or CuH, could be beneficial for increasing the volatilization rate. Later, Naotaka Sasahi et al. [41] developed a similar fundamental study to remove Sn at 1723 K and 2000 Pa. During the blowing, NH_3 gas decomposed into N_2 and H_2, which bubbled and agitated the molten bath. They believed that SnS would be the major volatilized species, rather than Sn-nitride or Sn-hydride. For a plant scale of 1×10^5 kg of hot metal with 0.05wt% dissolved sulfur [S], the removal rate could be 40% in 20 minutes. After this process, desulfurization would be required to eliminate the effect of excess sulfur in the steel product.

Tohru Matsuo et al. [42] initiated a nominally 1,000 kg scale experiment by blowing weak oxidizing powder, which could also be used for decarburization, to remove Cu and Sn from molten Fe (1923 K) under reduced pressure of about 130 Pa. The oxidizing powder, such as SiO_2, was decomposed to form dissolved oxygen [O], which could induce fine CO bubbles to agitate the surface due to the presence of dissolved carbon [C]. However, this method did not show a good removal rate of only 30% for both Cu and Sn in 2 hours. The removal rate of Sn could reach 80% with a high [S] content (0.1wt%) feed stock. Also combining this process with plasma heating could increase the removal rate of Cu and Sn by 2-3 times.

For the volatilization of Cu and Sn, the surface of the molten bath must be free from blocking by slag formation and reaction products. However, during the steelmaking process, slags are widely used to protect the oxidation of molten Fe. In addition, maintaining high vacuum and different atmospheres in the industrial vacuum furnace could be difficult to achieve, resulting in increasing operating costs.

B. Diffusing into slag phase

This process shares the same mechanism as fluxing with slags. Diffusion of Cu and Sn into the slag phase through chemical reactions with key components results in their removal as part of the slag during tapping.

Dinabandhu Ghosh [43] tried to use Al_2O_3-saturated Ca-$CaCl_2$ slag to remove Cu and Sn from molten Fe-Cu and Fe-Sn alloys, in alumina crucibles at 1448 to 1648 K. The initial weight ratio of slag to metal was 600 mg: 600 mg. The metal and slag were melted together in the alumina crucibles.

Based on their analysis, Cu and Sn could distribute into the slag phase at molten state to achieve the removal due to the difference of thermodynamic activity. It took almost 20 hours to reach equilibrium between the slag and metal. The removal rate was measured at 50% for Cu and 37% for Sn. He suggested that the inefficient removal could have resulted from preferential dissolving of alumina in calcium, which would probably lead to leakage of crucibles at higher temperature.

Xiaojun Hu et al. [44] studied the removal of Cu from molten steel using $FeO\text{-}SiO_2\text{-}CaCl_2$ slag at 1873 K. The following reactions were proposed for this process:

$$2[Cu]_{\text{in steel}} + FeO = Cu_2O + Fe(l) \quad (3\text{-}7)$$

$$Cu_2O + CaCl_2(l) = 2CuCl(g) + CaO \quad (3\text{-}8)$$

Eventually Cu was removed through the volatilization of CuCl into a gas phase. The ratio of metal to slag used in their experiment was 100 g: 15 g, respectively. Within 10 minutes, the removal rate of Cu was determined to be about 40%. They proposed that the removal rate would increase with time.

As mentioned earlier, ferrous sulfide can form a slag suitable to remove Cu. Adam Cohen and Milton Blander [45] researched this process in molten carbon-saturated Fe at 1638 K. They found that a binary slag of ferrous sulfide and aluminum sulfide could increase the distribution coefficient of Cu between the metal and slag. The Cu content could be reduced from 0.4wt% to 0.07wt% in about 3 hours by keeping the ratio of metal to slag as 90 g: 22.5 g.

Chao Wang et al. [46] also studied the distribution of Cu and Sn between $FeS\text{-}NaS_{0.5}$ slag and molten Fe at 1673 K. They found that the distribution of Cu raised with the addition of sodium sulfide. Therefore, this slag composition could be used to remove Cu, but would be ineffective for removal of Sn.

In 1949, James Fernando Jordan [47] patented a method of Cu removal (decopperization) using sodium sulfide, potassium sulfide, aluminum sulfide or their mixtures. At 1644 K, enough sulfur was added to the molten Cu-containing metal to further convert Cu into cuprous sulfide, which had a high distribution potential into the sulfide slag phase. In his tests, one pound of slag was used for one pound of metal to reduce the Cu content from 0.3wt% to 0.04wt%.

Deep injection of calcium into a molten bath while maintaining a reducing top-slag was applied to remove Sn in the research of S. Street, K. S. Coley and G. A. Irons [48]. The removal rate of Sn was 50% in the laboratory test. However, no reduction of Sn content during full-scale trials was observed. They believed being unable to maintain a high calcium activity may have been the reason.

In order to accelerate the distribution of impurities from molten metal phase to slag phase, the metal Ag and Pb have been researched and applied based on the quality of liquid immiscibility with Fe and good affinity to Cu and Sn. Katsuhiro Yamaguchi and Hideki Ono [49] carried out experiments to diffuse Cu from molten carbon-saturated Fe into sodium sulfide/B_2O_3 slag via Ag phase. With sodium sulfide slag, at 1473 K, the Cu content could be reduced from 0.1wt% to 0.068wt% in about 4 hours. With a B_2O_3 slag, at 1523 K, Cu could be oxidized firstly under an oxygen partial pressure of 0.6atm after diffusing into an Ag phase and then removed as Cu_2O due to the strong affinity with B_2O_3 slag. As a result, the oxidative removal

of Cu could be achieved with a decrease from 4wt% to below 0.2wt% in about 3 hours. Also Katsuhiro Yamaguchi and Yoichi Takeda [50] investigated the removal of Cu and Sn using liquid lead solvent at 1453 K. Maintaining the same amount of lead and scraps, a clear phase separation could be observed between the top layer of liquid carbon-saturated Fe phase and the bottom layer of liquid lead phase due to the difference in density. After about 60 minutes of heating, 70% of the Cu and Sn could be removed by diffusion into the lead layer. A higher removal rate was obtained with multiple stages of phase separation. However, considering the required amount and costs of Ag and Pb and the complexity of operation, the industrial feasibility of this technology would be low.

(3) Other methods

Instead of removing the impurities, such as Cu, Zhongzhu Liu et al. [51] studied the utilization of Cu and S in steel. Through a rapid solidification process, the precipitation of nanosized copper sulfide was detected in α-Fe phase at low temperature. This showed the potential to improve the strength and work hardening ability of steel.

In addition, alloying with other elements can suppress the surface hot shortness. Koji Shibata et al. [52] studied the effect of Si, Mn, S, B, P and Ni. They found P, Si, B and C could restrain the penetration of a Cu-enriched phase into grain boundaries. For examples, the internal oxidation of Si could cause the occlusion of a Cu-enrich phase into scale. Ni could increase the dissolving of Cu into steel and the melting point of a Cu-enriched phase. However, the high price of Ni must be considered for this application.

I. N. Zigalo et al. [53] investigated filtration of Cu from molten steel using Al_2O_3-ZrO_3 ceramics, which was chosen due to its small wetting angle with molten Cu ($\theta<90^o$) and large wetting angle with molten Fe ($\theta>90^o$). Thus Cu could be absorbed on the surface of ceramics, achieving a 30% removal rate. Liansheng Li et al. [54] added ZnO and C into the de-copperizing agents at 1873 K to improve this method. Due to the reducing reaction between ZnO and C, a Cu-Zn alloy could be formed to reduce the surface wetting angle between Cu and Al_2O_3 for better absorption performance. In their experiments, 0.23g Cu could be remove by 1g of reagents within 3 minutes.

Jianjun Wang et al. [55] studied the enrichment of Cu by exerting a negative electric field (-30 ~ 0 V) to the molten steel. Enrichment of Cu around the cathode was shown by testing due to the positive standard electrode potential of Cu based on their analysis. Then separating the molten steel containing enriched Cu by silica tube, a removal rate of 97% was shown for 200g steel scraps within 30 minutes.

4. Discussion

Based on the above analysis, a wide variety of technologies exist for impurity removal from steel scrap. Among these impurities, the key to reduced Cu content is the ability to significantly improve the quality of recycled steel scrap. Comparisons of different Cu removal technologies has been carried out, as shown in Figure 4-1. The Cu content of typical steel scrap can be assumed to be about 0.25wt% considering the impurity removal rate of regular shredding and magnetic separation in shredding plants. From this starting point, the expected Cu content of scrap subjected to differing technologies has been calculated based on their projected effective removal rates. Since less experimental data was available for sensor-based sorting of steel scraps, a 60% removal rate is adopted by referencing sortation efficiency in other application, such as 60%-90% for plastics sortation. The accuracy of demonstrated data is an estimate because they are based on laboratory experiments and commercialization will likely have a reduced efficiency. Furthermore, the treatment time and energy consumption for these technologies has not been fully considered in the comparison. Still the results illustrate past work done on impurity removal and suggests areas for future research. In particular the sensor-based sorting technology is just beginning and the knowledge of the source of Cu in scrap is key to the recycling steel scrap, and consequently to the realization of full commercial realization of the value of recycling steel.

Furthermore, incorporating one or more of these technologies into the existing steelmaking process would be beneficial for their operations. N. A. Warner [56] modeled the continuous desorption of Cu, Sn and Zn in molten scrap. In the melting loop of scraps, the radiant heat of combustion gases from the ironmaking loop was utilized to melt the preheated scraps. Also stannous sulfide, which could be removed by vacuum desorption before entering the steelmaking loop, was produced by the reaction between molten scrap and sulfur-containing gas derived from the ironmaking loop. Desorption of Zn and Cu at atmospheric pressure could be physically achieved under reduced pressure in the open-channel decarburization loop. After this process, the molten scrap could be introduced into the steelmaking loop. A vacuum pumping plant including a recirculating degasser and a Kawasaki top-blowing (KTB) lance has been proposed in his feasibility assessment. Finally, for nominal 0.5 Million Tonnes Per Annum (Mtpa) facilities, the Cu content is projected to be reduced from 0.5wt% to 0.05wt% at 250 Pa pressure; the Sn content could be reduced from 0.4wt% to 0.02wt% at 250 Pa pressure; and the Zn content could be reduced from 1.0wt% to 5 ppm at atmospheric pressure. Warner confirmed that it should be feasible to apply this fully incorporated system into engineering steelworks.

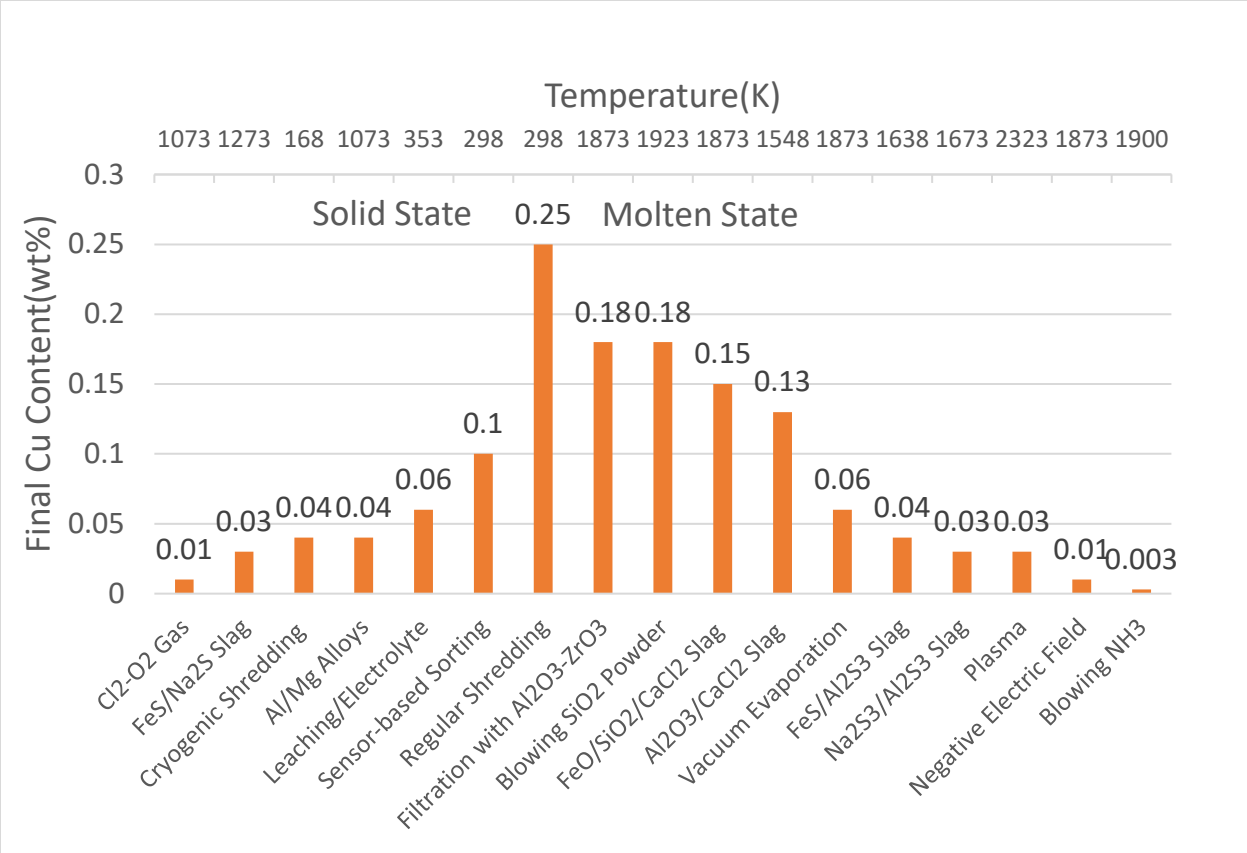

Figure 4-1 Comparison of different removal technologies for Cu

5. References

1. Ernst Worrell, Markus A. Reuter, 2014, "Handbook of Recycling – Chapter 6: Recycling of Steel," Elsevier, 65 pp.

2. R. J. Fruehan, O. Fortini, H. W. Paxton, R. Brindle, 2000, "Theoretic Minimum Energies to Produce Steel for Selected Conditions," Carnegie Mellon University, 43 pp.

3. Michael D. Fenton, 2001, "Iron and Steel Recycling in the United States in 1998," Report of U.S. Geological Survey, 11 pp.

4. D. Janke, L. Savov, H.-J. Weddige, and E. Schulz, 2000, "Scrap-based steel production and recycling of steel," Material in Tehnologije, Vol 34, No. 6, pp. 387-399.

5. U.S. Geological Survey, 2020, Iron and Steel Scrap Statistics and Information, accessed January 2020.

6. Hatayama, Hiroki, et al. "Outlook of the world steel cycle based on the stock and flow dynamics." Environmental science & technology 44.16 (2010): 6457-6463.8.

7. Oda, Junichiro, Keigo Akimoto, and Toshimasa Tomoda. "Long-term global availability of steel scrap." Resources, conservation and recycling 81 (2013): 81-91.

8. American Society for Metals, 1970, "Metals Handbook," Vol. 5, Forging and Casting, ASM.

9. Iain Le May, L. McDonald Schetky, 1982, “Copper in Iron and Steel - Chapter 3,” John Wiley & Sons, 45 pp.

10. K.E. Daehn, A. C. Serrenho, J. M. Allwood, 2017, “How will copper contamination constrain future global steel recycling,” Environ. Sci. Technol., Vol. 51, pp. 6599-6606.

11. M. Huellen, C. Schrade, U. Wilhelm, Z. Zulhan, 2006, “EAF-based flat-steel production applying secondary metallurgical processes,” IS’06, Linz/Austria, Secondary Steelmaking Session, No. 7.1, pp. 1-10.

12. S. Sato, M. Takeuchi, Y. Mizukami, J. P. Birat, 1995, “The Shinseiko Project: a new environment friendly steelmaking route based on scrap,” ATS International Steelmaking Conference, Session 1, pp. 473-483.

13. Pretorius, Eugene, Helmut Oltmann, and Jeremy Jones. "EAF fundamentals." New York, PA, LWB Refractories (2010).

14. T. Matsuto, C. H. Jung, N. Tanaka, 2004, “Material and heavy metal balance in a recycling facility for home electrical appliances,” Waste Management, Vol. 24, pp. 425-436.

15. SICON: PrimeScrap (2018), https://sicontechnology.com/en/sicon-primescrap/. Accessed January 2019.

16. H. Katayama, N. Sano, M. Sasabe, S. Matsuoka, 1996, “Research activities on removal of residual elements from steel scrap in Japan,” Mem. Fac. Sci. Shimane Univ., Series A, Vol. 30, pp. 99-114.

17. H. R. Manouchehri, 2003, “Sorting: possibilities, limitations and future. Proc. of Conference of Mineral processing, Luleå University of Technology, pp. 1-17.

18. F. Tanaka, T. Akagi, S. Naito, S. Kakimoto, M. Sakakibara, M. Ito, 1996, “Method of Automatically Discriminating and Separating Scraps Containing Copper from Iron Scraps,” United State Patent, No. 5911327, 26 pp.

19. Günter Buzanich, 2016, “A newly developed XRF-Sensor with high sensitivity for increasing sorting efficiency,” 7th Sensor-Based Sorting & Control 2016, pp. 221-232.

20. Alvin D. Shulman, 2008, “Method for Bulk Sorting Shredded Scrap Metal,” United States Patent, No. 7886915 B2, 24 pp.

21. S. Kashiwakura, K. Wagatsuma, 2013, “Characteristics of the calibration curves of copper for the rapid sorting of steel scrap by means of laser-induces breakdown spectroscopy under air atmosphers,” Analytical Sciences, Vol. 29, pp. 1159-1164.

22. H. Konishi, 2009, “Selective Separation and Recovery of Copper from Iron and Copper Mixed Waste by Ammonia Solution,” Osaka University, Report of Investigations, 7 pp.

23. Serdar Aktas, Ercan Acma, 2002, “Recovery of zinc from galvanized scraps,” Turkish J. Eng. ENv. Sci., Vol. 26, pp. 395-401.

24. Der-Tau Chin, 1977, “Electrochemical Extraction of Copper from Scrap Steel,” AlChE Journal, Vol. 23, No. 4, pp. 434-440.

25. Giezen Hendrik, 1984, “Method for the detinning of painted tinplate waste,” European Patent, No. 0105551, 15 pp.

26. F. J. Dudek, E. J. Daniels, 1992, "A Recycling Process for Dezincing Steel Scrap," Argonne National Laboratory, Report of U.S. Government, 16 pp.

27. R. J. Fruehan, and A. W. Cramb, 1991, "Copper Removal from Steel Scrap Using a Sulfur Matte," Carnegie Mellon University, CMP Report, No. 91-6, 218 pp.

28. Masanori Iwase, 1992, "Process for the Removal of Non-ferrous Metals from Solid Ferrous Scrap," United States Patent, No. 5090999, 5 pp.

29. Weol Dong Cho, Peng Fan, 2004, "Method and Systems for Removing Copper from Ferrous Scrap," United States Patent, No. 7789936 B2, 14 pp.

30. K. Matsumaru, 1993, "Removal of copper from iron-based scraps by Cl_2-O_2 gas mixtures," Current Advances in Materials and Processes, Vol. 6, pp. 1087.

31. A. D. Hartman, C. Williamson, D. Davis, 1996, Iron and Steelmaker, Vol. 23, No. 8, pp. 43-45.

32. F. Tailoka, R. V. Kumar, D. J. Fray, 2003, "Removal of tin from tin coated steel by chlorination in air," Ironmaking & Steelmaking, Vol. 35, No. 5, pp. 385-390.

33. J. K. S. Tee, D. J. Fray, 2006, "Separation of copper from steel," Ironmaking & Steelmaking, Vol. 33, No. 1, pp. 19-23.

34. J. K. S. Tee, D. J. Fray, 2005, "Recycling of galvanised steel scrap using chlorination," Ironmaking & Steelmaking, Vol. 32, No. 6, pp. 509-514.

35. Bahri Ozturk, R. J. Fruehan, 1996, "Vaporization of zinc from steel scrap," ISIJ International, Vol. 36, Supplement, pp. S239-S242.

36. K. Nakajima, O. Takeda, T. Miki, K. Matsubae, T. nagasaka, 2011, "Thermodynamic analysis for the controllability of elements in the recycling process of metals," Environ. Sci. Technol., Vol. 45, pp. 4929-4936.

37. Luben Savov, Dieter Janke, 1999, "Evaporation of Cu and Sn from induction-stirred iron-based melts treated at reduced pressure," ISIJ International, Vol. 44, No. 2, pp. 95-104.

38. Sung-Hong Jung, Youn-Bae Kang, 2016, "Simultaneous evaporation of Cu and Sn from liquid steel," Metallurgical and Materials Transaction B, Vol. 47B, pp. 2564-2570.

39. Tohru Matsuo, 1988, "Removal of copper and tin with plasma," Transactions ISIJ, Vol. 28, pp. 319-324.

40. K. Ono, E. Ichise, R. O. Suzuki, T. Hidani, 1995, "Elimination of copper from the molten steel by NH3 blowing under reduced pressure," Steel Research, Vol. 66, No. 9, pp. 372-376.

41. N. Sasaki, Y. Uchida, Y. Miki, H. Matsuno, 2014, "Fundamental study of Sn removal from hot metal by NH_3 gas blowing," ISIJ International, Vol. 54, No. 8, pp. 1807-1812.

42. T. Matsuo, K. Maya, and S. Anezaki, 1996, "Removal of copper and tin in molten iron with decarburization under reduced pressure," ISIJ International, Vol. 36, Supplement, pp. S62-S65.

43. Dinabandhu Ghosh, 2009, "Removal of tin and copper from liquid iron by Al_2O_3-saturated Ca-$CaCl_2$ slags at 1448 to 1648K," Metallurgical and Materials Transaction B, Vol. 40B, pp. 508-522.

44. Xiaojun Hu, and Kuochih Chou, 2013, "Removal of copper from molten steel using FeO-SiO2-CaCl2 flux," ISIJ International, Vol. 53, No. 5, pp. 920-922.

45. A. Cohen, and M. Blander, 1996, “Removal of copper from carbon-saturated iron with an aluminum sulfide/ferrous sulfide flux,” Metallurgical and Materials Transactions B, Vol. 27B, pp. 493-495.

46. C. Wang, T. Nagasaka, M. Hino, S. Ban-Ya, 1991, “Copper distribution between molten FeS-$NaS_{0.5}$ flux and carbon saturated iron melt,” ISIJ International, Vol. 31, No. 11, pp. 1300-1308.

47. J. F. Jordan, 1949, “Method of Desulfurizing and Decopperizing Ferrous Metal,” United States Patent, No. 2512578, 2 pp.

48. S. Street, K. S. Coley, G. A. Irons, 2001, “Removal of residual elements in the steel ladle by a combination of top slag and deep injection practice,” McMaster University, Report of investigation, 91 pp.

49. K. Yamaguchi, H. Ono, 2011, “Oxidation removal of Cu from carbon-saturated iron via Ag phase into B_2O_3 flux,” ISIJ International, Vol. 52, No. 1, pp. 18-25

50. K. Yamaguchi, Y. Takeda, 2003, “Impurity removal from carbon saturated liquid iron using lead solvent,” Materials Transactions, Vol. 44, No. 12, pp. 2452-2455.

51. Zhongzhu Liu, Y. Kobayashi, M. Kuwabara, K. Nagai, 2007, “Interaction between phosphorus micro-segregation and sulfide precipitation in rapidly solidified steel-utilization of impurity elements in scrap steel,” Materials Transactions, Vol. 48, No. 12, pp. 3079-3087.

52. K. Shibata, Soek-Jong Seo, M. Kaga, H. Uchino, A. Sasanuma, K. Asakura, C. Nagasaki, 2002, “Suppression of surface hot shortness due to Cu in recycled steels,” Materials Transactions, Vol. 43, No. 3, pp. 292-300.

53 I. N. Zigalo, Y. Baptizmanski, F. Vyatkin, A. G. Velichko, 1991, “Copper in steel and problems in removing it,” Steel in the USSR, Vol. 22, No. 7, pp. 299-302.

54. Liansheng Li, Changxiang Xiang, Pei Zhao et al., 1998, “Decopperization in steel melt through filtration,” Journal of Iron and Steel Research, Vol. 10, No. 3, pp. 5-7.

55. Jianjun Wang, Li Zhou, 2003, “Feasibility study of removing copper from molten steel by electric field,” Journal of Anhui University of Technology, Vol. 20, No. 4, pp. 89-90.

56. N. A. Warner, 2004, “Continuous oxygen steelmaking with copper-, tin-, and zinc- contaminated scrap,” Metallurgical and Materials Transactions B, Vol. 35B, pp. 663-674.

Appendix - B: Industry Survey

This page left BLANK intentionally

Summary of Industry Survey

Technologies	Product	Company	Cost	Note
Gamma Sensor	Cross Belt Analyzer	Thermo Fisher Scientific	Average $500,000	No sorting ability
Magnetic Separating	Shred 1™ Ballistic Metal Separator	Eriez	Capital Cost: $187,200 (60inch Feeding)	
XRT Sensor	COM XRT	Tomra	Capital Cost: $550,000 (1.2m Feeding)	Mining Sortor
XRF Sensor	REDWAVE XRF 1370	REDWAVE	Annual Fixed & Variable Costs: $504,874 (1.37m Feeding)	Sorting of ZORBA
	UHV IL-XRF	UHV Technologies	0.03$/kg (10 tons/hr)	Al Alloy Scrap
Optical Sensor	MultiWave	MSS	Approx. Cost: $185,000 (4,000 kg/hr)	Mainly used for sorting plastics
	Varisort	S&S	Capital Cost: Average $150,000 (0.5 to 2m Feeding)	
	Sirocco	Pellenc Selective Technologies	Approx. Cost: $175,000 (0.8 to 2.4m Feeding)	
	STEINERT LSS LIBS	STEINERT	Approx. Cost: Euro 240,000 (30 Euro/tonne, 8000 tonne/yr)	Mainly used for sorting of Al Scrap

Note: The above product may not mainly used for sorting steel scrap, but the cost should be similar based on their function.

1. Western Metals Recycling LLC

Introduction: Western Metals Recycling, LLC (WMR) is a wholly owned venture of Cincinnati-based, The David J. Joseph Company (DJJ). Founded in 1885, DJJ is one of the largest scrap broker/processors in US providing scrap brokerage, recycling and transportation services. DJJ is part of Nucor Corporation's family of companies.

DJJ operates six regional scrap metal recycling companies across the USA which includes a network of over 65 scrap metal facilities with the capacity to recycle 5 million tons of ferrous and 500 million pounds of nonferrous scrap annually.

WMR's largest consumers of products are EVRAZ steel mill in Pueblo, and Nucor Steel Mill in Plymouth UT.

General Manager: David Youngberg, with 25 years scrap industry experience, originally served in Provo, UT, then moved to Englewood, CO in 2003.

Description: WMR processes automobiles through a hammer mill shredder and two drum magnetic separators to produce shredded ferrous scrap. In the Denver facility, they don't apply any sorting method after magnetic separator. But manual picking up has been deployed to pick motors from the product stream. The Cu content of final shredded product is below 0.25%. David mentioned in some other yards, they apply Gamma Technology to control the composition of shredded scrap. Normally, the Cu content could be reduced to 0.16% with this technology. But the cost will increase and then influence the sale of final product. The flow sheet is as following. Also this gamma technology utilized at their facilities only validates the chemistry of the processed scrap. It has no sorting ability.

2. Gamma-tech (Information Collected from Manufacturer)

Introduction: Gamma-tech is a reseller for Thermo Fisher Scientific, who is the manufacturer of the Cross Belt Analyzer (CBA). Gamma-Tech customizes and calibrates the CBA for the metals industry and try to market the equipment in the scrap recycling, metals, and steel industries.

Product: Cross Belt Analyzer

Description: It is a Prompt Gamma Neutron Activation Analysis (PGNAA) system designed to integrate into an existing conveyor belt line and analyze, in real-time, the composition of bulk materials being transported by the conveyor belt. As the material passes through the tunnel of the analyzer, it is bombarded with neutrons from radioactive isotopes. The neutrons are captured by the atoms of the material and produce a secondary reaction in the form of gamma rays. This secondary gamma ray spectrum is de-compiled and analyzed to produce the composite elemental analysis of the material.

Clark Scott from Gamma-tech offers some information about this technology used in scrap yards. The analyzer is primarily used to provide a composite chemistry of a quantity of shredded scrap, i.e. a barge or train shipment. However, for most shipments, their contractual chemistry must be achieved, typically copper content in ferrous scrap. In the case of a shredder supplying a specified chemistry to a mill, the analyzer acts as a process control tool allowing the processer to monitor and control the quality of the shred. The quality is controlled by either changing the infeed material to the shredder, making adjustments to improve the downstream processing, adding pickers, or diverting out-of-spec material away from the shipment. PGNAA provides a full stream analysis of the shredded material on the conveyor belt, it does not sample the individual pieces.

The analyzer is used in the metal recycling applications of ferrous scrap, aluminum, and copper, as a quality control instrument to report the chemistry of a suite of elements specific to each industry/application.

According to R. C. Woodward, from Thermo Electron Corporation, the cost for PGNAA cross belt analyzer is $500,000 or more, depending upon the complexity of the installation.

Note: Information from “A Major Step Forward for On-line Coal Analysis”, R. C. Woodward, M. P. Evans, E. R. Empey, Thermo Electron Corporation

3. SciAps Inc. (Information Collected from Manufacturer)

Introduction: SciAps, Inc., is a Boston-based instrumentation company specializing in portable analytical instruments. They provide durable, field-tested, portable instruments to identify any compound, any mineral and any element, such as Handheld XRF and Handheld LIBS, which can be applied to scrap processing, geochemical and food industry.

More than 90% of all alloys can be identified in 1 second with excellent precision using the Alloy Model, which includes a large composition library for 500 metal and alloys.

David Walter, a local representative, said that they sell a lot of these instrument to scrap yards. The way they use them is to sort the metals prior to shredding. Prior to shredding, a fender, or an axel can be tested easily. But after shredding, testing every shredded piece will be too time consuming. Also he mentioned that XRF sensor above the conveyor belt has been used in industry. Considering the distance between conveyor and sensor, a more intense beam must be applied to avoid the drop off of its intensity. Otherwise it would influence the result of detector. As a result, millions dollar investment would be required for this type of sensor sorting.

LIBS has been used for more than 30 years as a laboratory technique, capable of analyzing any element in the periodic table. Recently, the technique has been miniaturized into a handheld device (HH LIBS), capable of analyze all elements, depending on the spectrometer range chosen for the device. But David thought LIBS may not be suitable for conveyor belt due to the small laser spot used to create plasma around the area struck.

4. Eriez Manufacturing Co. (Information Collected from Manufacturer)

Introduction: Eriez involves in the design and manufacture of separation, material handling and inspection equipment used throughout the process industries, such as food, plastics and chemical, mining, metalworking and recycling.

Product: Eriez Shred 1™ Ballistic Metal Separator

Description: Shred1 from Eriez uses ballistics to efficiently separate iron-rich ferrous from much of the mixed metals post-drum magnet flow. This separator delivers two distinct fractions: a premium low-copper ferrous product (in the range of 0.16-0.20% Cu) and a traditional #2 shred (over 0.20% Cu).

The Shred1 ballistic separator combined with a PokerSort to extract long, troublesome pokers, and a P-Rex™ permanent rare earth magnetic drum improves the entire process. Not only does this new CleanStream™ process recover more ferrous and concentrate 75% of the post-drum magnet flow into a low-copper premium shred, but it also reduces the hand picking and helps increase recovery of copper bearing materials.

Model	Feed Width	Approx. Weight	Price
Shred1-60	60 inches	26,000 lbs	$187,200

Note: Price information from an Area Sales Manager

5. Tomra (Information Collected from Manufacturer)

Introduction: TOMRA mainly offers suitable sorting solutions for the waste and metal recycling industries and continues to result in related machines and exceptional service.

Product: XRT Sensor Sorting

Description: High resolution X-ray (XRT), coupled with multi-density-channel capabilities, enhance the precision of sorting even the most complicated material mixing across a wide variety of metal applications. Their field-proven Dual Processing Technology, coupled with TOMRA's exclusive software development, means that the X-TRACT enables effective sorting of the highest throughput with reliable top-quality yield. Now equipped with the new intuitive ACT user interface, X-TRACT operators can easily see critical sorting information and real-time process data at a glance.

Harold Cline, area sales manager, offers some basic information about the price of XRT sensor.

XRT + Electromagnetic Sensor	Price $
Width of Conveyor: 1.2m	550k
Width of Conveyor: 2.4m	1.1M

Note: The estimated price is just for sortor only and doesn't include packing, shipping, commissioning, installation and spare parts.

6. REDWAVE (Information Collected from manufacturer)

Introduction: REDWAVE offers advanced sorting solution in the recycling and mining industry. Advanced optical sorting machines and complete plant solutions have been applied to sort glass, paper, plastics and scrap metal, including Camera based, Near Infra-Red (NIR) based, Induction based and XRF based sensor technology.

Product: REDWAVE XRF Chute Design

Description: a high level of detection is guaranteed even in the presence of material which is dirty or otherwise contaminated. Energy dispersive X-ray Fluorescence Spectrometer is used to generate elemental analysis of the feed materials. Up to 30t/h capacity can be achieved depending on the sorting width.

Considering the cost, a sales manager presents a payback calculation for REDWAVE XRF 1370 used to sort ZORBA, which is a mixture of aluminum, copper and other non-ferrous metals produced with the recycling of automobiles. The estimated annual fixed and variable costs are $504,874, including machine, compressor, pressurized air, electricity, spare and wear parts and manpower.

Payback Calcuation REDWAVE XRF 1370
Sorting of ZORBA, 10 000 t/a

Material stream	Composition of total	Quantity of total	Recovery Rate/ Yield	Quantity Recovered	Value		€
	[%]	[t]	[t]		[€/t]		
Inputmaterial		10000			1100		€ 11.000.000
Al 6061	60,0%	6000	95%	5700,00	1350		€ 7.695.000
Al mix	20,0%	2000	95%	1900,00	1000		€ 1.900.000
Cu	2,0%	200	99%	198,00	4200		€ 831.600
Brass	5,8%	580	99%	574,20	3000		€ 1.722.600
Zn	5,5%	550	95%	522,50	1000		€ 522.500
stainless steel	5,0%	500	95%	475,00	1050		€ 498.750
Pb	0,1%	10	95%	9,50	1500		€ 14.250
rest	1,6%	160	0%	0,00	0		€ -
total	100,0%						

Total value of recovered metals	€ 13.184.700
Minus costs for Input	€ 11.000.000
return per anno	€ 2.184.700
minus annual fixed and variable costs	€ 504.874
total annual profit 3 year amortization	**€ 1.679.826**
total annual profit 1 year amortization	**€ 1.036.493**

Assumptions
current market price for above mentioned metals
1 and 3 years amortization on machine and compressor
staff needed 2 person per shift
ca. 5000 operating hours needed per year, 2 shift operation
cost include machine, compressor, pressurized air, electricity, spare and wear parts service visits, manpower

Note: Information from "23rd International Recycled Aluminum Conference", Madrid 2015, Presented by Manuela Suttnig, Sales Manager from REDWAVE

7. UHV Technologies, Inc. (Information Collected from Manufacturer)

Introduction: UHV Technologies, Inc. involves the development and commercialization of advanced materials and devices. Their high throughput IL-XRF Metal Scrap Sorter is designed for commercial scale aluminum scrap sorting.

Description: Linear x-ray tube for parallel elemental composition measurement is applied on a fast moving conveyor belt.

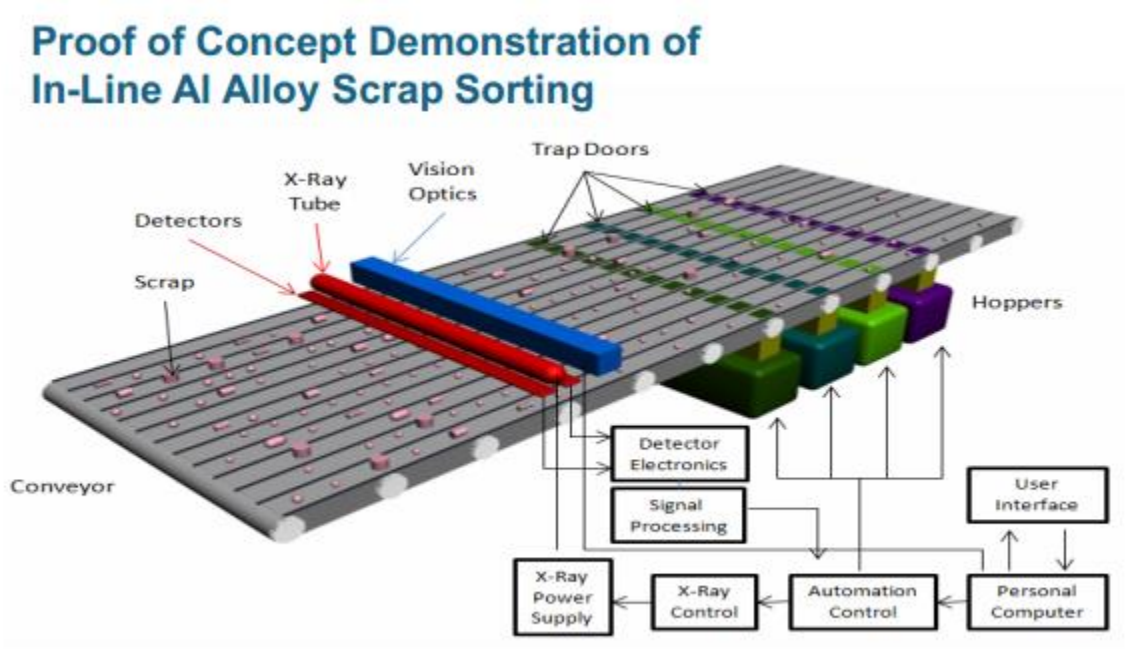

Metric	UHV IL-XRF
Sorting Capacity	> 10 tons/hr > 100 M pieces/yr
Cost	< $0.03/kg
Accuracy	> 99%
Sort Time/Piece	< 100 ms

Note: Information from “High Throughput IL-XRF Metal Scrap Sortor” METALS Annual Meeting, UHV Technologies, Inc.

8. Optical Sorting

(1) **MSS**: based in Nashville, TN. Its Aladdin system processes up to 4,000kg/hour and uses an integrated color sensor to differentiate between clear and green PET bottle or transparent and opaque, plus colored and natural HDPE bottles; able to identify and separate two eject streams from one pass stream; also counts bottles separated by size and type; approximate cost is US$185,000. Latest generation sensor technology is the MultiWave.

(2) **S&S Separation and Sorting Technology GmbH**: based in Germany, but has joint venture with California Company called Tectron Engineering. Varisort optical sorting equipment is produced for whole bottle sorting, which accommodates different sensors to achieve 99.5 percent purity. The mass-sort system works with different polymer types, colors and metals, as well as a commingled stream of mixed plastics. Unit capacity is between 500 kg/hr to 6,000 kg/hr and comes in four different belt widths from 500 to 2000 mm. Capital costs range from US$50,000 to US$250,000. S&S also offers SPECTRUM color sorters and PETMAG metal separation systems.

(3) **Pellenc Selective Technologies**: based in France. The Mistral is a multimaterial sorting system that uses NIR (near infrared spectroscopy) technology to identify all materials in one pass. The Sirocco uses Vision (sorting of hollow bodies by color vision) to identify each object by location, shape, transparency and color. The equipment offers random speeds of 2.5 to 2.8 m/s. Models range from 800mm to 2400mm belt widths, varying in output capacity from 900 kilograms to 3 t/hour to 8 to 10 t/hour. Purity levels of 90 to 98 percent are achieved. Efficiency is 90 to 96 percent. Approximate cost is US$100,000 to US$250,000, depending on sizes and options (binary, ternary).

Note: Information from “Plastics Optical-Sorting Technologies”, Canadian Plastics Industry Association & Association Canadienne De I’Industrie des Plastiques

9. STEINERT (Taken from Advertising Literature)

Introduction: STEINERT manufactures a complete line of magnetic and sensor-sorting equipment designed to recover a wide range of materials and provide different separation technology solutions for the scrap, waste, recycling and mining industries.

Product: STEINERT LSS LIBS with line sorting system

Description: It is additionally equipped with #D detection and a laser induced breakdown spectroscopy unit (LIBS). They have developed this efficient sorting machine especially for use in the sorting of aluminum scrap. But according to its mechanism, it could also be used for sorting steel scrap. It is ideally suited for stamping waste material 20 to 60 mm wide and 60 to 150 mm long.

The unit offered by STEINERT achieves an output of several tonnes per hour. “Yet, even with an output of just one tonne per hour, with 300 euros of additional proceeds and an operating time of 8,000 hours per year the additional proceeds amount to 2.4 million euros, comparing to the sorting costs of 20 to 30 euros per tonne” calculates Habich (CTO). In this example calculation, the unit would pay for itself in around half a year.

Note: Information from “New sorting technology for the separation into different aluminum alloys”, STEINERT

Appendix - C: Cost Analysis of Chemical Removal Methods

This page left BLANK intentionally

1. Fluxing with matte: FeS and Na_2S

Matte: 82% FeS and 18% Na_2S

Reactor: (TR21) Tilt Rotary kiln from Melting Solution with oxy-fuel burner

State of Scrap: Solid Shredded Scrap (rods, pipes, angles, plates)

State of matte: liquid

Temperature: 1000 ^oC

Mechanism: $FeS + 2Cu = Cu_2S + Fe$ $\Delta G = -3.26$ kcal/mol (1000^oC)

Description in literature: Reaction was carried out with 10 kg of matte per ton of scraps. The melting of matte takes about 30 minutes. The dissolution reaction rate is quite high and the overall reaction rate is limited by transfer of FeS in the matte to the reaction zone. So according to Cramb and Fruehan[24], assuming the rates of copper pick-up is linear. That means the content of Cu_2S in the matte will increase linearly. In their kiln trials, the process removed about 75% of the copper (from 0.4% to 0.1%) in 15 minutes. So if the final copper content is 0.03%, the required time is about 18 minutes.

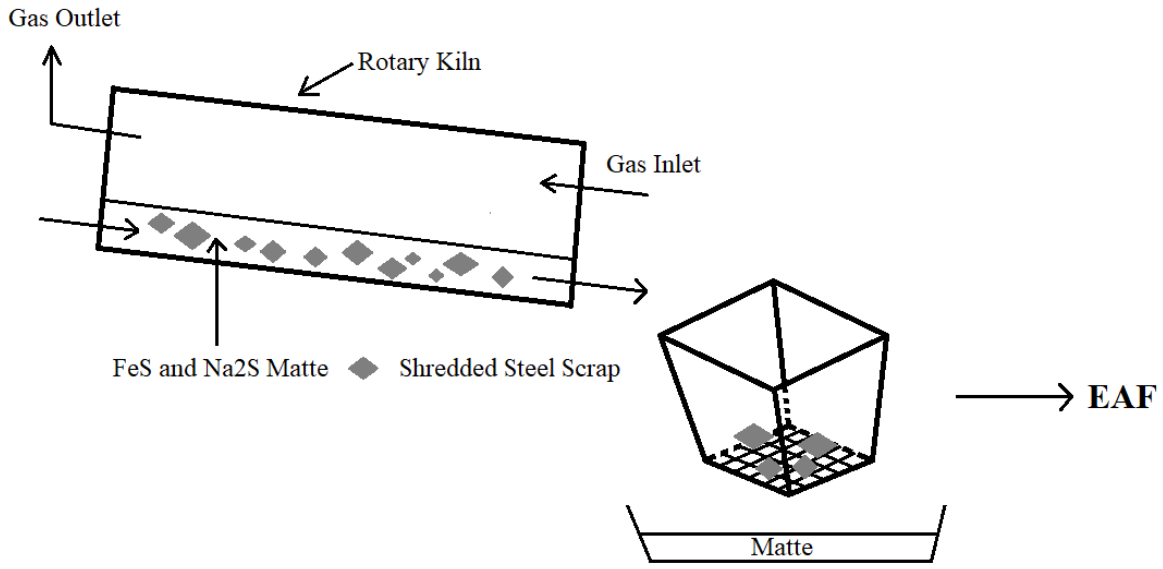

A. Energy consumption per ton scrap from 0.4% to 0.1%:

(1) Heating up input materials to 1000 ^oC

Input	Name	Weight /kg	Mole	ΔH(25 ^oC to 1000 ^oC)	Total Needed Heat	Energy Consumption /kWh
Matte	FeS	8.2	93.18	14.224 kcal/mol	1325.39 kcal	1.54
	Na_2S	1.8	23.08	23.756 kcal/mol	548.29 kcal	0.6

Scrap	Fe	996	17785.71	8.995 kcal/mol	159982.46 kcal	185.94
	Cu	4	62.5	6.434 kcal/mol	402.125 kcal	0.47

(2) Heating for the reaction

The reacted Cu from 0.4% to 0.1% is 46.92 mol

ΔH^{o}(1000 ^{o}C)= 7.854 kcal/mol FeS × 46.92 × 0.5 = 184.25 kcal = 0.21 kWh

(3) Heating for maintaining 1000 ^{o}C for 15 minutes reaction

From the specification of rotary kiln, it uses oxy-fuel burner. The burner energy per tonne of charge is 350 kW. To maintain 15 minutes, the energy consumption is 350 × 15/60 = 87.5 kWh.

(4) Heat loss

Assuming this kiln has a 60% heat efficiency.

(5) Maintaining rotating for 45 minutes

The drive power of this kiln is 125 kW with the capacity of 25 ton. So the energy consumption per tonne is 125/25 × 45/60 = 3.75 kWh.

(6) An extra 15 kWh/tonne is added to account for heat losses during the transition from the process furnace to the EAF.

During the normal steelmaking process, heating steel or Fe to high temperature is an essential process, so we don't need to include the energy consumption of heating steel (Fe) to 1000 ^{o}C.

So the extra energy consumption per tonne is:

(1.54+0.6+0.47+0.21+87.5)/0.6+3.75+15=**169.28 kWh**

B. Energy consumption per ton scrap from 0.4% to 0.03%:

(1) Heating up input materials to 1000 ^{o}C

Input	Name	Weight /kg	Mole	ΔH(25 ^{o}C to 1000 ^{o}C)	Total Needed Heat	Energy Consumption /kWh
Matte	FeS	8.2	93.18	14.224 kcal/mol	1325.39 kcal	1.54
	Na_2S	1.8	23.08	23.756 kcal/mol	548.29 kcal	0.6
Scrap	Fe	996	17785.71	8.995 kcal/mol	159982.46 kcal	185.94
	Cu	4	62.5	6.434 kcal/mol	402.125 kcal	0.47

(2) Heating for the reaction

The reacted Cu from 0.4% to 0.03% is 57.83 mol

ΔH^o(1000 ^oC)= 7.854 kcal/mol FeS × 57.83 × 0.5 = 227.1 kcal = 0.26 kWh

(3) Heating for maintaining 1000 ^oC for 18 minutes reaction

From the specification of rotary kiln, it uses oxy-fuel burner. The burner energy per tonne of charge is 350 kW. To maintain 18 minutes, the energy consumption is 350 × 18/60 = 105 kWh.

(4) Heat loss

Assuming this kiln has a 60% heat efficiency.

(5) Maintaining rotating for 48 minutes

The drive power of this kiln is 125 kW with the capacity of 25 ton. So the energy consumption per tonne is 125/25 × 48/60 = 4 kWh.

(6) An extra 15 kWh/tonne is added to account for heat losses during the transition from the process furnace to the EAF.

During the normal steelmaking process, heating steel or Fe to high temperature is an essential process, so we don't need to include the energy consumption of heating steel (Fe) to 1000 ^oC.

So the extra energy consumption per tonne is:

(1.54+0.6+0.47+0.26+105)/0.6+4+15=**198.78 kWh**

C. Material consumption per tonne:

Material		Price $	Amount	Sum $
FeS		0.254/g	4920g	1249.68
Na_2S		0.109/g	1080g	117.72
Burner	Natural Gas	0.203/m^3	35 m^3	7.105
	Fuel Oil	0.538/L	35 L	18.83
	Oxygen	11.92/m^3	70 m^3	834.4
Total				2227.735

D. Secondary Effects:

(1) If the treated scrap is transferred directly to the EAF without cleaning in order to have the heat retention, there will be some matte adhered on the surface, which could induce sulfur contamination during steelmaking. So desulfurization is required in the following ladle metallurgy. Since desulfurization has been existed in steelmaking, I think we don't need to consider this cost.

(2) If we don't control the atmosphere in the kiln, SO_2 would be produced in this process. So we need to remove SO_2 from the outgas using wet scrubber. According to the data from EPA, the cost for this process is 200-500 $/ton of pollutant removed.

2. Fluxing with Cl_2-O_2 gas

Gas: Cl_2-O_2 with flowrate 40/400 cm^3/min (laboratory)

Cl_2-O_2 with flowrate 0.7656/7.656 m^3/min (estimation based on total reaction with Cu on one tonne scrap)

Reactor: Horizontal tube furnace with gas feeding device

Material: Fe with copper winding

Temperature: 800 °C

Mechanism: Volatile copper chloride will be formed and formed Fe_2O_3 layer can stop the further oxidation of Fe and corrosion from chlorine

Description in literature: Based on the information of heat capacity, the heating time to 800 °C is about 1 h. Then Cl_2-O_2 gas is introduced into the furnace to have the reaction. The content of Cu could be reduced from 1.0% to 0.05% after 10 minutes reaction. According to Tee and Fray[30], the estimated reacting time for removing Cu from 0.4% to 0.1% is about 4 minutes. Also removing Cu from 0.4% to 0.03% is about 6 minutes reaction.

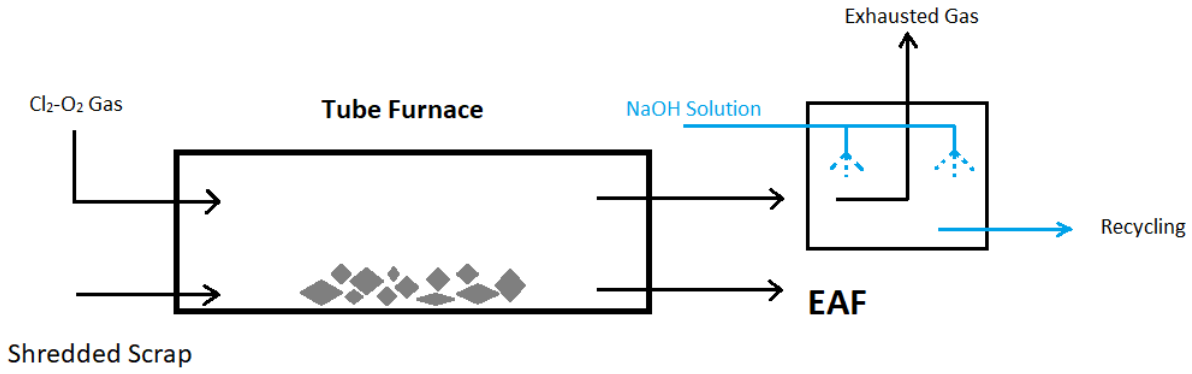

A. Energy consumption per tonne of scrap from 0.4% to 0.1%:

(1) Heating up input materials to 800 °C

Input	Name	Amount	Mole	ΔH(25 °C to 800 °C)	Total Needed Heat	Energy Consumption /kWh
Gas	Cl_2	7.656 m^3	312.5	6.766 kcal/mol	2114.375 kcal	2.46
	O_2	76.56 m^3	3418.9	6.040 kcal/mol	20650.16 kcal	24
Scrap	Fe	996 kg	17785.71	6.849 kcal/mol	121814.33 kcal	141.58
	Cu	4000 g	62.5	4.983	311.44 kcal	0.36

				kcal/mol		

(2) Heating for the reaction

The reacted Cu from 0.4% to 0.1% is 46.92 mol

$Cu+0.5\ Cl_2(g) = CuCl(g)$ ΔG= -4.433 kcal/mol (800°C)

ΔH^o(800 °C)= 16.734 kcal/mol Cu × 46.92 = 785.16 kcal = 0.91 kWh

(3) Heating for maintaining 800 °C for 4 minutes

Reactor: Tube furnace with gas-feeding device, equivalent to 200 W/dm^3. The volume of one tonne scrap is about 662.6 dm^3. Assume the usage efficiency of furnace is 80%. So the power of furnace is 200 × 662.6/0.8 = 165.65 kW.

Energy consumption: 165.65 kW × 4/60 = 11.04 kWh

(4) Heat loss

Assuming this kiln has a 60% heat efficiency.

(5) An extra 15 kWh/tonne is added to account for heat losses during the transition from the process furnace to the EAF.

So the extra energy consumption per tonne is:

(2.46+24+0.36+0.91+11.04)/0.6+15=**78.4 kWh**

B. Energy consumption per tonne of scrap from 0.4% to 0.03%:

(1) Heating up input materials to 800 °C

Input	Name	Amount	Mole	ΔH(25 °C to 800 °C)	Total Needed Heat	Energy Consumption /kWh
Gas	Cl_2	7.656 m^3	312.5	6.766 kcal/mol	2114.375 kcal	2.46
	O_2	76.56 m^3	3418.9	6.040 kcal/mol	20650.16 kcal	24
Scrap	Fe	996 kg	17785.71	6.849 kcal/mol	121814.33 kcal	141.58
	Cu	4000 g	62.5	4.983 kcal/mol	311.44 kcal	0.36

(2) Heating for the reaction

The reacted Cu from 0.4% to 0.03% is 57.83 mol

$Cu+0.5\ Cl_2(g) = CuCl(g)$ ΔG= -4.433 kcal/mol (800°C)

ΔH^o(800 °C)= 16.734 kcal/mol Cu × 57.83 = 967.73 kcal = 1.12 kWh

(3) Heating for maintaining 800 °C for 6 minutes

Reactor: Tube furnace with gas-feeding device, equivalent to 200 W/dm^3. The volume of one tonne scrap is about 662.6 dm^3. Assume the usage efficiency of furnace is 80%. So the power of furnace is 200 × 662.6/0.8 = 165.65 kW.

Energy consumption: 165.65 kW × 6/60 = 16.57 kWh

(4) Heat loss

Assuming this kiln has a 60% heat efficiency.

(5) An extra 15 kWh/tonne is added to account for heat losses during the transition from the process furnace to the EAF.

So the extra energy consumption per tonne is:

(2.46+24+0.36+1.12+16.57)/0.6+15= **89.18 kWh**

C. Material consumption per tonne:

Material	Price $	Amount	Sum $
O_2	11.92/m^3	76.56 m^3	912.6
Cl_2	0.45/lbs	48.92 lbs	22.014
Total			934.614

D. Secondary Effects:

(1) During this method, Fe would be oxidized into Fe_2O_3. But we can also use this method to remove Zn and Sn.

(2) Due to the toxicity of Cl_2, we need to use NaOH solution to neutralize the exhaust gas and dissolve the formed volatile CuCl. If we can use PVC waste as a source of reagent Cl_2, it should be possible to offset the cost for treating exhausted gas.

3. Vacuum Evaporation

Pressure: 50 Pa can be achieved in industrial scale

Reactor: existing vacuum degassing chamber with ladle furnace (inside d = 3.2 m, h= 2.9m)

Ladle Furnace: Capacity 90-100 t, 18000 kVA (14400 kW), about 152 kW/tonne

Temperature: 1600 ^{o}C

Mechanism: Due to different vapor pressure between Cu and Fe, Cu can be removed by evaporation. Vacuum can improve this process. Also the evaporation rate of Cu can be treated as first-order.

$$\text{In}\,([Cu_F]/[Cu_I]) = -k_{Cu}\times(A/V)\times t$$

According to the research of Luben Savov and Dieter Janke[34], $k_{Cu}=3\times10^{-5}$ m/s under 50 Pa and 1600 ^{o}C. Morales et al.[54] analyzed that the specific surface area (A/V) can be set to 0.5 m^{-1} (1.5 factor). So the estimated time for removing Cu from 0.4% to 0.1% is about 25.67 h. Also the removing time from 0.4% to 0.03% is about 47.97 h. The heating time to 1600 ^{o}C is about 2.5 h.

A. Energy consumption per tonne scrap from 0.4% to 0.1%:

(1) Maintaining 1600 ^{o}C for 25.67 h:

152 kW/tonne × 25.67 h = 3901.84 kWh

(2) Heat loss:

With a longer heating treatment, the temperature drop could be as high as 100 ^{o}C according to Ghosh's research. To overcome this heat loss, required additional energy is:

152 kW/tonne × 100 ^{o}C /300 (^{o}C/h) (heating speed) = 51 kWh/tonne

So the extra energy consumption per tonne is: **3952.84 kWh**

B. Energy consumption per tonne scrap from 0.4% to 0.03%:

(1) Maintaining 1600 ^{o}C for 47.97 h:

152 kW/tonne × 47.97 h = 7291.44 kWh

(2) Heat loss:

With a longer heating treatment, the temperature drop could be as high as 100 ^{o}C according to Ghosh's research. To overcome this heat loss, required additional energy is:

152 kW/tonne × 100 ^{o}C /300 (^{o}C/h) (heating speed) = 51 kWh/tonne

So the extra energy consumption per tonne is: **7342.44 kWh**

C. Material consumption per tonnes:

No directly material is need in this process.

D. Secondary Effects:

Although this method has a lower energy consumption, it would take more time if a good removal could be achieved. Lowering pressure to 10 Pa can increase the value of k, but this pressure is not easier to maintain in industry.

Also increasing the specific surface area can reduce the removing time, such as blowing NH_3, increasing the stirring intensity.

4. Blowing NH_3 under 2000 Pa

Method: Vacuum Evaporation

Reactor: existing vacuum degassing chamber with ladle furnace (inside d = 3.2 m, h= 2.9m)

Temperature: 1600 ^oC

NH_3 blow rate: 2L/min

Mechanism: Blowing NH3 can improve the evaporation of Cu and increase the specific area for the molten bath. According to Hidani et al.[55], the average rate constant is $k_{Cu} = 3.3\times10^{-5}$ m/s at 2000 Pa. M. A. Tayeb et al.[56] mentioned in ladle furnace the specific surface area can be considered as 3-14 times of flat area because of the emulsification. Blowing NH_3 can induce intense stirring. So A/C = 0.345 × 14 = 4.83. If we want to reduce the content of Cu from 0.4% to 0.1%, the time is 145 minutes, since the evaporation of Cu belongs to first order. Also the removing time from 0.4% to 0.03% is 270 minutes.

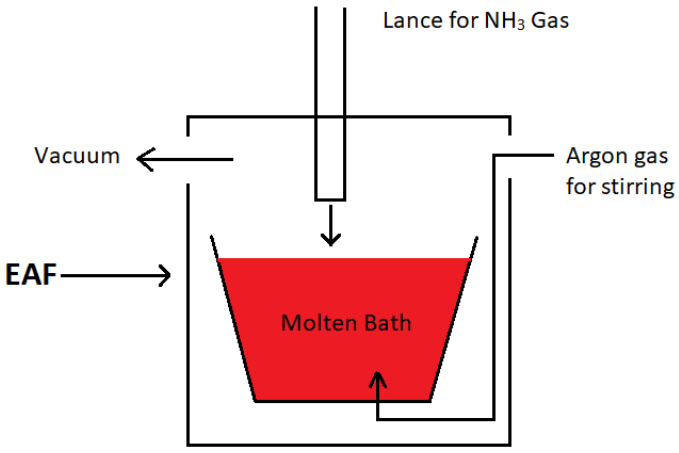

A. Energy consumption per tonne scrap from 0.4% to 0.1%:

(1) Maintaining 1600 ^oC for 145 minutes:

152 kW/tonne × 145/60 h = 367.33 kWh

(2) Heat loss:

This consumption is to maintain the heat lose during blowing NH_3 due to the increasing of exposed surface area. According to literature, the temperature loss rate for a 200t ladle during powder injection is about 3 ^oC/min. We can use this data to estimate the heat loss of blowing NH_3.

Temperature drop: 3 ^oC/min × 145 min = 435 ^oC

Energy consumption: 152 kW/tonne × 435 ^oC /300 (^oC/h) (heating speed) = 220.4 kWh/tonne

(3) Blowing NH_3 would influence the stable of vacuum. In order to maintain the required vacuum.an additional 10 kWh/tonne steel is needed.

So the extra energy consumption per tonne is: **597.73 kWh**

B. Energy consumption per tonne scrap from 0.4% to 0.03%:

(1) Maintaining 1600 ^{o}C for 270 minutes:

152 kW/tonne × 270/60 h = 684 kWh

(2) Heat loss:

This consumption is to maintain the heat lose during blowing NH_3 due to the increasing of exposed surface area. According to literature, the temperature loss rate for a 200t ladle during powder injection is about 3 ^{o}C/min. We can use this data to estimate the heat loss of blowing NH_3.

Temperature drop: 3 ^{o}C/min × 270 min = 810 ^{o}C

Energy consumption: 152 kW/tonne × 810 ^{o}C /300 (^{o}C/h) (heating speed) = 410.4 kWh/tonne

(3) Blowing NH_3 would influence the stable of vacuum. In order to maintain the required vacuum.an additional 10 kWh/tonne steel is needed.

So the extra energy consumption per tonne is: **1101.4 kWh**

C. Material consumption per tonnes:

Material	Price$	Amount	Sum $
NH_3	522/ton	290 L (0.4% to 0.1%)	0.111
		540 L (0.4% to 0.03%)	0.207

D. Secondary Effects:

During this process, nitrogen would be dissolved into the melting bath due to the decomposition of NH_3. So we may need additional degassing process after the treatment. The estimated energy consumption per minute is 2.53 kWh/tonne.

5. Blowing Weak Oxidizing Powder under Reduced Pressure

Temperature: 1923 K

Atmosphere: Ar atmosphere under 130 Pa

Reactor: existing vacuum degassing chamber with ladle furnace and top blowing lance (inside d = 3.2 m, h= 2.9m)

Scale: 1.0-1.5 metric tons iron with 0.4-1.0 % carbon.

Mechanism: Weak oxidizing powder SiO_2 was blown onto the molten bath and decomposed to form [O], which could induce fine bubbles of CO with C near the surface. The bubbles could agitate the bath and increase the surface area for evaporation.

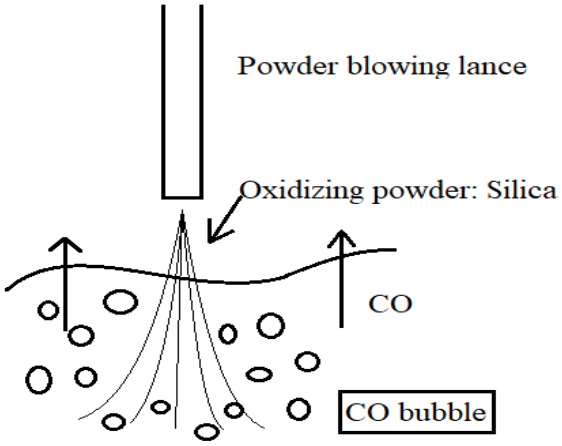

According to Matsuo et al.[39], the apparent removal rate constant of copper K_{Cu} ($k_{Cu} \times A/V$) = 7.1×10^{-5}. In 325 minutes, the content of copper is removed from 0.4% to 0.1%. In 10 h, the content of copper is removed from 0.4% to 0.03%. Also this reaction is endothermic and requires high carbon content to react with [O].

So if we want apply this method to steel scrap, which normally has a carbon content of 0.2%. So we need additional carbon to saturate the melt.

Long treating time, lower removal rate, additional carbon input and heating make this method impossible to incorporate into existing steelmaking process.

A. Energy consumption per tonne scrap from 0.4% to 0.1%:

(1) Maintaining 1650 °C for 325 minutes:

152 kW/tonne × 325/60 h = 823 kWh

(2) Heat loss:

Assuming it has a same energy loss (3 °C/min) as blowing NH_3.

152 kW/tonne × (325 × 3) °C/300 (°C/h) (heating speed) = 494 kWh/tonne

(3) Addition heating for the endothermic reaction:

$2C + SiO_2 = Si + 2CO(g)$ $\Delta H(1923K) = 168.433$ kcal/mol SiO_2

The blowing rate of SiO_2 is 0.2 kg/(min·ton). In 325 minutes, 65 kg SiO_2 is blown to the melt (assuming all SiO_2 has been reacted with C).

The energy required for maintaining this reaction is:

(65000/60) × 168.433 = 182469.08 kcal = 212.07 kWh/tonne

So the extra energy consumption per tonne is: **1529.07 kWh**

B. Energy consumption per tonne scrap from 0.4% to 0.03%:

(1) Maintaining 1650 ºC for 10 h:

152 kW/tonne × 10 h = 1520 kWh

(2) Heat loss:

Assuming it has a same energy loss (3 ºC/min) as blowing NH_3.

152 kW/tonne × (600 × 3) ºC/300 (ºC/h) (heating speed) = 912 kWh/tonne

(3) Addition heating for the endothermic reaction:

$2C + SiO_2 = Si + 2CO(g)$ $\Delta H(1923K) = 168.433$ kcal/mol SiO_2

The blowing rate of SiO_2 is 0.2 kg/(min·ton). In 600 minutes, 120 kg SiO_2 is blown to the melt (assuming all SiO_2 has been reacted with C).

The energy required for maintaining this reaction is:

(120000/60) × 169.433 = 338866 kcal = 393.84 kWh/tonne

So the extra energy consumption per tonne is: **2825.84 kWh**

C. Material consumption per tonnes:

Material	Price $	Amount	Sum $
SiO_2 (99.99%)	0.14/g	65 kg	9100
		120 kg	16800

D. Secondary Effects:

Adding Carbon into the melt would induce heating loss and generate CO in the exhausted gas.

Decarburization is needed after this process.

6. Using Slag to Remove Cu in Ladle Furnace

Composition of Slag: 94.65%FeO-1.93%Cu_2O-1.21%SiO_2-2.23%$CaCl_2$

Amount of Slag: 150 kg/tonne steel

Reactor: Ladle furnace (inside d = 3.2 m, h= 2.9m)

Temperature: 1873K

Mechanism: Cu reacts with FeO and is transferred to molten slag as Cu_2O. Then Cu_2O is chlorine by $CaCl_2$ to form volatile copper chlorides.

$2Cu(l) + FeO = Cu_2O + Fe(l)$ $\Delta G(1873K)= 24.908$ kcal

$Cu(l) = [Cu]_{steel}$ $\Delta G(1873K)= 33470-39.47\times1873=-40.27$ kJ = -9.63 kcal

$[Cu]_{steel} + FeO = Cu_2O + Fe(l)$ $\Delta G(1873K)= 44.168$ Kcal

$Cu_2O + CaCl_2 = 2CuCl(g) + CaO$ $\Delta G(1873K)=-0.244$ kcal

The reaction between [Cu] and FeO is thermodynamically difficult to happen. According to the research of Xiaojun et al.[41], a small amount of Cu_2O in the slag can react with $CaCl_2$. As a result, this process can make the first reaction move right.

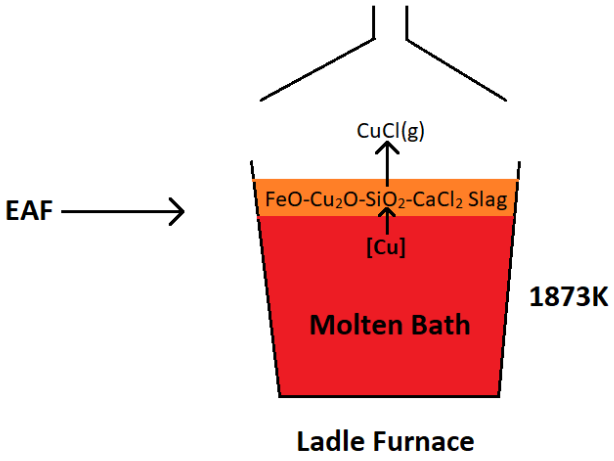

Also saturated carbon content will be helpful for the distribution of Cu from molten bath to slag phase.

We can assume the mass transfer of Cu in the melt controls the reaction rate and calculate the time using the same equation as evaporation.

No so much kinetic data can be found about this process, so we can assume average $k_{Cu}=5\times10^{-4}$ m/s and A=1 m^{-1} (factor 3)under electromagnetic stirring.

So the treating time to remove Cu to 0.1% is about 50 minutes. Also the removing time to 0.03% is 87 minutes.

A. Energy consumption per tonne scrap from 0.4% to 0.1%:

(1) Heating the slag to 1600 °C

Input	Name	Amount	Mole	ΔH(25 °C to 1600 °C)	Total Needed Heat	Energy Consumption /kWh
Slag	FeO	141.975kg	1970	28.289 kcal/mol	55730 kcal	64.77
	Cu_2O	2.895kg	20.1	47.223 kcal/mol	944 kcal	1.1
	$CaCl_2$	3.345 kg	30	41.312 kcal/mol	1240 kcal	1.44
	SiO_2	1.815 kg	30.3	26.422 kcal/mol	800 kcal	0.93

(2) Heating for the reactions:

$2Cu(l) + FeO = Cu_2O + Fe(l)$ $\Delta H(1873K)= 31.498$ kcal

$Cu_2O + CaCl_2 = 2CuCl(g) + CaO$ $\Delta H(1873K)=74.685$ kcal

To remove Cu from 0.4% to 0.1%, required energy is:

$62.5 \text{ mol} \times 0.75 \times 0.5 \times 31.498 + (62.5 \times 0.5 \times 0.75 + 20.1) \times 74.685 = 3989.83$ kcal

= 4.64 kWh

(3) Maintaining 1600 °C for 50 minutes:

152 kW/tonne × (50/60) h = 126.67 kWh

(4) Heating loss during treatment

Heat loss due to conduction through the ladle sides and bottom. According to Alexis et al., heat loss for a 100 ton furnace is 12.5 kWh/m^2.

$3.14 \times 1.6^2 \times 12.5 / 100 = 5$ kWh/tonne

So the extra energy consumption per tonne is:

64.77+1.1+1.44+0.93+4.64+126.67+5= **204.55 kWh**

B. Energy consumption per tonne scrap from 0.4% to 0.03%:

(1) Heating the slag to 1600 °C

Input	Name	Amount	Mole	ΔH(25 °C to 1600 °C)	Total Needed Heat	Energy Consumption /kWh
Slag	FeO	141.975kg	1970	28.289 kcal/mol	55730 kcal	64.77
	Cu_2O	2.895kg	20	47.223 kcal/mol	944 kcal	1.1
	$CaCl_2$	3.345 kg	30	41.312 kcal/mol	1240 kcal	1.44

	SiO_2	1.815 kg	30.3	26.422 kcal/mol	800 kcal	0.93

(2) Heating for the reactions:

$2Cu(l) + FeO = Cu_2O + Fe(l)$ $\Delta H(1873K)= 31.498$ kcal

$Cu_2O + CaCl_2 = 2CuCl(g) + CaO$ $\Delta H(1873K)=74.685$ kcal

To remove Cu from 0.4% to 0.1%, required energy is:

$62.5 \text{ mol} \times 0.925 \times 0.5 \times 31.498 + (62.5 \times 0.5 \times 0.925 + 20.1) \times 74.685 = 4570.52 \text{ kcal} = 5.31 \text{ kWh}$

(3) Maintaining 1600 °C for 87 minutes:

$152 \text{ kW/tonne} \times (87/60) \text{ h} = 220.4 \text{ kWh}$

(4) Heating loss during treatment

Heat loss due to conduction through the ladle sides and bottom. According to Alexis et al., heat loss for a 100 ton furnace is 12.5 kWh/m^2.

$3.14 \times 1.6^2 \times 12.5 / 100 = 5 \text{ kWh/tonne}$

So the extra energy consumption per tonne is:

64.77+1.1+1.44+0.93+5.31+220.4+5= **298.95 kWh**

C. Material consumption per tonne:

Material	Price $	Amount	Sum $
FeO (99.5%)	9.68/g	141.975kg	Couldn't find the bulk price
Cu_2O (99%)	788.2/2.5kg	2.895kg	912.74
$CaCl_2$ (97%)	92.054/kg	3.345 kg	307.92
SiO_2 (99.99%)	0.14/g	1.815 kg	254.1
Total			1474.76+$FeO

D. Secondary Effects:

Decarburization is needed after this process.

Due to the unclear mechanism, the removal rate may not be easier to achieve in the above time.

Appendix - D: Calculation for the Blending of Scrap Sources with Virgin Ferrous Materials

This page left BLANK intentionally

1. Virgin Ferrous Materials

Most commonly used ferrous materials in EAF to dilute steel scrap with high Cu content include pig iron, hot briquetted iron (HBI) and direct reduced iron (DRI). Table 1.1 shows the composition of these ferrous materials used in the EAF.

Table 1.1 Composition of Virgin Ferrous Materials

%	Pig Iron	HBI	DRI
Total Fe	91.0-95.7	91-93	90-94
Metallic Fe	91.0-95.7	83-88	83-89
Silica (SiO_2)	/	1.5-2.5	1.5-2.5
Si	0.3-3.0	/	/
Alumina (Al_2O_3)	/	0.4-1.5	0.4-1.5
Mn	0.4-1.0	/	/
P	0.08-0.5	0.02-0.05	0.2-0.09
S	Max 0.04	0.002-0.02	0.005-0.03
CaO	/	0.3-1.8	1.5
MgO	/	0.5-1.8	0.45
C	3.5-4.5	1.2-2.2	1-2.5

Due to the lower processing temperature of producing HBI and DRI, few FeO could be contained in the final product. That's why we need to consider the Metallic Fe content in HBI and DRI. So the FeO content can be calculated by (Total Fe% - Metallic Fe%)×72/56. But during the dilution process in EAF, we can assume FeO can be reduced into Fe. So in the following calculation, the data of Total Fe% will be used to estimate the overall amount of virgin ferrous materials. Also we can assume these materials don't contain any Cu.

2. Scrap Sources

Besides shredded automobile scrap, other types of scrap are also used as scrap source in EAF, including #1 Bundles, Bushelling, Heavy Metal Scrap (HMS), and Plate & Structural. Institute of Scrap Recycling Industries (ISRI) issues guidelines for these ferrous scrap commodities. Also different steelmaking companies have their own specification manual for various scrap sources. Table 2.1 shows the composition of these scrap sources.

Table 2.1 Composition of Scrap Sources

Scrap Sources	Cu(%)	Sn(%)	Ni(%)	Mo(%)	Cr(%)
Shredded Scrap	0.22	0.015	0.3	0.03	0.2
Bushelling	0.1	0.015	0.3	0.03	0.2
HMS	0.3	0.05	0.3	0.03	0.5
#1 Bundles	0.08	0.015	0.3	0.03	0.2
Plate & Structural	0.17	0.03	0.3	0.03	0.2

In the following calculation, two type of scrap sources, including (1) only shredded scrap and (2) the mixture of scrap in Table 2.1, will be considered to evaluate the blending process.

3. Cu content of steel product

Due to different application, various steel product have specific requirement for the content of Cu. Table 5.2 shows the limitation of Cu content for most commonly applied steel product.

Table 3.1 Limitation of Cu Content in Steel Product

Steel Product	IF Steel	Deep Drawing Steel	Commercial Steel	Structural Steel
Cu content (Z%)	0.03	0.04	0.1	0.12

4. Assumption:

(1) Weight of scrap sources: Ms

(2) Cu content of scrap sources: A%

(3) Weight of required pure Fe for dilution: Mp

(4) Weight of required virgin ferrous materials: Mv

(5) Total Fe content of virgin ferrous materials: Total Fe%

(6) Cu content of final steel product: Z%

5. Mathematic Description

$$Z = \frac{\frac{Ms \times A}{100} + \frac{Mp \times 0}{100}}{Ms + Mp} \times 100 \ (1)$$

$$Z = \frac{Ms \times A}{Ms + Mp} (2)$$

$$Mp = \frac{A - Z}{Z} Ms (3)$$

$$Mv = \frac{Mp}{Total\ Fe\%} \times 100 (4)$$

$$Mv = \frac{\frac{A - Z}{Z} Ms}{Total\ Fe\%} \times 100 (5)$$

6. Calculation

(1) Required amount of virgin ferrous materials for diluting shredded scrap

Due to the different value of Total Fe% in pig iron, HBI and DRI, we carry out the calculation respectively.

Table 6.1 Total Fe% of Virgin Ferrous Materials

Virgin Materials	Total Fe%	Equation (5)
Pig Iron	95.7	$Mv = \frac{\frac{A - Z}{Z} Ms}{95.7} \times 100 (5)$

HBI	93	$Mv = \frac{\frac{A-Z}{Z}Ms}{93} \times 100 (5)$
DRI	94	$Mv = \frac{\frac{A-Z}{Z}Ms}{94} \times 100 (5)$

At this situation, for shredded scrap, A=0.22%. Based on equation (5), the required amount of virgin ferrous material for diluting per ton shredded scrap (Ms = 1ton) is calculated and demonstrated by Fig. 6.1 with the change of Cu content in final steel product.

As shown in Fig 6.1, because of the really small difference of Total Fe% among pig iron, HBI and DRI, it is convenience to treat them as one kind of material in the following calculation. Also, the required amount of virgin ferrous materials is increased exponentially if much lower Cu content is achieved.

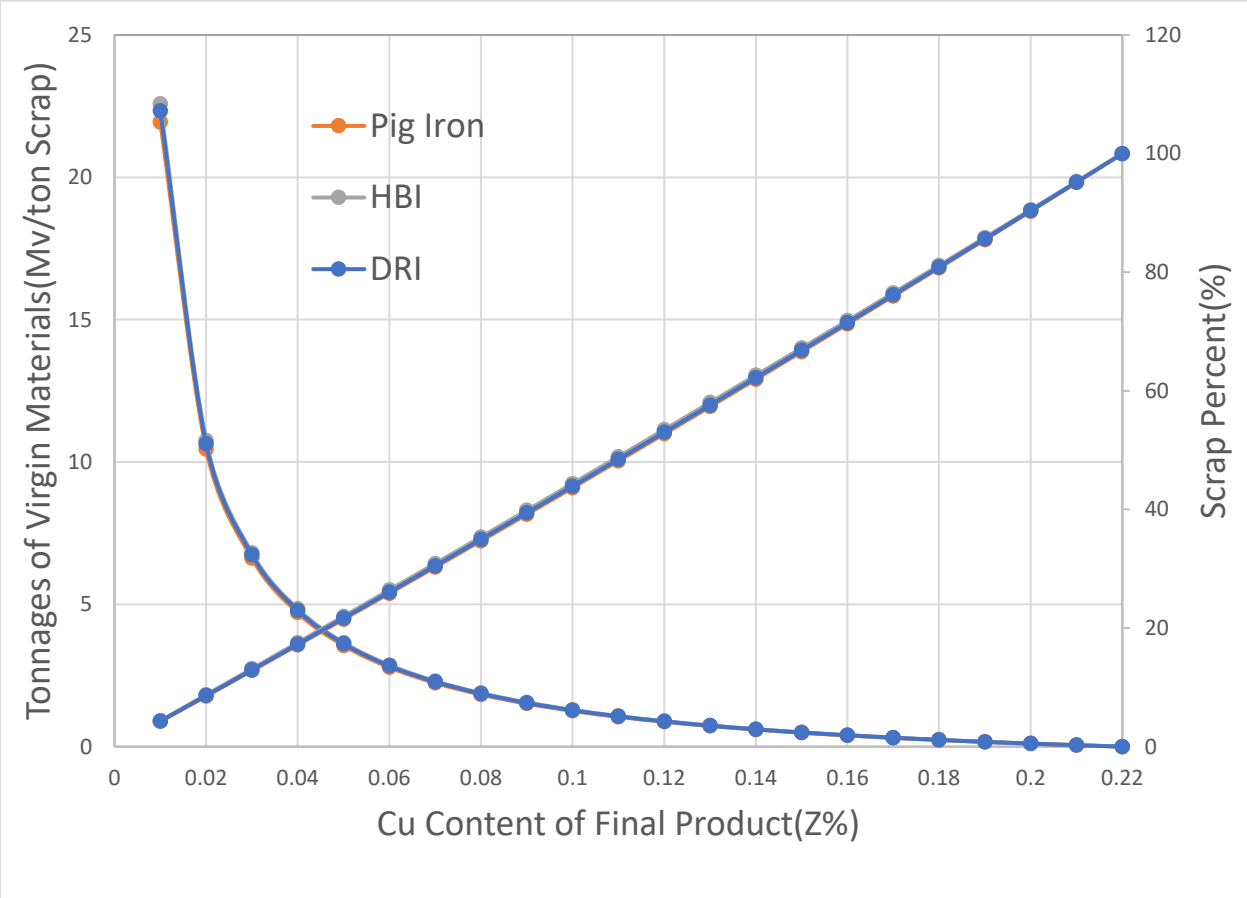

Fig 6.1 Required Amount of Virgin Materials for Diluting per ton Shredded Scrap into Specific Cu Content

(2) Required amount of virgin ferrous materials for diluting mixture of scrap sources

In the industry, a mixture of scrap sources is used in the EAF. So we can assume the makeup of scarp sources in Table 6.2:

Table 6.2 Makeup of Scrap Sources

Scrap Sources	Weight Percentage/%	Cu Content/%
Shredded Scrap	y_1	a_1=0.22
Bushelling	y_2	a_2=0.1
HMS	y_3	a_3=0.3
#1 Bundles	y_4	a_4=0.08
Plate & Structural	y_5	a_5=0.17
Sum	100	A

$$A = \frac{Ms \times (\frac{y_1 \times a_1}{100 \times 100} + \frac{y_2 \times a_2}{100 \times 100} + \frac{y_3 \times a_3}{100 \times 100} + \frac{y_4 \times a_4}{100 \times 100} + \frac{y_5 \times a_5}{100 \times 100})}{Ms} \times 100$$

$$A = \frac{y_1 \times a_1 + y_2 \times a_2 + y_3 \times a_3 + y_4 \times a_4 + y_5 \times a_5}{100}$$

$$(0 \ll y_1, y_2, y_3, y_4, y_5 \ll 100)$$

$$A = \frac{\sum_{j=0}^{j=5}(y_j \times a_j)}{100} \quad (6)$$

$$100 = y_1 + y_2 + y_3 + y_4 + y_5$$

Assuming Total Fe% is 94.2 (average value of pig iron, HBI and DRI) for the virgin ferrous materials and Ms = 1ton,

$$Mv = \frac{100A - 100Z}{94.2Z}$$

$$Mv = \frac{\sum_{j=0}^{j=5}(y_j \times a_j) - 100Z}{94.2 \times Z} (7)$$

For steelmaking companies, the makeup of mixture will be different from each other. Equation (6) can be used to calculate the overall Cu content of the mixture. Based on Equation (6) and Table 5.2, the value of A has a range:

$$0.08 \ll A \ll 0.3$$

Table 6.3 demonstrates some examples for different mixture of scrap sources and their makeup.

Table 6.3 Different Mixture of Scrap Sources

Scarp Sources	Percent of Mixture					
Shredded Scrap	0	10	20	30	62.5	0
Bushelling	0	30	50	15	0	0
HMS	0	0	10	30	37.5	100
#1 Bundles	100	60	10	15	0	0
Plate & Structural	0	0	10	10	0	0
Overall Cu Content (A%)	0.08	0.1	0.149	0.2	0.25	0.3

Based on the overall Cu content (A%) in Table 6.3,we can calculate the required amount of virgin ferrous material for diluting per ton shredded scrap and get a similar plot as Fig 6.1.

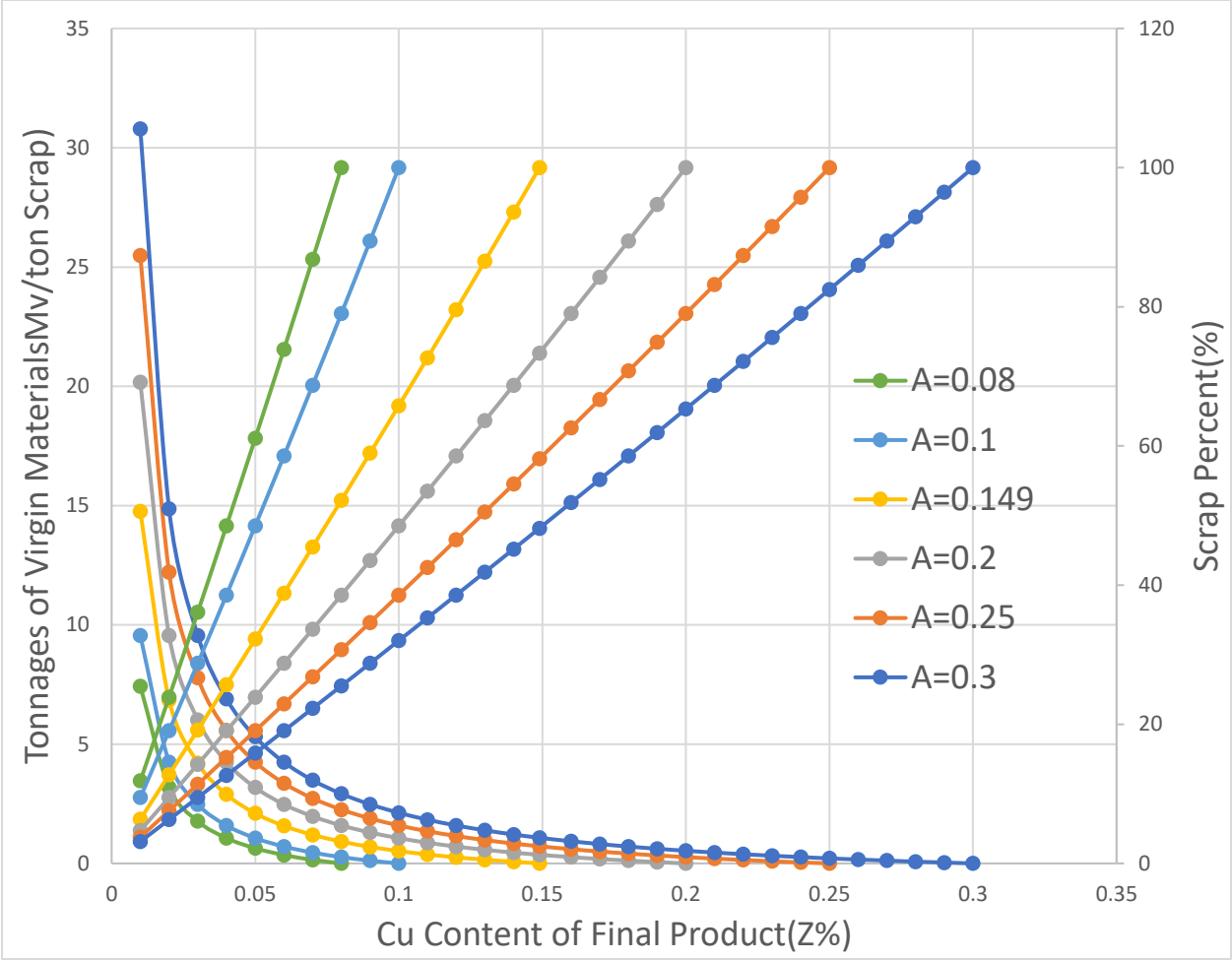

Fig 6.2 Required Amount of Virgin Materials for Diluting per ton Scrap Mixture into Specific Cu Content

(7) Conclusion

With the help of equation (5), Fig 6.1 and 6.2, industry can decide the amount of virgin ferrous materials in EAF based on the Cu content of final steel product.

Also, with the given value for scrap percent in EAF and Cu content of final steel product, industry can know the exact Cu content of scrap sources, which can offer a direction for the mixture of different types of scrap.

Appendix F

Colorado State University - Fort Collins

Project Name: Colorado State University Extension Industrial Assessment Center
Primary Investigator: Jason Quinn
Description and Progress in 2020:

The Colorado State University Industrial Assessment Extension program officially kicked off in September 2019. Before the extension program was funded, the Colorado State University Industrial Assessment Center (CSU IAC) and its predecessor programs (the Energy Analysis and Diagnostic Center and the Waste Minimization Assessment Center) had been providing manufacturers with plant assessments and suggestions for improved operations since 1984. There was a funding gap that occurred from 2017 to 2019 and as a result the IAC program had to be dismantled. In 2019 the IAC extension program was awarded funding through the DOE and cost share through the Colorado Higher Education Competitive Research Authority. This funding allowed for the restart of the program. The Industrial Assessment Center is designed to provide industrial energy audits by engineering students to small and medium sized manufacturing facilities. As a result of performing these assessments, engineering students receive unique hands-on assessment training and gain knowledge of industrial process systems, plant systems, and energy systems. A team of students will conduct a site visit, take energy system measurements, and acquire utility bills along with other energy related documentation from the manufacturing plant. From these measurements and usage bills, the team performs a detailed analysis for specific energy recommendations, estimating performance, implementation costs, and payback times. These calculations are included in a report that details the analysis, findings, and strategic energy management recommendations. Lastly, a follow up Implementation survey will be conducted with the plant manager to verify which recommendations the plant intends to implement within the following year.

The relaunch of the program proved to be more demanding than originally anticipated due to the impacts from the Coronavirus. Although the impacts were significant and sustained, the IAC was still able to actively prepare for the relaunch of the IAC. This included the development of the website, request for IAC office space, development of the pre-assessment questionnaire and operational documentation, building a formal database of potential assessment clients, and the shadowing of an assessment conducted by the University of Utah IAC. CSU also located the data acquisition systems from the previous program and purchased new instrumentation and PPE to replace damaged and outdated equipment. A total of 6 students have been trained by the program and we recently brought on our first graduate student.

In addition to completing the background work needed to prepare the IAC, in November we were able to secure university approval for our first in-person assessment. The completion of the first assessment was a significant achievement and a needed accomplishment. Moving forward we have secured three additional companies looking for assessments and we are excited to schedule them into the program. The University is supportive of our continued in person activity and we are excited to meet our manufacturing neighbors.

The industrial assessment program offers an incredibly valuable service to our local manufacturing community. The assessments are offered to companies that don’t have the necessary internal resources to perform the energy and waste assessments, and they provide explicit assessment reconditions. The recommendations facilitate the saving of energy while also helping our manufactures stay competitive in a dynamic manufacturing environment. These are

very direct and repeatable positive outcomes. Not only does the program provide these direct benefits, but there is evidence suggesting that the program has the ability to change long term energy related decision making. This can partially be attributed to IAC graduates entering the workforce and taking with them the experiences of the program.

Not only does the program provide these direct, measurable benefits to or local manufacturing community, it also provides training and applied experience for our next generation of energy engineers. Students get a wide variety of training including the use of modern data acquisition devices, comprehensive data analysis, emerging energy analysis techniques, energy systems evaluation, waste reduction opportunities, report writing, and professional development. This training comes from the IAC internally and also from industry partners. The most impressive training is the student to student interactions. These combined experiences anchor the skills learned in the traditional academic environment and at the same time enhance personal leadership skills and confidence.

Appendix G

MRI: Acquisition of a High-Sensitivity Low-Energy Ion Scattering (HS-LEIS) Spectrometer with Multiple Reactive Environment Transfer for Interrogating Surfaces and Interfaces

Description: Materials interact with their environment through their surfaces. Knowledge of surface properties of materials is crucial to understanding structure-function relationships and designing next-generation materials with targeted characteristics spanning chemical, optical, electronic, thermal, mechanical, biological, and other applications. Recent developments in ion scattering spectroscopy provide unprecedented resolution and sensitivity for the top atomic layer of materials, which most critically affects behaviors such as catalytic reactivity, coating permeability, or charge transport in photovoltaics. This proposal seeks to acquire a high-sensitivity low-energy ion scattering (HS-LEIS) spectrometer, which will be a vital resource for the greater Rocky Mountain Region and its many researchers studying catalysis, atomic layer deposition and coatings, photovoltaics, and solid state structure and interfaces, among other areas. The instrument will stimulate the establishment of new collaborations and will be leveraged in creating a new annual, web-based surface science symposium to connect the geographically diffuse researchers of the region. As a publicly available resource, the instrument will advance the scientific missions of local academic, government, and industrial researchers.

This funding is being applied toward the purchase of a new instrument for a scientific user facility on the CU Boulder campus. The first year of the funding period was used for iterating on a final design for custom components with the manufacturer and their subsequent building of the instrument. Construction has been recently completed (January 2021), but delivery has been postponed until completion of some facilities updates in the final CU Boulder campus location that will house the instrument (a room is being expanded to fit the instrument as the original slated room was reallocated between the time of grant and delivery). We anticipate the instrument will become operational in late 2021 and begin servicing the scientific mission described in the abstract starting then.

Several graduate students were involved in the instrument design process, but until it is commissioned later this year, there is little to report.